ABSTRACT

DEACTIVATION AND ENHANCEMENT EFFECTS OF SULFUR ON SUPPORTED PLATINUM OXIDATION CATALYSTS

by
Mark Ladolcetta

The effects of sulfur poisoning on the oxidation activity of 1.5 % Pt/γ-Al_2O_3, Pt/TiO_2, Pt/ZrO_2, and Pt/SiO_2 were investigated in this study. Each catalyst was poisoned with an H_2S/air or SO_2/air mixture at 400°C for 24 hours and a sulfur concentration of 200 ppm. The complete oxidation of mixtures of 1 % CO, methane, ethane, ethene, ethyne, propane, propene, and n-butane in air were measured over fresh and sulfur-poisoned catalysts.

Non-methane alkane oxidation activity was enhanced significantly after sulfur poisoning on all four catalysts. The temperatures at which 50 % conversion to CO_2 was achieved (T_{50}) ranged from 10 to 72°C lower for the sulfur-poisoned catalysts than the corresponding fresh catalyst samples. CO oxidation activity was severely deactivated on all four sulfur-poisoned catalysts and T_{50} values were 24-75°C higher than the fresh catalyst T_{50}'s. Methane oxidation activity was moderately deactivated on all sulfur-poisoned catalysts with the exception of Pt/SiO_2, for which no effect was found. The effects of sulfur poisoning on alkene and alkyne oxidation activity were small on each catalyst sample.

Catalyst characterization studies, including H_2 chemisorption, BET surface area, FTIR spectroscopy, and temperature-programmed reduction and desorption studies were conducted to determine the nature of sulfur interactions on the catalysts' surface and the mechanisms responsible for associated changes in observed catalyst activity. Alkane

oxidation enhancement for Pt/γ-Al_2O_3, Pt/TiO_2, and Pt/ZrO_2 was primarily associated with the formation of new active sites, which facilitate the oxidation reaction. New active sites are formed due to the combination of sulfate formation on the catalyst support and sulfur-induced Pt crystal growth. Enhanced alkane oxidation activity on sulfur-poisoned Pt/SiO_2 was the result of Pt crystal growth and the formation of a small amount of sulfate on Pt sites. Deactivation of CO and methane oxidation reactions was a result of pore blocking and active site inhibition due to sulfate formation.

DEACTIVATION AND ENHANCEMENT EFFECTS OF SULFUR ON SUPPORTED PLATINUM OXIDATION CATALYSTS

by
Mark Ladolcetta

A Dissertation
Submitted to the Faculty of
New Jersey Institute of Technology
in Partial Fulfillment of the Requirements for the Degree of
Doctor of Philosophy in Environmental Science

Department of Chemical Engineering,
Chemistry and Environmental Science

August 2000

APPROVAL PAGE

DEACTIVATION AND ENHANCEMENT EFFECTS OF SULFUR ON SUPPORTED PLATINUM OXIDATION CATALYSTS

Mark Ladolcetta

Dr. Henry Shaw, Dissertation Advisor — Date
Professor of Chemical Engineering, Chemistry,
and Environmental Science, NJIT

Dr. Richard Trattner, Committee Member — Date
Associate Chairman for Environmental Science and Professor of
Chemical Engineering, Chemistry, and Environmental Science, NJIT

Dr. Robert Pfeffer, Committee Member — Date
Distinguished Professor of Chemical Engineering, Chemistry,
and Environmental Science, NJIT

Dr. Howard Perlmutter, Committee Member — Date
Professor of Chemical Engineering, Chemistry,
and Environmental Science, NJIT

Dr. Robert Farrauto, Committee Member — Date
Research Fellow, Research and Development, Engelhard Corp. and
Adjunct Professor of Chemical Engineering, Chemistry,
and Environmental Science, NJIT

BIOGRAPHICAL SKETCH

Author: Mark Ladolcetta

Degree: Doctor of Philosophy in Environmental Science

Date: August 2000

Undergraduate and Graduate Education:

- Doctor of Philosophy in Environmental Science
  New Jersey Institute of Technology, Newark, NJ, 2000

- Bachelor of Science in Chemistry
  Catholic University of America, Washington, D.C., 1994

Publications and Presentations:

"The Effect of Sulfur on the Oxidation of Hydrocarbons and CO Over Pt Catalysts Supported on Various Acid Substrates", 8th Annual Uni-Tech Student Conference on Science & Technology.; NJIT; April 24, 1998.

"The Effect of Sulfur on the Oxidation of Hydrocarbons and CO Over Pt Catalysts Supported on Various Acidic Substrates", 1998 Annual Meeting of the American Institute of Chemical Engineers; Miami Beach, Nov. 18, 1998.

"The Activation/Deactivation Effects of Sulfur On Hydrocarbon and CO Oxidation by Pt Catalysts Supported on Various Acidic Substrates", 16th North American Meeting of the Catalysis Society; Boston, May 30-June 4, 1999.

"Exxon – Harvesting Clean Energy" Technology Observer, Vol. 1(2), 58-61, 1999.

"H Power; Small Today...Big Tomorrow" Technology Observer, Vol. 1(2), 62-66, 1999.

ACKNOWLEGMENT

The work described in this dissertation could not have been completed without the assistance of many people. I wish to express my sincere gratitude to everyone who has made this research possible. I express my deepest appreciation to my thesis advisor, Dr. Henry Shaw for his constant support, encouragement, and advice, which made the completion of my doctoral studies possible.

I would like to specially thank Dr. Robert Farrauto for supporting me in this work, serving on my dissertation committee, and providing valuable advice. I am also thankful to Dr. Farrauto and Engelhard Corp. for graciously providing materials used in this research. I also would like to thank Dr. Robert Pfeffer, Dr. Howard Perlmutter, and Dr. Richard Trattner for serving on my dissertation committee and for continual support.

This research would not have been possible without the initial funding of the Hazardous Substance Management Research Center as well as support from the Department of Chemical Engineering, Chemistry, and Environmental Science.

I have been fortunate to work alongside many outstanding students who have assisted me in numerous ways, especially, Dr. Yi Wang, Dr. Paul Yu, Shan Xiao, and Tian Sang. Appreciation is also reserved for Clint Brockway and Larisa Krishtopa for valuable instrumentation assistance.

I also wish to specially thank the friendly folks at Warren Plaza, without whom I probably would have starved.

Finally, I am deeply grateful to my parents, family, and friends for their continued support throughout my studies at New Jersey Institute of Technology. A special thanks is due to everyone who has asked the question, "When will you be finished?"

TABLE OF CONTENTS

TABLE OF CONTENTS

(Continued)

TABLE OF CONTENTS
(Continued)

Chapter **Page**

LIST OF TABLES

Table **Page**

LIST OF FIGURES

Figure **Page**

LIST OF FIGURES
(Continued)

Figure **Page**

LIST OF FIGURES
(Continued)

Figure **Page**

LIST OF FIGURES
(Continued)

Figure **Page**

LIST OF FIGURES
(Continued)

Figure **Page**

CHAPTER 1

INTRODUCTION

The field of heterogeneous catalysis has been instrumental in curbing many of the environmental ills stemming from the rapid industrialization of the second half of the 20th century. Catalysts are heavily employed to reduce air pollutants produced as byproducts of various forms of energy generation. This includes transportation-related pollution sources such as automobiles, trucks, and buses as well as stationary sources such as fossil fuel-burning power plants. Additionally, many chemical manufacturing plants utilize catalysts as an end-of-pipe treatment method to reduce and eliminate waste emissions. Furthermore, catalysts are used to improve the efficiency of various chemical processes thereby eliminating pollution at the source. The development of catalysts for all of these applications has been driven by increasingly stringent environmental regulations and it is quite evident that the field of catalysis will continue to play an important role in meeting environmental challenges of the future. This is reflected in the large number of international meetings and symposia devoted entirely to the field of environmental catalysis. A prominent catalysis journal (Applied Catalysis) spun off a separate journal, Applied Catalysis B: Environmental, devoted exclusively to this subject.

Air pollution, which plagues most industrialized nations throughout the world, is inherently coupled with energy usage. As long as fossil fuels continue to provide the bulk of the world's energy output, scientists and engineers will have to continually develop innovative methods to abate the associated emissions. Burning fossil fuels results in the secondary production of carbon monoxide and hydrocarbons, which are

both products of incomplete combustion. Also, the high temperatures characteristic of combustion systems result in the combination of nitrogen and oxygen in air to form nitrogen oxides. Both carbon monoxide and nitrogen oxides are direct respiratory irritants and have other harmful effects on humans. Additionally, nitrogen oxides and volatile organic hydrocarbons react in the presence of sunlight in the troposphere to form photochemical smog, which afflicts many urban areas throughout the world. Ozone, a primary component of smog, is also a strong respiratory irritant and is responsible for free radical-associated tissue and chromosomal damage. Nitrogen oxides also react with water vapor to form acidic nitrogen compounds, which are responsible for the acidification of soils and water bodies in many areas of the world. Consequently, the U.S. Environmental Protection Agency (EPA) has regulated emissions of these pollutants under the Clean Air Act (CAA) since the early 1970's.

1.1 Automotive Three-Way Catalysts

One of the most successful applications of catalysis in the environmental field has been the use of so-called three-way catalysts (TWC's) in automobile exhaust systems. TWC's are named as such because of their ability to simultaneously oxidize CO and unburned hydrocarbons to carbon dioxide and reduce NO_x (NO and NO_2) to nitrogen (N_2). A summary of the reactions carried out by TWC's in the automotive catalytic converter is given in Figure 1.1. Automotive TWC's have evolved into extremely complex active systems with the ability to conduct the necessary reactions efficiently in an extremely hostile environment.

Figure 1.1 Summary of TWC catalytic reactions [1,2]

CO and Hydrocarbon Oxidation:

$$CO + \frac{1}{2}O_2 \rightarrow CO_2 \quad (1.1)$$

$$C_yH_x + \left(y + \frac{x}{4}\right)O_2 \rightarrow yCO_2 + \frac{x}{2}H_2O \quad (1.2)$$

Steam Reforming of CO and Hydrocarbons:

$$CO + H_2O \rightarrow CO_2 + H_2 \quad (1.3)$$

$$C_yH_x + 2yH_2O \rightarrow yCO_2 + 2\left(y + \frac{x}{4}\right)H_2 \quad (1.4)$$

NO and NO_2 reduction:

$$NO + CO \rightarrow \frac{1}{2}N_2 + CO_2 \quad (1.5)$$

$$NO_2 + 2CO \rightarrow \frac{1}{2}N_2 + 2CO_2 \quad (1.6)$$

$$NO + H_2 \rightarrow \frac{1}{2}N_2 + H_2O \quad (1.7)$$

$$NO_2 + 2H_2 \rightarrow \frac{1}{2}N_2 + 2H_2O \quad (1.8)$$

$$2\left(y + \frac{x}{4}\right)NO + C_yH_x \rightarrow \left(y + \frac{x}{4}\right)N_2 + yCO_2 + \frac{x}{2}H_2O \quad (1.9)$$

$$\left(y + \frac{x}{4}\right)NO_2 + C_yH_x \rightarrow \left(\frac{y}{2} + \frac{x}{8}\right)N_2 + yCO_2 + \frac{x}{2}H_2O \quad (1.10)$$

TWC's have generally been composed of a mixture of precious metals (Pt, Pd, Rh) supported on a high surface area γ-Al_2O_3 washcoat. The washcoat is deposited on a ceramic honeycomb monolith with open parallel channels consisting of approximately 400 cells per square inch and 0.006 in. wall thickness. Monoliths are effective for automotive catalyst applications for several reasons. The high cell density and narrow wall thickness provide an open frontal area of greater than 70 %, resulting in a low pressure drop, which is important in automotive applications in order to maximize engine power and fuel efficiency. Also, monoliths are manufactured from ceramic materials with low thermal expansion coefficients that can be matched to the thermal expansion properties of the support (γ-Al_2O_3) washcoat. These properties are critical for maintaining catalyst durability despite rapid temperature fluctuations and periodic high temperature excursions experienced under various operating conditions. Additionally, the ceramic monoliths provide a large amount of contact between reactants and catalyst washcoat, necessary for the efficient removal of various exhaust components. In some specialized applications, metal monoliths are used with extremely narrow wall thickness resulting in open frontal areas greater than 90 %.[1,2]

First generation catalytic converters consisted of a mixture of Pd and Pt deposited on γ-Al_2O_3. These catalysts were only required to oxidize CO and hydrocarbons since NO_x emissions standards could be attained through engine modifications such as exhaust gas recirculation. More stringent NO_x regulations took effect in 1979 and led to development of the precursor to today's TWC. Early TWC's were composed of a mixture of Pt and Rh in a ratio of 5:1 with a total metal content of 0.1-0.15 % by weight on a γ-Al_2O_3 support. In this system, oxidation reactions are primarily carried out on Pt

while NO_x reduction occurs mostly on Rh. A variety of additives were also incorporated within the metal-support system to instill several desirable properties. Small amounts (1-2 % by weight) of La_2O_3 and BaO were added to γ-Al_2O_3 to stabilize the support and prevent support sintering. CeO_2 (10-20 % by weight) was added to the support along with smaller amounts of ZrO_2 to improve the oxygen storage capabilities of the system as discussed further below.[1,2]

Effective operation of the TWC required the concomitant development of both oxygen sensor with associated engine technology, and the CeO_2 oxygen storage component. In order to effectively conduct oxidation and reduction reactions simultaneously, it is necessary for the engine to operate within a very small range of air to fuel ratio. The stoichiometric air/fuel ratio on a weight/weight basis is 14.6 and optimal operation of the TWC requires this ratio to vary within a window of only $\pm$ 0.05. This was accomplished through the development of the exhaust oxygen sensor. This sensor, located before the catalytic converter in the exhaust manifold, is composed of a high surface area Pt electrode with a stabilized ZrO_2 solid electrolyte (note: another successful use of catalysis!). The sensor detects the amount of oxygen present in the exhaust gas and relays this information to an onboard computer, which adjusts the air/fuel ratio accordingly. Oxygen concentration data is transmitted by the sensor at a rate of 0.5-1 Hz. A result of the oxygen sensor and associated electronics is that the catalytic converter operates under alternating oxidizing and reducing conditions. Under reducing conditions, an additional source of oxygen is required to oxidize unreacted CO and hydrocarbons.[1,2]

The required oxygen is supplied by a CeO_2 oxygen storage component (OSC). The redox properties of CeO_2 are such that oxygen is efficiently liberated under reducing conditions yielding a reduced Ce_2O_3. When the exhaust gas reverts to oxidizing conditions, CeO_2 is re-formed storing oxygen for future use. In addition to providing oxygen for the CO and hydrocarbon oxidation reactions (Fig. 1.1, reactions (1.1) and (1.2)), CeO_2 is also an efficient catalyst for the steam reforming reactions, which convert CO and hydrocarbons to CO_2 and H_2 under rich conditions (Fig. 1.1, reactions (1.3) and (1.4)). The generation of H_2 further enhances the reduction of NO_x to N_2. Small amounts of ZrO_2 are added to the CeO_2, which increases the oxygen mobility on the CeO_2 surface and improves the thermal stability of CeO_2.[1,2]

In the last decade, catalyst manufacturers have altered the catalyst composition of TWC's from a 5:1 Pt/Rh mixture to a mostly Pd formulation with small amounts of Pt and Rh added or, in some cases, a Pd only catalyst. The shift from Pt and Rh to Pd has been driven by the higher costs of Pt and Rh compared to Pd. Pd catalysts tend to be more susceptible to various forms of deactivation than Pt or Rh. However, improvements in fuel quality, higher engine operating temperatures, more precise control of the air/fuel ratio, and improved catalyst formulations have enabled Pd catalysts to become viable for automotive emission control.[1,2]

The evolution of the modern automotive TWC has occurred largely due to U.S. EPA regulations that have steadily increased in stringency since the early 1970's. Current standards for vehicle emissions are shown in Table 1.1. These standards have been completely in effect since 1996 and it is likely that further reductions in each pollutant will be required in the near future. Already, a more stringent NO_x standard was

promulgated recently in conjunction with a rule requiring reductions in the sulfur content of fuel (see discussion below).[4] The new NO_x legislation establishes a 0.07 g/mile standard and applies to all vehicle categories listed in Table 1.1. The scheduled phase-in period begins in 2004.

Table 1.1: Current light-duty vehicle and truck emission standards (g/mile)[a] [3]

Vehicle type	CO	THC[e]	NMHC[f]	NO_x
LDV[b]	3.4 (4.2)	0.41	0.25 (0.31)	0.4 (0.6)
LDT1[c]	3.4 (4.2)	(0.80)	0.25 (0.31)	0.4 (0.6)
LDT2[d]	4.4 (5.5)	(0.80)	0.32 (0.40)	0.7 (0.97)

Notes: a) The listed standards are so-called Tier 1 standards which were completely phased in by 1996. The first number in each column is the standard that must be met for 5 years/50,000 miles. The number in parentheses is the 10-year/100,000 mile standard. A blank space indicates that there is no applicable standard.
b) Light-duty vehicle
c) Light-duty truck $\leq$ 3750 lbs. Gross Vehicle Weight (GVW)
d) Light-duty truck > 3750 lbs. GVW, but $\leq$ 8500 lbs.
e) Total hydrocarbons
f) Non-methane hydrocarbons

1.2 Sulfur Poisoning

Many of the innovations in automotive TWC's described above were developed as methods for combating various forms of catalyst deactivation. Typical emission control catalysts are deactivated by high temperatures; thermal cycling; lubricating oil-derived phosphorous, zinc, and lead deposition; and sulfur poisoning. Sulfur poisoning, in particular, has been extensively studied by catalyst researchers and the interactions between various sulfur compounds and catalysts can be extremely complex. In general, sulfur poisoning occurs on automotive TWC's when organosulfur compounds, present in current gasoline blends at an approximate concentration of 300 ppm, are oxidized during the combustion process to SO_2. SO_2 can interact with the TWC in several ways

depending on the exhaust gas temperature and composition as well as the composition of the TWC.

At low temperatures (< 300°C), SO_2 adsorbs on the metal surface thereby inhibiting catalytic reactions by blocking active sites. At higher temperatures and under oxidizing conditions, SO_2 can be oxidized to SO_3, which can react with the γ-Al_2O_3 support to form $Al_2(SO_4)_3$. $Al_2(SO_4)_3$ is less dense than Al_2O_3 and can cause the blockage of pores on the γ-Al_2O_3 surface. The extensive pore network common to high surface area Al_2O_3 is one of several important properties that make it an effective catalyst support material. However, when pore blockage occurs, the precious metal particles that are deposited in the pores become unavailable as reaction sites. Under reducing conditions and high temperatures, the γ-Al_2O_3 surface can be partially regenerated as SO_4^{2-} is reduced to H_2S. H_2S can then adsorb on the metal particles and block catalytically active sites or it can be emitted to the atmosphere. Furthermore, SO_2 in the exhaust gas can react with the oxygen storage component to form $Ce(SO_4)_2$, which inhibits its oxygen storage, and release properties.

The adsorption of sulfur compounds on active metal sites and the formation of sulfate on both metal sites and the support material are fairly well established in the catalysis literature. However, the mechanisms for the subtle changes in reactivity caused by the interactions between sulfur species and active catalytic sites are not as well established despite extensive study by many researchers over several decades. Studies on emission control catalysts have shown that, in most cases, the oxidation of carbon monoxide is severely inhibited by the presence of sulfur compounds in the feedstream and/or on the catalyst surface. This observation holds regardless of whether the

feedstream exhibits oxidizing or reducing conditions, although the deactivation mechanism may be different in each case. Methane oxidation activity is generally deactivated slightly under both oxidizing and reducing conditions. While there is substantial agreement in the literature on the carbon monoxide and methane oxidation reactions, the effects of sulfur compounds on hydrocarbon oxidation reactions are not clearly understood and appear to depend substantially on sulfur concentration, reaction conditions, catalyst composition, and the specific hydrocarbon compound being studied.

A large number of laboratory studies have examined the effect of sulfur on the oxidation activity of Pt and Pd catalysts for propane oxidation. In general, Pt and Pd catalysts are deactivated for propane oxidation under reducing conditions where the steam reforming reaction is dominant (Fig. 1.1, reaction (1.4)). It is presumed that sulfur compounds on the catalyst surface interfere with the reaction between adsorbed hydrocarbons and surface hydroxyl groups.[5] Pd catalysts are also substantially deactivated for propane oxidation in oxidizing conditions. However, many researchers have observed an activity ***increase*** for propane oxidation on Pt catalysts when adsorbed sulfur compounds are present. Although the subject has been studied extensively, a review of the literature indicates that there is not one singular explanation for the activity increase observed for the propane reaction on Pt catalysts. A variety of mechanisms have been proposed including: (1) sulfur-induced restructuring of the Pt crystal surface from substantially (111) crystal planes to (100) planes which are more active for the propane reaction; (2) sulfur-induced electronic effects on Pt crystals which result in active sites for the propane reaction; (3) formation of sulfate on Pt sites leading to additional active reaction sites; (4) formation of sulfate at the Pt/support interface which yields additional

active sites for propane reaction; and (5) sulfur-induced crystal growth of Pt metal particles yielding larger particles more active for the propane reaction.

The concept of activity enhancement in catalysis due to the presence of trace adsorbed compounds is not new and has been utilized to improve the function of catalysts for a variety of chemical reactions. Examples of catalytic reactions enhanced by sulfur poisoning include: (1) increased selectivity of Fischer-Tropsch catalysts for heavier hydrocarbons in the CO + H_2 reaction, (2) increased selectivity for partial hydrogenation of di-olefins to the corresponding mono-olefins, and (3) minimization of excessive hydrocracking in the reforming of naptha.[6] However, in these examples, the mechanism for activity enhancement appears to involve the suppression of one or more competing reactions in favor of the desired reaction rather than an absolute increase in activity for the desired reaction. That is, the overall rate of the desired reaction may be inhibited by sulfur poisoning, but competing reactions are inhibited to a much greater extent. In contrast, activity promotion for propane oxidation on Pt catalysts appears to occur because of an enhancement in activity for the dissociative chemisorption of propane involving C-H bond activation. In fact, this step is generally thought to be the rate-limiting step in a wide variety of hydrocarbon conversion reactions including hydrocarbon oxidation.[7]

As a consequence of the importance of catalytic hydrocarbon conversion reactions in many industrial processes as well as in emission control applications, it is desirable to obtain a better understanding of the interactions between sulfur compounds and Pt catalysts and their associated effects on reaction activity.

1.3 Importance of Sulfur Interactions on Precious Metal Catalysts

In emission control applications, it is essential to understand the interactions of sulfur on catalyst surfaces since sulfur is a trace component of most solid and liquid fuels. Combustion of sulfur- containing fuels results in the production of residual amounts of SO_2, which often inhibits emission control catalysts. In addition to activity changes on automotive TWC's, sulfur effects have important implications for a variety of present and future emission control applications of precious metal catalysts.

For example, catalysts designed for diesel engine exhaust treatment are subject to sulfur poisoning due to the fact that diesel engines operate with a lean air/fuel mixture. A consequence is the lower exhaust temperatures at which diesel engine exhaust catalysts must operate as compared to gasoline engine exhaust catalysts.[1] At lower temperatures, oxidized sulfur compounds tend to adsorb on active metal sites and inhibit the reduction of NO_x by hydrocarbons and soot in the exhaust. Additionally, oxidized sulfur compounds can desorb and be emitted as particulates, which are strictly regulated for diesel engines.[1]

The reduction of NO_x by hydrocarbons and CO to form N_2 and CO_2 in a lean environment is an important catalytic reaction for the development of emission control systems for lean-burn gasoline and lean-burn natural gas engines, which are currently being developed for use in the transportation sector.[1] This reaction is difficult to perform catalytically in a lean exhaust environment and interactions of sulfur with potential catalysts are important. A similar technology known as partial lean-burn is also being studied. In this case, an engine would operate primarily on a lean air/fuel mixture for which catalysts can easily be designed to oxidize CO and hydrocarbon emissions.

The catalysts would contain a type of NO_x storage material such as BaO, which would adsorb NO_x while the engine is operating in the lean mode. Periodically, the engine would switch to a rich air/fuel ratio, at which time the NO_x would desorb and react with available carbon compounds. Unfortunately, sulfur also has an inhibiting effect on many potential NO_x storage materials.[1]

One strategy for eliminating the effects of sulfur on emission control catalysts is to reduce the amount of sulfur in fuels. Automakers have complained to the U.S. EPA for several years that it is impossible to reduce tailpipe emissions to meet proposed emission standards without a simultaneous reduction in the sulfur content of gasoline. However, petroleum refiners argue that further decreases in the sulfur content of gasoline would result in significant increases in gasoline prices and cause initial fuel shortages. The U.S. EPA recently issued regulations mandating reductions in the amount of sulfur contained in gasoline.[4] The sulfur regulation was issued in conjunction with regulations requiring cuts in NO_x emissions from automobiles and light trucks. Currently, the average sulfur content of gasoline in the U.S. is 330 ppm and the new regulations would reduce that concentration to 30 ppm. The regulation requires a scheduled phase-in period from 2005 to 2009. The US. EPA estimates that the rule will result in a 2 cent per gallon gasoline price increase while petroleum refiners estimate the additional cost to be three times as much. Additionally, the U.S. EPA is considering a proposed rule, currently under review by the Office of Management and Budget, which would cut sulfur levels in diesel fuel from current levels of 500 ppm to 15 ppm by 2006.[8]

Obviously, it would be economically advantageous to fuel producers as well as fuel consumers if catalysts could be designed to minimize deleterious effects of sulfur

while incorporating the promotional effects. Current sulfur concentrations of 330 ppm in gasoline already require substantial investments in desulfurization technology to remove high levels of sulfur in crude oil. A reduction of sulfur content to 30 ppm will certainly require new innovations in desulfurization technology that will not be inexpensive. Thus, the high costs of further sulfur removal may be averted if it can be shown that sulfur has beneficial effects on emission catalysts.

In addition to the effects on emission control catalysts, sulfur also interacts with many catalysts used in the petroleum refining industry. Refiners use a variety of noble metal catalysts supported on metal oxide supports to improve the yields of reactions used to produce gasoline from crude oil including fluidized catalytic cracking, reforming, and isomerization reactions. Since organosulfur compounds are present in crude oil in varying amounts, the catalysts used in these reactions are subject to interactions with sulfur. In some cases, sulfur proves to be beneficial while in others sulfur decreases the efficiency and/or lifetime of the catalysts. Consequently, research on the reactions of carbon-containing compounds on sulfur-exposed catalysts has important implications for petroleum refining processes as well as for emission control catalysts. Additionally sulfur compounds have effects on typical catalysts used for processes such as Fischer Tropsch synthesis of hydrocarbons from synthesis gas ($CO + H_2$), coal gasification, and gas-to-liquids technology.

An emerging technology for which precious metal catalysts will play an important role is the use of fuel cells for both stationary power production and vehicle propulsion. Current fuel cell prototypes utilize the H_2 plus O_2 reaction to produce an electric current. The current thinking is that H_2 will be produced by catalytic reforming of a hydrocarbon

source such as gasoline, natural gas, or methanol. In this system, two different catalyst units would be required. In the first unit, a process such as steam reforming or partial oxidation of the hydrocarbon fuel would be used to produce a mixture of CO and H_2. In a second unit, the water-gas shift reaction would be used to remove CO produced in the first process by reaction with H_2O to produce H_2 and CO_2. As noted previously, sulfur compounds are present in various concentrations in each of the fuels listed above and will, thus, play an important role in the type of reforming catalysts used for hydrogen production in fuel cell applications.

As this discussion indicates, the interaction of sulfur with precious metal catalysts is a topic that is relevant and extremely important to a vast array of chemical and industrial processes. A better understanding of the mechanisms behind the effects of sulfur on catalysts has the potential to benefit a large number of chemical processes.

1.4 Objective

The objective of this study was to investigate the effects of sulfur poisoning on supported Pt oxidation catalysts and to attempt to find a mechanism or mechanisms that account for the observed effects. The catalysts included in this study were Pt supported on several different oxide supports and were similar, but simplified versions of typical emission control catalysts. Different support materials were studied in order to determine whether activity changes on sulfur-poisoned Pt catalysts were influenced by the support structure. The support materials included γ-Al_2O_3, TiO_2, ZrO_2, and SiO_2.

Catalyst activity was evaluated for the complete oxidation reactions of CO and several light hydrocarbons including, CH_4, C_2H_6, C_2H_4, C_2H_2, C_3H_8, C_3H_6, and n-C_4H_{10}.

While CO, CH_4, and C_3H_8 have been commonly studied in the past by catalysis researchers as representative exhaust compounds, the other hydrocarbons were chosen to evaluate differences in catalytic activity between alkanes, alkenes, alkynes, and CO. It was assumed that sulfur effects on reactivity are strongly dependent on the reaction mechanism. Thus, the compounds chosen for this study provided the opportunity to determine the effects of sulfur on several different reaction mechanisms.

In these experiments, one specific form of sulfur poisoning was studied. Each catalyst was poisoned with a mixture of H_2S in air ***prior*** to conducting various activity and characterization experiments. Thus, the effects studied were those due to sulfur poisoning under ***oxidizing*** conditions and ***did not*** include the additional effects of sulfur present in the reaction feedstream during activity experiments. Fresh and sulfur-poisoned catalysts were compared based on their activity for the complete oxidation of the compounds listed above.

In addition to activity experiments, a range of catalyst characterization experiments was conducted to elucidate the nature of the effects of sulfur on Pt catalysts. Techniques such as H_2 chemisorption, BET surface area, FTIR spectroscopy, temperature-programmed reduction, and temperature programmed desorption were utilized to evaluate changes in catalyst properties due to sulfur poisoning. Detailed experimental procedures are presented in Ch. 3.

Experimental results were compared to results found in the literature and some conclusions were made regarding the mechanisms for observed effects of sulfur poisoning on the reactivity of Pt catalysts. The sulfur-induced activity promotion for alkane oxidation activity on Pt was specifically emphasized.

CHAPTER 2

LITERATURE REVIEW

As stated in Ch. 1, the interactions of sulfur compounds with catalyst surfaces have wide ranging implications for many chemical processes in which practical catalyst systems are employed. Accordingly, an extensive amount of research has been conducted on this subject. A summary of pertinent research results describing the specific interactions of sulfur compounds with Pt catalysts and the associated effects on various catalytic reactions is presented below. This is preceded by a brief discussion of the properties of catalyst support materials including a review of the interactions of sulfur compounds with the support materials alone.

2.1 Catalyst Support Materials

In general, materials used as catalyst supports are characterized by a high surface area and a complex pore network in which the active metal catalyst particles are deposited. The primary purpose of the support is to provide a large surface area and a stable surface on which the metal catalyst can be deposited. A support material is chosen for a given application on the basis of several important characteristics including its inertness to undesired side reactions, appropriate mechanical properties (attrition resistance, strength, etc.), stability under reaction conditions, a surface area and pore size distribution appropriate for the desired reactions, and its cost. [9]

The support material can have other beneficial properties as well. Often, metal catalysts are more active for a particular reaction when they exist as highly dispersed

particles with small particle diameters. Other reactions are favored on larger particles. In either case however, a support material can be used which stabilizes the catalyst particles at the desired dispersion by preventing metal sintering or re-dispersion. Additionally, support materials can be designed to inhibit catalyst deactivation resulting form exposure to poisonous reactive compounds. Support materials can also interact with the deposited metal and impart additional catalytic activity not intrinsic to the metal itself. This phenomenon is often referred to as strong metal-support interactions (SMSI). In other cases, support materials have catalytic activity independent of the deposited metal catalyst. This occurs in so-called bi-functional catalysts where a reaction intermediate present on an active metal site reacts with another reaction intermediate present on the support surface. The reaction occurs at the metal/support interface.

A discussion of the physical properties of the four catalyst support materials used in this study is presented in the sections below. Included in each discussion is a brief review of the interactions of sulfur compounds on each catalyst support.

2.1.1 γ-Al_2O_3

Alumina (Al_2O_3) is the most commonly used catalyst support material. It exists in a large number of crystallographic structures with greatly varying surface area, pore size distribution, and surface acidity. The crystallographic form depends on the preparation method, purity, and thermal history. Of the many forms, γ-Al_2O_3 is the most common for use as a catalyst support. It is used in wide variety of catalyst applications because it possesses many of the important attributes of an ideal catalyst support including its inertness toward many catalytic reactions. (Although, in some instances it is used alone

as a catalyst; i.e. the Claus reaction and alcohol dehydration.) It also has many desirable physical characteristics that make it a successful commercial catalyst support including attrition resistance, hardness, and compressive strength. The gamma form of Al_2O_3 is stable at temperatures up to 500-600°C, which covers a useful temperature range for many catalytic reactions. This temperature stability can be increased however, by the addition of various trace components, such as La_2O_3. Additionally, γ-Al_2O_3 has a high surface area and the pore size distribution can be easily controlled by varying the preparation procedure. [2,9]

The surface of γ-Al_2O_3 is characterized by varying amounts of surface –OH groups depending on the preparation conditions and reaction environment. Heating γ-Al_2O_3 causes the surface –OH groups to react and form water, leaving behind surface oxides as well as exposed Al atoms. γ-Al_2O_3 is known to be weakly acidic and contains both Bronsted and Lewis acid sites resulting from surface -OH groups and Al metal atoms, respectively. [9]

A review of pertinent literature allows several observations and conclusions to be made regarding the activity of sulfur compounds on γ-Al_2O_3. Most notable, is the formation of surface sulfate even in the absence of a metal catalyst such as Pt. The formation of sulfate by oxidation of SO_2 was observed on γ-Al_2O_3 both in the presence and the absence of gas phase O_2 at temperatures $\geq$ 400°C. Deo et al. [10] observed the formation of a chemisorbed "sulfate-like species" when room temperature-adsorbed SO_2 was heated to 400°C in the absence of O_2. The "sulfate-like species" was identified based on the formation of two broad IR transmission bands at 1375 and 1110 cm^{-1}. Chang [11] found that treating γ-Al_2O_3 with a mixture of 7 torr SO_2 and 7 torr O_2 at temperatures

greater than 400°C resulted in the formation of two broad and intense IR peaks at 1400 and 1100 cm^{-1} which were attributed to the formation of aluminum sulfate. Chang also showed that the room temperature adsorption of SO_3 on γ-Al_2O_3 resulted in the same broad IR bands characteristic of aluminum sulfate formation. Okamoto et al. [12] found that the adsorption of H_2S at room temperature on γ-Al_2O_3 followed by treatment with O_2 at 500°C resulted in the appearance of an IR band at 1380 cm^{-1}, which the authors attributed to the formation of surface sulfate anions.

It can be concluded from these reports that sulfur compounds (H_2S and SO_2) are readily oxidized on γ-Al_2O_3 to form aluminum sulfate and/or adsorbed sulfate anions when O_2 is present at temperatures $\geq$ 400°C. Although sulfate formation is observed in the absence of Pt or any other catalytic metal, it is expected to occur to a much greater extent on Pt/ γ-Al_2O_3 catalysts. Pt is an effective catalyst for the oxidation of H_2S to SO_2 and SO_3 and, since SO_3 has been shown by Chang [11] to readily react with γ-Al_2O_3 to form aluminum sulfate, the formation of sulfate on Pt/γ-Al_2O_3 catalysts is expected to occur by spillover of oxidized SO_3 on active Pt sites to the support with subsequent reaction on the γ-Al_2O_3 surface. This process is important because it results in the formation of sulfate sites on the γ-Al_2O_3 support that are in close proximity to the active Pt sites and leads to the formation of active catalytic sites at the Pt/support interface.

2.1.2 TiO_2

TiO_2 occurs in three natural crystallographic forms with the anatase form being the most commonly used in catalysis because of its higher surface area. This structure is stable

below 500°C. TiO_2 is more acidic than γ-Al_2O_3 and is reported to be less susceptible to sulfate formation than γ-Al_2O_3. [2,9]

Recent research has been conducted by Yi et al. [13] comparing the adsorption and reactivity of H_2S and SO_2 on TiO_2 and Al_2O_3. It had been suggested previously that TiO_2 is a more active Claus catalyst than γ-Al_2O_3 due to the fact that TiO_2 is less susceptible to sulfate formation. The authors found that both TiO_2 and Al_2O_3 were deactivated for the hydrolysis of CS_2 reaction following a pre-sulfation treatment with a mixture of SO_2 and air at 450°C. Over time, however, TiO_2 recovered much of its original activity while Al_2O_3 did not. This led the authors to conclude that sulfate formed on a TiO_2 surface is unstable and that surface activity can be recovered under reaction conditions while a sulfated Al_2O_3 surface cannot be easily regenerated. These results indicate that the formation of surface sulfate should be less extensive on Pt/TiO_2 catalysts than Pt/ γ-Al_2O_3.

Additional work performed by Yi et al. [13] showed that the adsorption of sulfur compounds (H_2S and SO_2) on TiO_2 has a strong effect on the conductivity of the surface as determined by temperature-programmed electronic conductivity experiments. The same effect was not observed on Al_2O_3. This conductivity effect was expected since TiO_2 is an n-type semiconductor and it has important implications for the effects of sulfur compounds on Pt/TiO_2 catalysts. It seems to indicate that electronic effects on Pt particles due to adsorbed sulfur compounds on the support may be more likely to occur on Pt/TiO_2 than for Pt supported on other materials. A discussion of the electronic effects of sulfur compounds on Pt catalysts is presented in section 2.2.2.

2.1.3 ZrO_2

ZrO_2 is stable at high temperatures but its use as a catalyst support is limited as a result of its considerable expense relative to more commonly used supports [9]. It is commonly sulfated to form a ZrO_2-SO_4^{2-} solid superacid catalyst with is active for a variety of acid-catalyzed hydrocarbon conversion reactions [14]. Sulfate groups apparently result in additional Bronsted acid sites, which serve as active catalytic sites for certain reactions.

2.1.4 SiO_2

SiO_2 is characterized as having an extremely large surface area. It is, in general, less mechanically stable than γ-Al_2O_3 but more inert to many reactants. SiO_2 is reported to be unreactive towards sulfur compounds and is slightly acidic due to the presence of surface hydroxyl groups. [2,9]

2.2 Effects of Sulfur on Pt Catalysts

A review of the catalysis literature reveals the existence of several major mechanisms that are employed to describe the effects of sulfur compounds on supported Pt catalysts. Some of these mechanisms are well established and generally accepted to be true, while others require additional experimental evidence to prove their validity. A brief description is presented below for each mechanism that is believed to be important and relevant to the sulfur poisoning conditions and oxidation reactions investigated in this study. Each one of the mechanisms listed below is not taken directly from a single reference but, rather, is a summary of ideas presented in numerous reports in the catalysis

literature. More detailed discussions of each mechanism, including specific references, are presented in the ensuing sections.

1) The reactions of sulfur gases on Pt metal surfaces followed by subsequent reactions on the support surface can cause Pt particles to restructure from predominantly (111) crystal planes to (100) crystal planes. The change in crystal structure is accompanied by a change in Pt activity. The result is that certain reactions may be enhanced on (100) surfaces while others are deactivated. Still other reactions may not be affected at all.
2) The presence of sulfur compounds or sulfate ions on the catalyst support or on the Pt surface can effect changes in the electronic properties of Pt particles, which can alter the activity of Pt catalytic sites. Sulfur compounds and anions act as electron acceptors, which can withdraw electron density from the Pt particles and, consequently, affect the activity of Pt sites. These electronic effects are proposed to inhibit or enhance a variety of chemisorption, dissociation, and reaction processes.
3) The formation of sulfate compounds and anions on the catalyst support and/or at the Pt/support interface may result in the creation of new active sites for certain reactions. In some cases, this can create a so-called bi-functional catalyst on which an adsorbed intermediate on the Pt surface can react at the Pt/support interface with an adsorbed intermediate on the sulfated support. Although sulfate may create active sites on the support for some reactions, it can also block active sites for others.
4) Reactions of sulfur compounds on Pt can also lead to the formation of oxidized sulfur compounds and anions on Pt metal sites. This results in the formation of new active catalytic sites for certain reactions as described in the mechanism above. However, it

also results in the blocking of active Pt sites, which is expected to inhibit reactions that take place on bare Pt metal sites.

5) The reaction of sulfur compounds on supported Pt catalysts can cause the reduction and agglomeration of Pt metal crystals forming larger Pt particles. An increase in particle size can result in enhancement or deactivation of various catalytic reactions. Other reactions may be unaffected by changes in particle size.
6) Reactions of sulfur compounds with the support material to form support-sulfate compounds can result in the blockage of the support pore network. Pore blockage can also occur as a result of thermally induced sintering of the support material. The pores of Pt catalyst supports contain a considerable amount of deposited Pt particles, and substantial deactivation in reactivity can occur as a result of pore blockage.

2.2.1 Restructuring of Pt Crystal Surfaces From a (111) Orientation to (100)

Many researchers have observed the rearrangement of the surface structure of Pt crystals following interaction with sulfur compounds. In fact, these observations have not been limited to Pt or sulfur compounds only. Other metal surfaces are structurally altered by the presence of adsorbed species. For example, Ni(111) and Cr(110) surfaces have both been observed to undergo rearrangement of the surface structure to a 100 crystal plane orientation when adsorbed sulfur compounds are present.[15] The restructuring of Ni(111) to Ni (100) was also observed in the presence of C_2H_4 or benzene.[15]

Many of the experiments in which these phenomena have been observed were conducted on single crystal surfaces under ultra high vacuum conditions, which are definitely not conditions characteristic of real catalyst systems. Consequently, there is

much debate in the literature over the applicability of such results to real systems. Nevertheless, many researchers have attributed changes in Pt reactivity to structural modifications of the metal surface, so it is still important to consider these results when studying the effects of sulfur compounds on supported Pt catalysts.

Early work on the subject of Pt crystal surface restructuring was conducted by Schmidt and Luss [16] who studied Pt-10 % Rh gauze catalysts used for HCN production from NH_3, CH_4, and air. They found that, upon addition of 100 ppm H_2S to the reaction mixture, a 4 % increase in reaction yield was obtained. Electron microscopy results revealed that this activity increase was accompanied by considerable faceting (reorientation of the crystal surface structure) of the catalyst. The H_2S-poisoned surface exposed predominantly 100 crystal planes, whereas the original catalyst exposed mainly 111 planes. The authors concluded that the surface energy of the 100 plane is most likely lower than that of other crystal planes in the presence of sulfur compounds.

A mechanism for an adsorbed surface impurity-induced crystal surface reorientation was proposed by Somorjai [15] in an important commentary and is summarized here. Somorjai suggested that the surface rearrangement is due to rapid diffusion of surface metal atoms induced by an adsorbed impurity. Specifically, the adsorbed impurity lowers the surface energy of one crystal plane relative to the orientation exhibited by the clean metal surface. Generally, the lowest free energy corresponds to the surface structure with the highest atomic density. For platinum and other face-centered cubic crystals, the (111) plane has the highest atomic density. According to Somorjai, the adsorption of sulfur on Pt crystals lowers the surface free

energy of the (100) plane so that it is favored over the (111) structure. Thus, sulfur promotes the recrystallization of Pt crystals from (111) surfaces to (100) surfaces.

Using this model, reactions that are inhibited (or enhanced) by sulfur poisoning are said to be "structure-sensitive" while reactions unaffected by sulfur are referred to as "structure-insensitive". Several researchers have suggested that the promotion of propane oxidation on sulfur-poisoned Pt catalysts occurs because the propane oxidation reaction is favored on the (100) Pt surface. Although this may be true, it is important to recognize that practical Pt catalysts do not exist as single crystal surfaces and, generally, expose a combination of various crystal surface orientations. Therefore, the applicability of single crystal studies to observed effects on practical catalysts is not clear.

Additionally, sulfur poisoning of supported Pt catalysts such as $Pt/\gamma\text{-}Al_2O_3$, is expected to result in the presence of sulfur compounds and anions primarily on the support surface. It is uncertain whether support surface-adsorbed sulfur can have a long-range effect on Pt crystal structure. Although it is possible, however, that sulfur can effect changes in the Pt crystal structure of supported Pt catalysts during the short period of time in which sulfur compounds adsorb and oxidize on Pt before the resulting sulfur compounds spillover to the support surface.

One of the few studies showing Pt crystal surface restructuring due to sulfur poisoning of supported Pt catalysts was performed by P.J.F. Harris [17] who used transmission electron microscopy to show that sulfur adsorption can change the surface morphology of Pt/Al_2O_3 catalysts. In these experiments, the Pt crystals, which initially appeared as well-rounded or rounded octahedral crystals characteristic of 111 faceting, restructured in the presence of H_2S to form crystals exposing mainly square profiles

indicative of (100) faceting. Sulfur adsorption was carried out using a mixture of 100 ppm H_2S in H_2 at 400°C and this study was the first case where sulfur-induced faceting was observed for Pt/Al_2O_3 catalysts. However, one drawback to this study was the fact that the Pt/Al_2O_3 catalysts were heated in air at 700°C to increase the particle size to 113 Å prior to sulfur adsorption experiments. Larger particle sizes were necessary to observe the changes in catalyst morphology given the available instrumentation. The small particles typical of highly dispersed supported Pt catalysts (generally, $\leq$ 50 Å) would not necessarily behave in exactly the same manner. Normally, as particle size increases, the physical, chemical, and electronic properties approach that of bulk Pt metal.

2.2.2 Electronic Perturbations of Pt Crystals Due to Sulfur Deposition

In a review article, J. Oudar [6] noted that the adsorption of sulfur compounds on metal catalysts can cause modifications in both the structural ***and*** electronic properties of the metal and that the observed effects of sulfur poisoning on metal catalysts are not simply related to the blockage of active sites. In a review of various studies of model catalytic reactions on single crystals, Oudar concluded that sulfur could change the reactivity of a metal surface by weakening the electronic density of the surface as a result of sulfur's electronegative character.

Again, it is necessary to note that many of these studies involved single metal crystal surfaces investigated at very low pressures and are not representative of practical catalyst systems. It is certainly not clear that sulfur compounds adsorbed on a catalyst support can have the same electronic effect as sulfur adsorbed directly on an active metal

site. Oudar [6] states that, "the transposition of the results obtained on single crystals and under low pressures in the case of technical and supported catalysts which operate under atmospheric pressure or under high pressures raises certain reservations."

2.2.2.1 Theoretical Predictions In a theoretical study of the effects of adsorbed impurities on Pt, Ruckenstein et al. [18] claim that the structural changes described by Somorjai do not always explain experimental facts. Although calculations and experiments have shown that adsorbed contaminants with electron-withdrawing properties such as S and Cl can induce the restructuring of Pt from (111) to (100) crystal planes due to the weakening of the bond strength between Pt atoms, Ruckenstein et al. believe that adsorbed impurities can have electronic effects independent of structural modifications that may or may not occur. This is supported by their extended Huckel method calculations describing the effects of S and Cu on the oxidation of C_2H_4 and CO over Pt/Al_2O_3 catalysts.

Ruckenstein et al. [18] performed calculations on model Pt clusters consisting of either 10 Pt atoms in the (111) orientation or 9 Pt atoms in the (100) orientation. Both clusters yielded similar results when one Cu or S atom was adsorbed to a single Pt atom in the cluster. The following conclusions were made:

- Adsorbed S atoms decreased the electron density of the cluster or, in other words, yielded more positively charged Pt atoms.
- Adsorbed Cu atoms had the opposite effect although the effect of S was considerably stronger.

- Adsorbed S atoms inhibit the dissociative chemisorption of O_2 on Pt by inhibiting the electron transfer from Pt to the π^* antibonding molecular orbitals of O_2.
- Cu atoms have the opposite effect. The dissociative chemisorption of O_2 is enhanced through improved electron transfer from Pt to the π^* antibonding molecular orbitals of O_2 and a weakening of the O-O bond.
- Electron density changes due to adsorbed Cu are limited to the Pt atom on which Cu is adsorbed and its nearest neighbors only.
- In addition to localized effects on atomic charge density, adsorbed S atoms caused a significant decrease in the bond population of the entire cluster.
- Based on the charge transfer effects calculated for O_2 activity, adsorbed S is also expected to inhibit the dissociative chemisorption of CO while Cu adsorption is expected to have an enhancement effect for CO activity on Pt clusters.

Ruckenstein's [18] observations have several implications for Pt catalyst activity. Due to the combined effects on CO and O_2 chemisorption, adsorbed S would be expected to deactivate Pt for CO oxidation. On the other hand, adsorbed Cu would be expected to enhance the oxidation of CO on Pt. Additionally, the oxidation of C_2H_4 on Pt is expected to be inhibited by the presence of adsorbed S if the reaction occurs through the interaction between dissociatively adsorbed O_2 and gas-phase C_2H_4. Each of these observations is consistent with laboratory results.

Kummer [19] found that Cu treatment of a pre-reduced Pt/Al_2O_3 catalyst yielded significant increases in activity for both CO and ethylene oxidation compared to the copper-free catalyst, while the presence of sulfur in the feedstream caused a significant decrease in activity for CO and ethylene oxidation. It was also observed that Cu addition

could only partly negate the effects of sulfur indicating that the effects of adsorbed S are stronger than that of Cu.

Yates et al. [20] observed a strong reduction in the CO adsorption capacity of a single Pt (111) crystal due to the adsorption of sulfur. This adsorption inhibition was attributed to a combination of the physical blocking of active Pt sites by sulfur and a perturbation in next-nearest neighbor Pt sites causing a reduction in the adsorption rate and a decrease in the adsorption binding energy.

In section 2.2.1, several uncertainties were discussed regarding the applicability of surface structure reorientation studies conducted on single Pt crystal surfaces to practical supported Pt catalysts. Similar objections can be raised when discussing the electronic effects of adsorbed sulfur on Pt catalysts. First, the effects of a sulfur atom or compound adsorbed on a Pt site may be extremely localized and the effects on overall catalyst activity may be minimal. Although Ruckenstein et al. [18] calculated a decrease in the bond population over a entire 10 atom Pt cluster resulting from one adsorbed S atom, other investigators have predicted electronic effects to be limited to nearest neighbor Pt atoms. Secondly, it is doubtful that adsorbed sulfur compounds located on a Pt catalyst support material could have long range electronic effects on deposited Pt particles.

Feibelman and Hamann [21] studied the distance dependence of adsorbed sulfur on transition metal properties and suggested that sulfur-induced changes in reactant sticking probability, coverage, and activity on transition metal surfaces is, in fact, a result of perturbations in the electronic properties over distances exceeding nearest neighbor metal sites. Using surface linearized-augmented-plane-wave calculations of electronic

perturbations caused by S adsorbed on a Rh (001) surface, they found that the charge transfer effects described by Ruckenstein et al. [18] are only applicable at a distance not exceeding that of the neighboring metal atom. There is a "screening" effect that limits the charge transfer effects of adsorbed S to a localized environment. However, it was also found that adsorbed S causes a reduction in the Fermi-level local density of states (LDOS), which extends significantly beyond the distance of the nearest neighbor Rh atom.

Wimmer et al. [22] suggested that calculations based on Pt clusters have the disadvantage of a poor accounting for the metallic nature of the catalysts. Consequently, studies such as those of Ruckenstein et. al. [18], do not effectively explain long-range electrostatic effects. Wimmer et al. used an all-electron full-potential linearized-augmented-plane-wave calculation method to determine the effects of pre-adsorbed K or S on the co-adsorption of CO on a Ni(001) surface. Calculations confirmed earlier reports and showed that pre-adsorbed K, an electron donor like Cu, enhances the dissociative chemisorption of CO on Ni through electrostatic interactions resulting in a shift of the molecular energy levels to a larger binding energy and a larger population of the antibonding $2\pi^*$ molecular orbital levels. As the $2\pi^*$ antibonding orbital of CO is filled the C-O bond is destabilized and, as a result, dissociation is favored. The poisoning effect of adsorbed S was found to be more complex involving covalent bonding between S and Ni, a small transfer of electronic charge from Ni to S, and a direct interaction between adsorbed S and CO molecules. These effects cause the Ni surface to be deactivated for the dissociative chemisorption of CO. The authors conclude that

promoting and poisoning effects of catalyst additives such as K and S are complex in nature and that classification into long-range and localized effects may be meaningless.

2.2.2.2 Laboratory Experiments In one of the few laboratory studies presenting evidence of electronic effects due to adsorbed sulfur, Apesteguia et al. [23] used infrared spectroscopy to determine the effects of pre-adsorbed sulfur on the adsorption of CO on a Pt/Al_2O_3-Cl catalyst. The frequency shift of adsorbed CO was used to evaluate the S-Pt interaction following the treatment of the catalysts with a mixture of 0.1 % H_2S/H_2 at 773 K followed by treatment with H_2 for 8 hrs. at 773 K. Experiments showed a decrease in the CO adsorption band intensity and a positive 15 cm^{-1} shift in band frequency for CO adsorbed on sulfur-treated Pt when compared to CO adsorption on a clean Pt surface. Shifts in CO absorption frequency can be caused by electronic or geometric changes effected by adsorbed compounds on the catalyst. An adsorbate such as sulfur, which acts as an electron acceptor, would be expected to increase the vibration frequency. This is because the electron acceptor (S) decreases the back-donation of electrons from the metal to the $2\pi^*$ antibonding orbitals of adsorbed CO resulting in a strengthening of the C=O bond and a decrease in the force constant of the Pt-C bond.

Additional experiments showed that decreasing the coverage of CO on the sulfur-treated Pt catalyst causes the original IR peak attributable to CO stretching vibrations to split into two smaller peaks [23]. Apesteguia et al. identify the resulting peaks as the vibrations of CO molecules adsorbed on Pt sites with S adsorbed on the same site or on a neighboring site and CO molecules adsorbed some distance away from any adsorbed S

atoms. The authors conclude from these experiments that sulfur does alter the electronic properties of Pt catalysts but that these effects are extremely localized.

Apesteguia et al. [23] confirmed the occurrence of electronic effects by measuring the competitive adsorption of benzene and toluene on a sulfur-poisoned Pt/Al_2O_3-Cl catalyst. Toluene is a better electron donor than benzene and, since sulfur is expected to increase the electrophilic character of the Pt sites, it is expected that toluene adsorption would be favored. Experiments showed that the ratio of toluene adsorbed to benzene adsorbed was indeed higher on the sulfided catalyst than on the non-sulfided catalyst.

2.2.3 Formation of Sulfate on Pt Particles

The formation of sulfate on Pt catalyst support materials has been proposed by many researchers to be responsible for a wide range of catalytic effects due to sulfur poisoning, including both deactivation and promotion of certain reactions. This effect is discussed in further detail in section 2.2.4. However, an additional effect of sulfur poisoning was recognized by Lambert et al. [7], who showed that adsorbed sulfur compounds on Pt surfaces can promote the oxidation of alkanes without any contribution from a support material. The activity enhancement was attributed to the formation of an SO_x compound on the Pt surface, which was determined in subsequent experiments to be sulfate.

Specifically, Lambert et al. [7] found that the chemisorption of SO_2 on an O_2 pre-covered Pt (111) surface yielded a surface which was active for the dissociative chemisorption of C_3H_8 under ultra high vacuum (UHV) conditions. This leads to enhanced C_3H_8 oxidation since the usual rate-limiting step in catalytic hydrocarbon conversions is proposed to involve H atom abstraction by the catalytic surface.

Dissociative chemisorption of C_3H_8 was observed only on a Pt (111) surface that had been pre-adsorbed with O_2 followed by SO_2. No C_3H_8 adsorption was found on a clean Pt (111) surface or on a Pt (111) surface pre-adsorbed with SO_2 only. Reversing the adsorption steps (i.e., adsorption of SO_2 followed by O_2) also did not yield a surface active for C_3H_8 adsorption. Additionally, the enhanced C_3H_8 chemisorption was observed when O_2 and SO_2 adsorption was conducted at 300 K but was not observed at 160 K. Lambert et al. [7] suggested the following mechanism to account for the enhanced activity:

1) Propane reacts with an adsorbed sulfur complex by hydrogen atom abstraction.

$$SO_x + C_3H_8 \longrightarrow C_3H_y + HSO_x$$

2) At higher temperatures, C-C bond cleavage occurs, which yields CH_x fragments that are further oxidized to H_2O, CO, and CO_2

3) CO forms a surface complex with sulfur compounds and dissociatively desorbs.

$$CO\text{-}SO_{x(a)} \longrightarrow CO_2 + SO_2 + (x\text{-}2)O_a$$

Subsequent HREELS and XPS experiments by Lambert et al. [24] identified the chemisorbed sulfur complex responsible for enhanced C_3H_8 activity as chemisorbed SO_4 bound to Pt in a bi-dentate geometry through two O atoms. This structure was observed to form when SO_2 was adsorbed on an O_2 pre-adsorbed Pt (111) surface under UHV conditions and temperatures higher than 250 K. HREELS experiments also confirmed that the abstraction of a H atom to form a surface $H\text{-}SO_4^-$ complex is the initiation step for C_3H_8 oxidation. Additionally, Lambert et al. [24] found that CH_4 and C_2H_6 do not show similar activation due to the presence of stronger C-H bonds and it is assumed that the initial H atom abstraction occurs on the secondary C atom in C_3H_8.

2.2.4 Formation of Sulfate on the Support Surface and/or on the Pt/Support Interface

Treatment of supported Pt catalysts with sulfur compounds (H_2S, SO_2, and SO_3) is well known to result in the formation of sulfate on certain types of catalyst supports when the treatment is carried out in an oxidizing environment at sufficiently high temperatures ($\sim \geq 400^{\circ}C$). If sulfate formation occurs as proposed, by the spillover of SO_3 to the support surface followed by subsequent oxidation to SO_4^{2-}, then it is likely that the sulfate groups occur at the Pt/support interface.

The formation of sulfate on the catalyst support can have a number of effects on catalyst reactivity. One of the earliest observed effects of sulfate formation on Pt catalysts was the blockage of pores on the support surface. Thus, sulfate formation can inhibit various catalytic reactions by preventing or inhibiting the diffusion of reactant gases into the pores of the support where many active Pt sites are located. (This topic will be discussed in more detail in section 2.2.6.) Additionally, the formation of sulfate on the support can enhance certain reactions by providing additional or new active adsorption or reaction sites. A third effect of sulfate formation on the catalyst support is the possible perturbation of the electronic properties of active Pt metal sites. Although several researchers have proposed that electronic interactions are responsible for their observed experimental results, there is little conclusive evidence available in the catalyst literature proving that these effects do occur on supported Pt catalysts. As discussed in section 2.2.2, electronic effects are more likely to occur due to sulfur compounds adsorbed directly on Pt metal sites but, even in this case, the effects may be extremely localized.

The hydrocarbon oxidation activity of a Pt-Rh/CeO_2-Al_2O_3 three-way catalyst was investigated by Golunski et al. [5] for reducing and oxidizing simulated exhaust-gas mixtures containing SO_2. For a reducing simulated fuel-rich exhaust gas mixture, the presence of 20 ppm SO_2 in the feedstream caused severe deactivation for CH_4 and C_3H_8 oxidation reactions. A comparable fuel-lean oxidizing gas mixture showed enhanced oxidation activity for C_3H_8 and a negligible effect for CH_4 oxidation when 20 ppm SO_2 was included in the feedstream.

Rich ageing of the Pt-Rh/CeO_2-Al_2O_3 catalyst (i.e., treatment of the catalyst in a reducing exhaust gas mixture including 20 ppm SO_2 at various temperatures) caused the CO chemisorption capacity of the catalyst to be severely reduced.[5] Golunski et al. attributed some of this decrease to thermally induced sintering (<2%) and sulfate formation (<55 %). The remainder of the decrease, according to the authors, was a result of the combined effects of site-blocking and adsorption inhibition. XPS studies of the rich-aged catalyst confirmed the presence of small amount of S^{2-}, but a majority of the sulfur present was in the form of S^{6+} (SO_4^{2-}).

Additional experiments by Golunski et al. [5] showed that a Rh-only catalyst was deactivated by SO_2 poisoning for alkane oxidation in rich conditions despite the fact that no S^{2-} species were observed to form on Rh. The authors concluded that the steam reforming reactions of CH_4 and C_3H_8, which are dominant under reducing conditions, were inhibited by the presence of sulfate on the support. It was postulated that hydrocarbon compounds adsorb on the Pt metal surface and react with surface hydroxyl groups on the support. Formation of sulfate on the support inhibits this interaction. Golunski et al. [5] also concluded that sulfate formation on the support results in the

enhancement of alkane activity under oxidizing conditions as a result of the modification of electronic properties of the Pt metal particles. However, no actual evidence of this effect was presented and it is more likely that sulfate formation results in the formation of new active sites for alkane adsorption, which may facilitate the oxidation reaction on the sulfated catalyst.

Burch et al. [25] investigated the effect of SO_2 poisoning on the activity of a 1 % Pt/Al_2O_3 catalyst for C_3H_8 oxidation. They reported that pre-treatment of the catalyst for 2 hrs. in a 36:1 O_2:SO_2 mixture (SO_2 conc. = 500ppm; O_2 conc. = 1.8 %; N_2 balance) at 500°C, resulted in significantly enhanced activity for C_3H_8 oxidation when compared to the fresh catalyst sample. Additionally, it was found that the sulfated catalyst exhibited a sharper light-off profile. Similar experiments performed on a 1 % Pt/SiO_2 catalyst showed no increase in catalytic activity following sulfur treatment and no effect was found by physically mixing γ-Al_2O_3 with the Pt/SiO_2 catalyst either. Calculations showed that sulfation of the Pt/Al_2O_3 sample results in an increase in the apparent activation energy for propane oxidation from 78 to 129 kJ/mol, but that this is more than compensated for by an increase in the pre-exponential factor by seven orders of magnitude. The authors point to these results as evidence for the formation of sites active for C-H bond activation.

Additional experiments by Burch et al. [25] on Pt/Al_2O_3 showed a large transient promotional effect and a smaller permanent promotional effect for C_3H_8 oxidation when pulses of SO_2 were added to the feedstream. Two mechanisms were proposed for these effects. First, it may be that the rapid oxidation of SO_2 to SO_3 on oxygen-covered Pt sites frees up some of the metal sites for the propane reaction resulting in a large temporary

enhancement effect. A second mechanism involves the formation of sulfate complexes at the Pt metal-support interface. The diffusion of SO_3 from Pt to the support results in a sulfate site at the metal-support interface that is highly active for the combustion reaction. Over time, the sulfate sites migrate to more stable adsorption sites on Al_2O_3 that are not as active.

Burch et al. [25] conclude by proposing a model for propane oxidation enhancement in which electronegative SO_4^{2-} anions form in close proximity to the edge of Pt particles. Electron density is withdrawn from the Pt particle creating a site active for C-H bond activation. Although a similar mechanism is proposed by Golunski et al. [5], neither group presents any experimental evidence proving that electronic effects are responsible for the observed results, and it seems more likely that the promotion effects on alkane oxidation activity resulting from sulfate formation on Pt catalysts involves the formation of new active sites on the support and at the Pt/support interface.

In one of the few studies completed on the effects of sulfur poisoning of Pt/TiO_2 catalysts, Burch et al. [26] examined the activity of an SO_2-poisoned 1% Pt/TiO_2 catalyst for CO and propane oxidation. Following poisoning by 0.05 % SO_2 in air at 300°C for 30 min., it was found that the catalysts were severely deactivated for CO oxidation and promoted significantly for C_3H_8 oxidation. It was assumed that the mechanism for promotion of C_3H_8 oxidation was similar to that proposed by other researchers for Pt/Al_2O_3, involving the formation of sulfate at the metal-support interface which enhances C-H bond activation in C_3H_8. Although it was not discussed by Burch et al., the concept of electronic interactions between sulfate formed on the support and Pt particles seem to be more plausible on Pt/TiO_2 considering its properties as an n-type

semiconductor. Still, there is little information in the literature regarding electronic effects of sulfur compounds adsorbed on Pt/TiO_2 catalysts.

In a follow-up study to their work on Pt (111) surfaces (see section 2.2.3), Lambert et al. [27] conducted experiments on a Pt (111) surface on which an AlO_x film had been deposited. Since previous reports had shown that C_3H_8 oxidation was promoted on Pt/Al_2O_3 by SO_2 treatment and, that no effect of SO_2 was found on either Pt/ZrO_2 or Pt/SiO_2, the effect of Al_2O_3 on activity promotion was investigated. Experiments showed an even greater enhancement for propane oxidation on $AlO_x/Pt(111)$ following O_2 and SO_2 adsorption than that observed for a similarly treated Pt (111) surface. The increased activity is suggested to be a result of an AlO_x-induced stabilization of an adsorbed SO_4 complex, yielding a bi-functional catalyst. Subsequent experiments by Lambert et al. [28] showed that annealing the AlO_x film at 1100 K resulted in the formation of crystalline γ-Al_2O_3. CO chemisorption studies indicated that γ-Al_2O_3 multi-layers were present as islands on the Pt (111) surface.

The experiments by Lambert et al. [24] on Pt (111) surfaces, discussed in section 2.2.3, showed that chemisorbed SO_4 was the activating species responsible for the promotion of C_3H_8 oxidation. However, XPS experiments showed that the stability of SO_4 on Pt (111) is less than that on Al_2O_3 [28]. In their experiments on γ-$Al_2O_3/Pt(111)$, Lambert et al. [28] observed the formation of $Al_2(SO_4)_3$ after adsorption of O_2 and SO_2 on the catalyst surface. Therefore, they found that the presence of Al_2O_3 on Pt (111) increases the total SO_4 coverage and concluded that $Al_2(SO_4)_3$ provides additional adsorption sites for C_3H_8, which can react at the Pt-Al_2O_3 interface. The formation of $Al_2(SO_4)_3$ results in a bi-functional catalyst on which propane is dissociatively

chemisorbed on sulfated-Al_2O_3, and O_2 is dissociatively chemisorbed on bare Pt sites. Subsequent reaction between the two adsorbed species occurs at the Pt-Al_2O_3 interface [28].

The experiments by Lambert et al. [24,27,28] described above were conducted under UHV conditions on model Pt (111) single crystal surfaces. In an attempt to determine the relevance of these experiments to practical highly dispersed catalyst systems, Lambert et al. [29] continued their studies on several Pt/Al_2O_3 catalysts with Pt metal loadings of 0.05, 3 and 9 % by weight. A combination of XRD, TEM, and BET studies determined that SO_2 poisoning resulted in Pt sintering as well as the formation of aluminum sulfate. Poisoning was carried out by treatment of Pt/Al_2O_3 catalysts with a 1:1 mixture of SO_2 and O_2 at 1 bar and 673 K. Additional experiments showed that, at low metal loadings, Pt exists mainly as oxidic particles (PtO_2), which are inefficient for C_3H_8 oxidation. Considering the results of experiments on Pt (111), Al_2O_3/Pt(111), and Pt/Al_2O_3, Lambert et al. [29] propose the following additive mechanisms to account for the sulfur-induced enhancement of C_3H_8 oxidation:

1) *Formation of aluminum sulfate* Experiments have shown that the formation of aluminum sulfate greatly enhances the dissociative chemisorption of propane and subsequent oxidation on Pt metal sites. Sulfate sites increase the presence of adsorbed hydrocarbon fragments resulting from hydrogen abstraction and therefore increases the oxidation activity of sulfated catalysts compared to fresh catalysts.
2) *Formation of surface sulfate at Pt metal sites.* Experiments have also shown the formation of chemisorbed sulfate on single crystal Pt (111) surfaces. On these surfaces, the dissociative chemisorption is enhanced compared to the clean Pt (111)

surface. The stability of sulfate species on metallic surfaces is much lower than on Al_2O_3 surfaces, however. (A discussion of this topic was presented in section 2.2.3.)

3) *Sulfate-induced reduction and sintering.* Experiments also show that SO_2 treatment of highly dispersed (low Pt loading) Pt/Al_2O_3 catalysts reduces platinum oxide particles to metallic Pt and causes Pt sintering. This results in the formation of larger metallic Pt particles on which C_3H_8 oxidation is favored. The larger particles provide active sites for both oxygen dissociation and heterolytic C-H bond scission. Pt sintering and crystal growth is discussed further in section 2.2.5.

The sulfate-induced promotion of alkane oxidation activity by enhanced C-H bond scission (H atom abstraction) involves a free-radical reaction mechanism. An alternative mechanism for the increased alkane activity resulting from sulfate formation involves the increase in catalyst acidity that accompanies sulfate formation. Lewis acid sites on the catalyst surface act as electron acceptors and can remove a hydride ion from a hydrocarbon, leading to the formation of carbocations on the catalyst surface. Carbocations are intermediates in reactions such as hydrocarbon cracking, polymerization, and isomerization and may also be intermediates in alkane oxidation reactions. Increased catalyst acidity would be expected to enhance carbocation formation and subsequent reaction with chemisorbed O_2.[9]

Trimm et al. [30] studied the activity of a 0.2 % Pt/Al_2O_3 catalyst for the oxidation of CH_4 and found that the addition of either 20 ppm H_2S or 20 ppm SO_2 to the reactant gas stream (1.8 % CH_4, 21 % O_2, He balance) resulted in a slight activity *increase* for CH_4 oxidation. However, this observation is contrary to many reports in the literature, including those of Golunksi et al. [5] and Wang [31], showing either a negligible effect or

a slight deactivation of CH_4 oxidation due to sulfur poisoning of Pt/Al_2O_3 catalysts. Trimm et al. suggest that the observed effects are a result of the increased catalyst acidity due to the formation of aluminum sulfate. However, changes in acidity do not entirely explain the sulfur-induced enhancement of hydrocarbon oxidation as shown by Burch et al. [25].

In order to determine whether increased surface acidity due to sulfation of Al_2O_3 is in fact responsible for the promotion of alkane oxidation, Burch et al. [25] conducted experiments in which Pt/Al_2O_3 was pretreated with CHF_3 at 500°C. Replacing surface OH^- groups with F^- would be expected to increase the surface acidity to a greater extent than sulfation would. The fluorination procedure did result in increased activity for C_3H_8 oxidation, but the activity increase was less than that observed for SO_2 treatment. Treating the fluorinated catalyst with SO_2 resulted in a further increase in activity but the activity increase was still not as great as that observed for SO_2 treatment only. These fluorination experiments show that the activity enhancement is not solely related to changes in catalyst acidity since fluorination did not increase the activity of the catalyst for C_3H_8 oxidation as much as sulfation did.

2.2.5 Pt Sintering & Crystal Growth

Pt crystal growth on supported catalysts occurs when small Pt crystals become mobilized on the support surface and coalesce with other Pt crystals to form larger Pt particles. This process can be thermally induced (sintering) or can be promoted by various compounds in a reactant feedstream such as sulfur compounds. Pt crystal growth yields larger Pt particle sizes which may exhibit altered activity for certain reactions when compared to

smaller Pt particles. Some reactions are inhibited on larger Pt particles while others are enhanced. For other reactions, there may be no observed effect on activity at all.

Lambert et al. [29], in experiments described in section 2.2.4, found that the sintering of Pt/Al_2O_3 catalysts caused by SO_2 poisoning resulted in the enhancement of the catalysts' activity for C_3H_8 oxidation. Their experiments determined that SO_2 treatment of highly dispersed Pt/Al_2O_3 catalysts causes a reduction of oxidic Pt particles and an associated sintering of Pt to form larger metallic Pt particles. These larger particles serve as active sites for both O_2 dissociation and heterolytic C-H bond scission. A mechanism was proposed by Lambert et al. [29] to account for the observed sulfur-induced reduction and sintering. When a surface that has been pre-adsorbed with O_2 is exposed to SO_2, a reaction occurs between SO_2 and weakly bound oxygen at the Pt-O-Al interface resulting in the formation of interfacial sulfate and the reduction of Pt. Additionally, the weakening of the Pt-O interaction promotes the migration and agglomeration of metallic Pt particles.

A similar enhancement effect of Pt sintering on hydrocarbon activity was observed in a recent study by Burch et al. [32]. It was observed that conversion activity for the NO_x/n-octane reaction was enhanced when a 1 % Pt/Al_2O_3 catalyst was sintered by treatment in a 5 % O_2/He mixture at 740°C.

2.2.6 Pore Blockage Due to Sulfur Poisoning

Pore blockage on supported Pt catalysts results in the inhibition of the diffusion of gaseous reactants to the active catalytic sites located in the pore network of the support material. There are several ways in which pore blockage can occur that are relevant to

this study including both sulfate formation and thermally-induced support sintering. The presence of SO_2 in automotive exhaust gases is well known to result in the formation of $Al_2(SO_4)_3$ on the γ-Al_2O_3 support surface of three-way catalysts (TWC's) [2]. $Al_2(SO_4)_3$ is a low-density material and its formation on the surface of γ-Al_2O_3 results in the partial occlusion of the γ-Al_2O_3 pore network. This causes deactivation of TWC's by preventing the interaction of reactants on active metal sites. Thermally induced sintering of the support occurs at high temperatures, which cause modifications of the support surface leading to the narrowing or complete blockage of pore openings [2]. The end result is the same as the effects of aluminum sulfate formation. Reactants are prevented from contacting the active catalytic sites in the occluded pores, thereby inhibiting catalytic activity.

CHAPTER 3

EXPERIMENTAL METHODS

3.1 Catalysts

Catalyst samples were prepared in powdered form by Engelhard Corp., Iselin, NJ. The catalysts consisted of platinum metal supported on various oxide supports with a constant metal loading of 1.5 % Pt by weight. Four different support materials were evaluated including γ-Al_2O_3, TiO_2, ZrO_2, and SiO_2. There were no special procedures followed in terms of catalyst storage. That is, catalyst samples were not stored in a dessicator, so, it is likely that the catalysts contained significant amounts of H_2O and other adsorbed gases on the surface. The catalysts were pre-treated in nitrogen at temperatures up to 600°C in order to remove these surface adsorbates prior to conducting many of the characterization studies. (More detailed descriptions of the experimental procedures are presented in the following sections.) However, the catalysts were used as received for activity and poisoning experiments; i.e., the catalysts were not pre-treated in any way prior to conducting activity or poisoning experiments.

The catalysts studied in these experiments were similar to those used in a wide variety of emission control technologies. Generally, the feedstreams in most of these applications contain significant amounts of water vapor and trace amounts of other gaseous compounds. Thus, activity and poisoning experiments were conducted on catalyst samples exposed to conditions similar to the conditions experienced by commercial catalysts. It was assumed that water vapor, both in the adsorbed form and in the gas phase, had little effect on the results of the activity and poisoning experiments

conducted during this study. However, this assumption may not be completely valid for sulfur-poisoning experiments and a discussion of this topic will be presented in Ch. 4, section 4.7.

3.2 Activity Experiments

Catalyst activity was determined for fresh and sulfur-poisoned catalysts by measuring the oxidation of CO or one of several light hydrocarbons in air to CO_2 and H_2O as a function of temperature. Increases and decreases in catalyst activity were observed as shifts in the activity curves to lower or higher temperatures, respectively.

Activity experiments were carried out individually with CO, CH_4, C_2H_6, C_2H_4, C_2H_2, C_3H_8, C_3H_6, and n-C_4H_{10}. Each gas was purchased from Matheson Corp. as a mixture in dry air and a concentration of approximately 1 %. GC analysis of each gas mixture revealed minimal carbon-containing decomposition products and the actual component concentrations were assumed to be equal to the concentrations analyzed by Matheson Corp. Specific concentrations and gas specifications are given in Appendix A. The experimental setup used to measure the activity of fresh and sulfur-poisoned Pt catalysts is shown in Figure 3.1. Reactions were carried out in a cylindrical quartz reactor supplied by Q-Glass Corp. The reactor measured 59.4 cm. in length with a 2.5 cm. i.d. (inner diameter) and was equipped with a course-fritted quartz disc located 32.4 cm. from the top of the reactor.

The quartz reactor was located inside an Applied Test Systems, Inc. Series 3210 clamshell-style 3-zone furnace. Two Omega type-K chromel alumel thermocouples were used to measure furnace and sample temperatures. One was located in the center of the

Figure 3.1: Experimental Setup

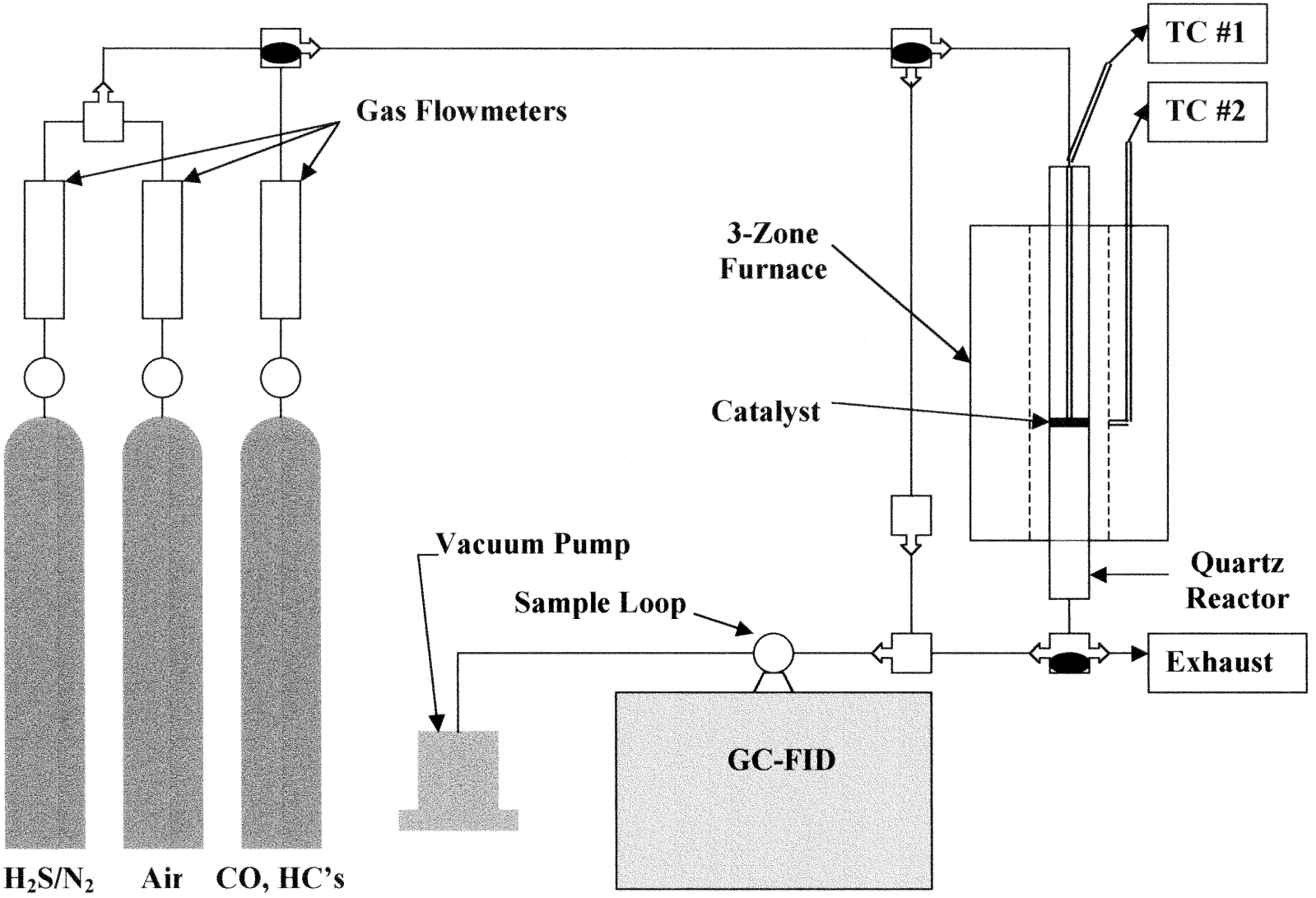

furnace while the second was located directly in the catalyst bed. Other components of the activity experiment setup shown in Figure 3.1 included a Cole-Palmer flowmeter, Parker three-way and two-way ball valves with 1/8" Swagelok fittings, 1/8" Swagelok stainless steel unions, 1/8" Swagelok stainless steel ferrules and nuts, 1/8" O.D. Parflex PP flexible tubing, and 1/8" O.D. stainless steel tubing.

In each activity experiment, 0.250 g ± 0.002 g of catalyst sample was physically mixed with 1.500 ± 0.002 g of γ-Al_2O_3 and loaded onto the fritted disc in the reactor. The γ-Al_2O_3, supplied by Engelhard Corp., was used as a diluent in order to minimize the amount of catalyst used while ensuring adequate contact time for the reactants. Also, the diluent served to absorb heat generated by the oxidation reactions, most of which are very exothermic, and enabled the reaction temperature to be easily controlled. To ensure that γ-Al_2O_3 did not contribute to the oxidation reactions being studied, activity experiments were performed using only γ-Al_2O_3. Results and a brief discussion on this topic are included in Ch 4, section 4.1.5.

For each activity experiment, the reactant gas flow rate was 250 cm^3/min. Constant amounts (0.250 g) of catalyst sample were used in each activity experiment, so that the total amount of Pt metal was the same in each experiment given that the Pt metal loading was 1.5 % on each support material. However, since the bulk density of each catalyst support was different, the experimental space velocities were different for each of the four supported Pt catalysts studied. Space velocity is defined as the actual volumetric flow rate of the reactant gases at the experimental temperature divided by the catalyst bed volume including void space. Since the flow rate in all activity experiments was 250 cm^3/min and the catalyst bed volumes were different for each support material,

the space velocities were also different. The measured bulk density and calculated space velocity for each catalyst are presented below in Table 3.1.

Table 3.1: Measured bulk density data and calculated space velocities for catalyst activity experiments

Catalyst	Bulk density (g/cm^3)	Space Velocity[a] (V/V/hr)[b]
1.5 % $Pt/\gamma\text{-}Al_2O_3$	0.920	55,200
1.5 % Pt/TiO_2	0.873	52,380
1.5 % Pt/ZrO_2	1.422	85,320
1.5 % Pt/SiO_2	0.250	15,000

Notes: a) Space velocity was calculated by dividing the volumetric flow rate (250 cm^3/min) by the catalyst bed volume; catalyst bed volume equals the catalyst mass (0.250 g) divided by the bulk density.
b) The flow rate (250 cm^3/min) was converted to an hourly rate to obtain the unit "V//V/hr" typically used to express space velocity data. "V" stands for a volume unit.

The products of the reaction were analyzed using a Hewlett-Packard HP 5890 Gas Chromatograph equipped with a flame ionization detector (GC-FID). Reaction samples were injected to the GC column using a Rheodyne 6-way gas sampling valve equipped with a 20 mm^3 sample loop. The column was a 2.4 m. stainless steel packed-column with Porapak Q 80-100 mesh packing purchased from Alltech. A nickel hydrogenation catalyst system was installed between the column outlet and the detector inlet in order to analyze CO and CO_2. After separation on the column, CO and CO_2 were hydrogenated to CH_4 and then analyzed by FID. A constant flow rate of 30 cm^3/min H_2 was maintained over the Ni catalyst. Other GC-FID operating conditions are shown below in Table 3.2. All analytical gases were purchased from Matheson Corp. and specifications are listed in Appendix A. Peak data was collected and analyzed using either an HP 3396A integrator or a Fisons Instruments VG Chromatography server interfaced with a personal computer running Minichrom v. 1.62 software.

Each activity experiment was conducted in the following manner. Reactor effluent was analyzed at room temperature first. Subsequent measurements were made as the temperature was increased stepwise until a conversion of approximately 100 % was obtained. Conversion of CO and hydrocarbons to CO_2 at each temperature was calculated as follows:

$$\text{Conversion } \% = 100 * \frac{(\text{Influent Conc.} - \text{Effluent Conc.})}{\text{Influent Conc.}} \qquad (3.1)$$

As shown in equation 3.1, conversion was calculated based on the disappearance of the reactant gas rather than the production of CO_2. CO_2 peaks were measured, however, to ensure that mass balance was maintained. In all experiments, the production of CO_2 closely matched that which would be expected given the complete oxidation of each carbon-containing compound. Product gas concentrations were determined by preparing calibration curves for each gas compound. A two-point linear calibration fitted through zero was used for CO, CH_4, and C_3H_8 while a one-point linear calibration fitted through zero was used for all other gases. Gas concentrations and specifications are given in Appendix A.

Table 3.2: GC-FID operating conditions

Carrier gas (He) flow rate:	35 cm^3/min
H_2 flow rate:	68 cm^3/min
Air flow rate:	415 cm^3/min
Injection Temperature:	350°C
Oven (Column) Temperature:	~25°C (for CO and CH_4 experiments) 45°C (for C_2H_6, C_2H_4, and C_2H_2 experiments) 100°C (for C_3H_8 and C_3H_6 experiments) 150°C (for C_4H_{10} experiments)
Detector Temperature:	250°C

3.3 Catalyst Poisoning Experiments

Catalyst poisoning was carried out using the experimental setup shown in Figure 3.1. In all experiments, 2.000 g ± 0.002 g of catalyst was weighed and placed into the quartz reactor (described previously). A 200 ppm mixture of H_2S in air with a flow rate of 250 cm^3/min. was obtained by mixing the appropriate amounts of an H_2S/N_2 mixture with air using two Aalborg flowmeters. Gas concentrations and specifications are given in Appendix A. Experimental space velocities are shown in Table 3.3.

Table 3.3: Calculated space velocities for catalyst poisoning experiments

Catalyst	Bulk density[a](g/cm^3)	Space Velocity[b] (V/V/hr.)[c]
1.5 % Pt/γ-Al_2O_3	0.920	6900
1.5 % Pt/TiO_2	0.873	6550
1.5 % Pt/ZrO_2	1.422	10,700
1.5 % Pt/SiO_2	0.250	1880

Notes: a) from Table 3.1
b) Space velocity was calculated by dividing the volumetric flow rate (250 cm^3/min) by the catalyst bed volume; catalyst bed volume equals the catalyst mass (2.000 g) divided by the bulk density.
c) The flow rate (250 cm^3/min) was converted to an hourly rate to obtain the unit "V//V/hr" typically used to express space velocity data. "V" stands for a volume unit.

All poisoning experiments were conducted in the following manner. The catalyst sample was heated in air from room temperature to 400°C over approximately 10 minutes. When the catalyst reached 400°C, the gas stream was switched from air to the 200 ppm H_2S/air mixture with a flow rate of 250 cm^3/min. The temperature and flow rate were maintained for 12 hrs., at which point, the H_2S/air mixture was turned off and the catalyst was allowed to cool overnight to room temperature in air. This procedure was repeated the following day for a total poisoning time of 24 hours. At the conclusion, the catalyst sample was removed from the reactor and stored in a glass jar.

A poisoning temperature of 400°C was chosen based on previous studies conducted by Wang who showed that sulfur was completely oxidized to SO_4^{2-} over a $Pt/\gamma\text{-}Al_2O_3$ catalyst at this temperature.[31] Many other studies have yielded similar results. In fact, it has been suggested that H_2S can, in the presence of excess O_2, completely react with an Al_2O_3 surface to form aluminum sulfate with or without Pt being present.[33] In a study of Claus catalysts, George noted that, for a mixture of SO_2 and O_2, maximum sulfation of alumina occurred at a temperature of 240°C.

3.4 H_2 Chemisorption Experiments

The selective chemisorption of hydrogen was used as a technique to determine the Pt metal dispersion on fresh and poisoned catalyst samples. Dispersion is defined as the ratio of exposed surface metal atoms to the total number of metal atoms present:

$$\%\,\text{Dispersion} = \frac{\#\ \text{of surface metal atoms}}{\text{total metal atoms}} * 100 \qquad (3.2)$$

The selective chemisorption technique requires several assumptions to be made. First, the stoichiometry of the chemisorption process must be known. In the case of Pt catalysts, each H_2 molecule dissociatively adsorbs on the exposed Pt atoms so that one hydrogen atom adsorbs to each exposed Pt metal atom for an overall H_2/Pt ratio of 0.5. Additionally, it is assumed that this stoichiometry does not change as the Pt particle size changes. Finally, the adsorbing gas (H_2) must adsorb only on Pt atoms and not on the catalyst support material.[2,34,35]

Several methods are available for performing chemisorption measurements. In this study, a dynamic technique was employed in which pulses of hydrogen gas were injected into an inert carrier gas stream (Argon) and passed through the catalyst sample. The amount of hydrogen gas adsorbed on the catalyst sample was calculated by comparing the inlet and outlet concentrations of hydrogen gas. This dynamic technique yields rapid chemisorption results. However, a disadvantage is that only strongly chemisorbed species are detected while weakly adsorbed species are not detected. Thus, dispersion results are often slightly lower than results obtained using static volumetric techniques.[2,36]

In this study, an Altamira AMI-1 catalyst characterization system was used to perform all H_2 chemisorption experiments. The AMI-I instrument is a computer-controlled system incorporating two electronic mass flow controllers, several three-way and six-way valves, a furnace, a U-shaped tubular quartz reactor, sample and furnace thermocouples, and a thermal conductivity detector all in one apparatus. It is capable of performing a variety of catalyst characterization experiments including pulse chemisorption, BET surface area, and a range of other temperature-programmed techniques.

In each H_2 chemisorption experiment, a 0.04-0.2 g catalyst sample was heated in 50 cm^3/min N_2 at 600°C for 2 hours. The catalyst was then cooled to 25°C in flowing N_2. Fifteen - 50 mm^3 H_2 pulses were injected into a 50 cm^3/min Ar stream, which passed through the catalyst sample. The breakthrough pulses, defined as the pulses in which no hydrogen was adsorbed, were used to calibrate the hydrogen peak areas. Dispersion data was calculated using all peaks smaller than the breakthrough peaks.

3.5 BET Surface Area

Overall surface area of the catalyst samples was measured using the Brunauer, Emmett, and Teller (BET) method.[37] In this method, the adsorption of nitrogen is measured as a function of partial pressure of nitrogen at liquid nitrogen temperature. By calculating the number of nitrogen molecules forming a monolayer on the catalyst surface, and assuming a cross-sectional area of 16 $Å^2$ for a nitrogen molecule, the surface area of the catalyst can be calculated. The relationship between the volume adsorbed at a given partial pressure and the volume adsorbed at monolayer coverage is given by the BET equation:

$$\frac{P}{V(P_o - P)} = \frac{1}{V_m C} + \frac{(C-1)P}{V_m C P_o} \qquad (3.3)$$

where

P = partial pressure of N_2
P_o = vapor pressure of N_2 at liquid N_2 temperature
V = volume adsorbed at P
V_m = volume of N_2 adsorbed at monolayer coverage
C = constant. (related to ΔH_{ads} and liquefaction of adsorbate)

The slope and intercept of a plot of

$$\frac{P}{V(P_o - P)} \text{ vs. } \frac{P}{P_o},$$

can be used to calculate V_m and the surface area in m^2/g.[2,37]

BET surface area measurements were conducted using the Altamira AMI-1 system described previously. A dynamic technique was employed in which the adsorption and desorption of various concentrations of N_2 were measured at liquid N_2 and ambient temperatures, respectively. N_2 concentrations were 10, 20, and 30 % in helium (See Appendix A for gas specifications) and the flow rate used in all experiments was

30 cm^3/min. Catalyst samples weighing approximately 0.05 g were loaded into a quartz tubular reactor and purged with N_2 for 30 min. prior to performing the BET experiment.

3.6 Diffuse Reflectance-FTIR Studies

Fresh and sulfur-poisoned catalysts were analyzed by diffuse reflectance FTIR spectroscopy for the presence of sulfur compounds on the catalyst surfaces. All experiments were performed using a Bio-Rad FTS-40 FTIR spectrometer and the resultant spectra were analyzed using Bio-Rad's WIN-IR software. The FTIR spectrometer was outfitted with a diffuse reflectance sampling apparatus that was installed in the sample compartment.

Diffuse reflectance is defined as radiation collected from the surface of a material that scatters or diffuses incident radiation. Unlike specular reflectance, diffuse reflectance is independent of the angle of incident radiation. The diffuse reflectance technique is useful for analyzing samples that have a low transmittance, are IR opaque, or highly scattering. An advantage of this method is that a solid sample can be directly analyzed and preparation of KBr discs is unnecessary. This technique has proven to be successful for the analysis of catalyst samples.[38]

The following procedure was performed for each catalyst sample. The diffuse reflectance apparatus contained four individual sample holders. The first was left empty and was used to record the single beam background spectrum. The second sample holder contained a fresh powdered catalyst sample while the third sample holder contained the corresponding sulfur-poisoned powdered catalyst sample. An absorbance spectrum was recorded for both catalyst samples. Using the WIN-IR software, the fresh catalyst

spectrum was subtracted from the sulfur-poisoned catalyst spectrum and the difference spectrum was further analyzed for the presence of sulfur compounds. Data collection parameters were the same for each experiment and are shown in Table 3.4.

Table 3.4: Diffuse reflectance-FTIR data collection parameters

# Scans:	64
Scan delay:	0 s
Speed:	5 kHz
Filter:	1.12 kHz
UDR:	2
Resolution:	4
Aperture:	2 cm^{-1}
Sensitivity:	1
Collection range:	4000-400 cm^{-1}

3.7 Temperature-Programmed Reduction Experiments

Temperature-programmed reduction experiments are typically carried out by measuring the amount of a reductant, usually hydrogen, which is taken up by a catalyst as a function of temperature. In this case, a mixture of 5 % H_2 in Argon was used as the reducing gas. Experiments were conducted on fresh and H_2S-poisoned catalysts.

The Altamira AMI-1 instrument was also used to conduct these experiments. Samples weighing 0.05-0.2 g were heated to 600°C and held at 600°C in 50 cm^3/min N_2 for 2 hours. This treatment step was conducted in order to provide a clean catalyst surface. After cooling to room temperature, the sample was heated at a rate of 20°C/min in 5 % H_2/Ar with a flow rate of 50 cm^3/min up to 600°C. Uptake of hydrogen by the catalyst samples was determined by passing the inlet and outlet gases through the

reference and sample cells of a thermal conductivity detector. Uptake of hydrogen by the catalyst sample was observed as an increase in the detector signal.

3.8 Temperature-Programmed Desorption Experiments

Temperature-programmed desorption (TPD) experiments, using C_3H_8 and CO as adsorbates, were conducted on fresh and sulfur-poisoned catalyst samples. These experiments yielded information regarding the number and strength of adsorption sites on the catalyst samples for each particular adsorbate. Since the adsorption of reactants on the catalyst surface is an important step in most heterogeneous catalytic reactions, TPD experiments can reveal effects of sulfur treatment by correlating changes in the number and strength of adsorption sites with changes in catalyst activity.

Experiments were conducted on fresh and sulfur-poisoned Pt catalysts on all four support materials. Adsorbing gases included mixtures of 1207 ppm C_3H_8 and 984 ppm CO in helium balance gas. (See Appendix A for gas specifications.) The desorption of each gas was measured in separate experiments.

Experiments were performed using the Altamira AMI-1 instrument and the following procedure. Catalyst samples weighing 0.04-0.2 g were heated at 600°C for 2 hrs. in 50 cm^3/min N_2 in order to remove any surface adsorbates. After cooling to the adsorption temperature, the catalyst sample was treated with the adsorbing gas mixture at a flow rate of 50 cm^3/min for 60 min. The adsorption temperature varied for each catalyst sample and adsorbate. Adsorption temperatures were chosen as the highest temperature at which no catalytic reactivity was observed for each catalyst sample and adsorbate as determined from the activity curves. Adsorption temperatures are shown in

Table 3.5. At the conclusion of the adsorption step, the catalyst sample was cooled to 25°C, flushed with 50 cm^3/min carrier gas, and heated in 50 cm^3/min of the carrier gas at a heating rate of 20°C/min up to 600°C. The carrier gas was argon for CO experiments and N_2 for C_3H_8 TPD experiments. TCD signal versus time plots yielded desorption peaks at various temperatures.

Table 3.5: Adsorption temperatures for CO and C_3H_8 mixtures on Pt catalysts. All temperatures are reported in °C.

Catalyst	984 ppm CO/He	1207 ppm C_3H_8/He
1.5 % Pt/γ-Al_2O_3	50	100
1.5 % Pt/TiO_2	50	150
1.5 % Pt/ZrO_2	75	150
1.5 % Pt/SiO_2	50	150

3.9 Dry Poisoning Studies

Experiments were conducted to determine the effect of water vapor on catalyst poisoning and subsequent oxidation activity. The catalysts (1.5 % Pt/γ-Al_2O_3 and 1.5 % Pt/SiO_2) were dried by heating a 2.000 ± 0.002 g sample in 250 cm^3/min N_2 at a temperature of 400°C for 2 hrs. using the experimental apparatus shown in Figure 3.1. After 2 hrs., the gas flow was switched to a mixture of 200 ppm SO_2 in air at 250 cm^3/min. After 12 hrs. of SO_2-treament at 400°C, the catalyst was allowed to cool to room temperature in flowing air overnight. On the following day, the catalyst was heated in air to 400°C, at which point the mixture of 200 ppm SO_2 in air was turned on. The poisoning gas was once again maintained for 12 hrs. At this point, the catalyst was cooled to room temperature in flowing air, transferred to a glass jar, and stored in a dessicator for future experiments.

Catalyst activity experiments were conducted on SO_2-poisoned Pt/γ-Al_2O_3 and Pt/SiO_2 for CO, CH_4, and C_4H_{10} oxidation. Experimental procedures for these activity experiments were identical to those described above in section 3.2.

CHAPTER 4

RESULTS & DISCUSSION

4.1 Activity Experiments

As discussed in Ch. 3, four different catalysts were evaluated, including 1.5 % Pt/γ-Al_2O_3, 1.5 % Pt/TiO_2, 1.5 % Pt/ZrO_2, and 1.5 % Pt/SiO_2. For each catalyst, the activity of the fresh sample was compared to the activity of an H_2S-poisoned sample for the complete oxidation of CO, CH_4, C_2H_6, C_2H_4, C_2H_2, C_3H_8, and C_4H_{10} to CO_2 and H_2O. A description of the sulfur poisoning conditions was also presented in Ch. 3. The effects of sulfur poisoning on catalyst activity were observed as changes in the conversion versus temperature plots for each reactant. For each reaction, the temperature at which 50 % conversion was obtained was determined from the activity curve and used as a single figure of merit for catalyst activity. Results of the activity experiments are presented and discussed below.

4.1.1 CO Oxidation

Activity curves for CO oxidation on fresh and H_2S-poisoned catalyst samples are shown in Figures 4.1, 4.2, 4.3, and 4.4. The experiments show that each of the four catalysts were severely deactivated for CO oxidation following H_2S poisoning, in agreement with numerous laboratory studies including those of Kummer [19], Burch et al. [26], and Wang [31].

Tables 4.1, 4.2, 4.3, and 4.4 show the 50 % conversion temperatures for CO and hydrocarbon oxidation on fresh and H_2S-poisoned catalysts. Also shown in these tables is the quantity, ΔT_{50}, defined as the difference between the 50% conversion temperatures

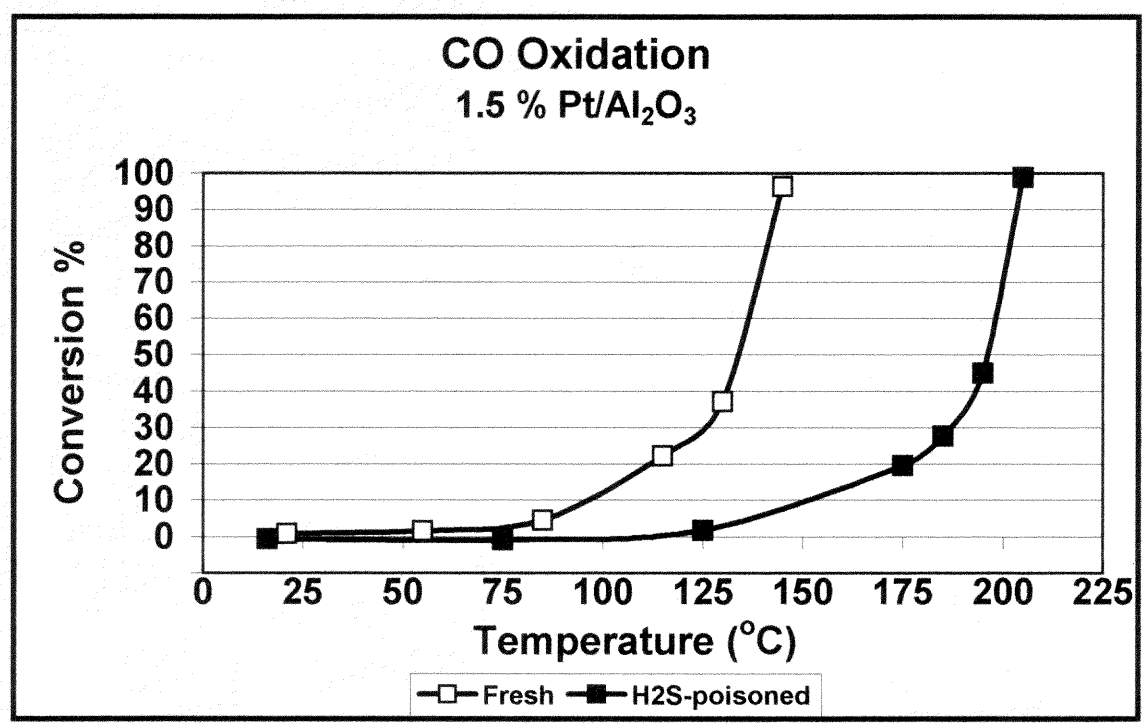

Figure 4.1: Fresh vs. H_2S-poisoned catalyst activity for the oxidation of 1 % CO in air on 1.5 % Pt/γ-Al_2O_3; GHSV = 55,200; (Poisoning: 200 ppm H_2S/Air @ 400°C for 24 hrs.; GHSV = 6900)

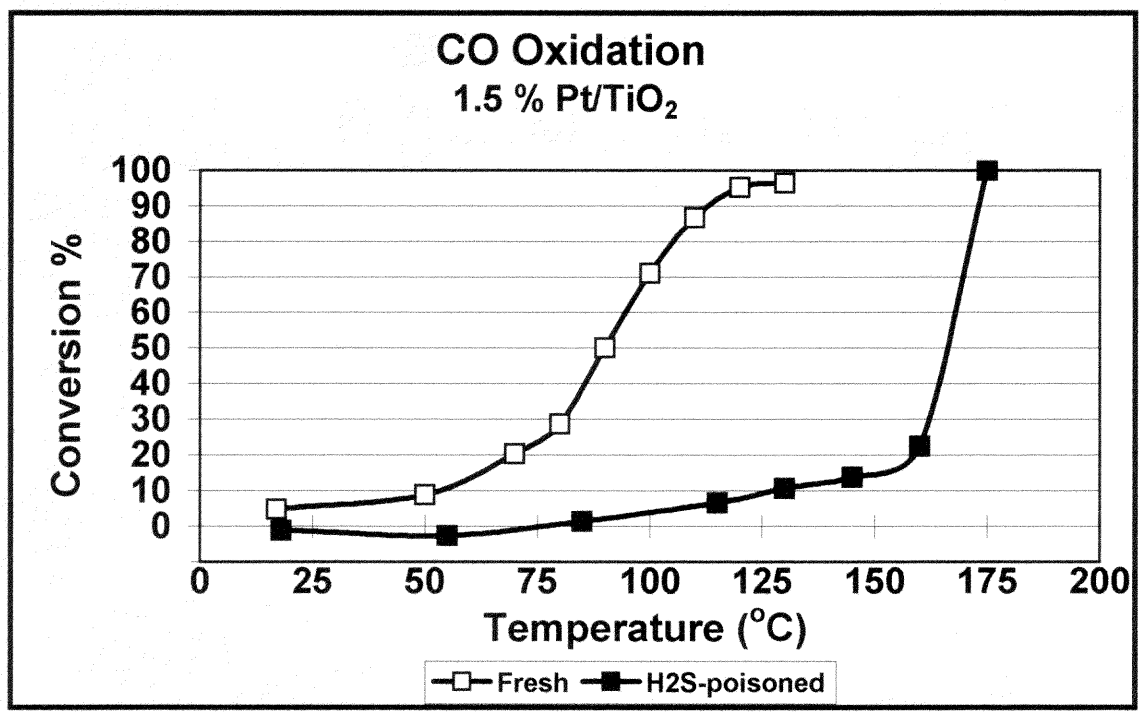

Figure 4.2: Fresh vs. H_2S-poisoned catalyst activity for the oxidation of 1 % CO in air on 1.5 % Pt/TiO_2; GHSV = 52,380; (Poisoning: 200 ppm H_2S/Air @ 400°C for 24 hrs.; GHSV = 6550)

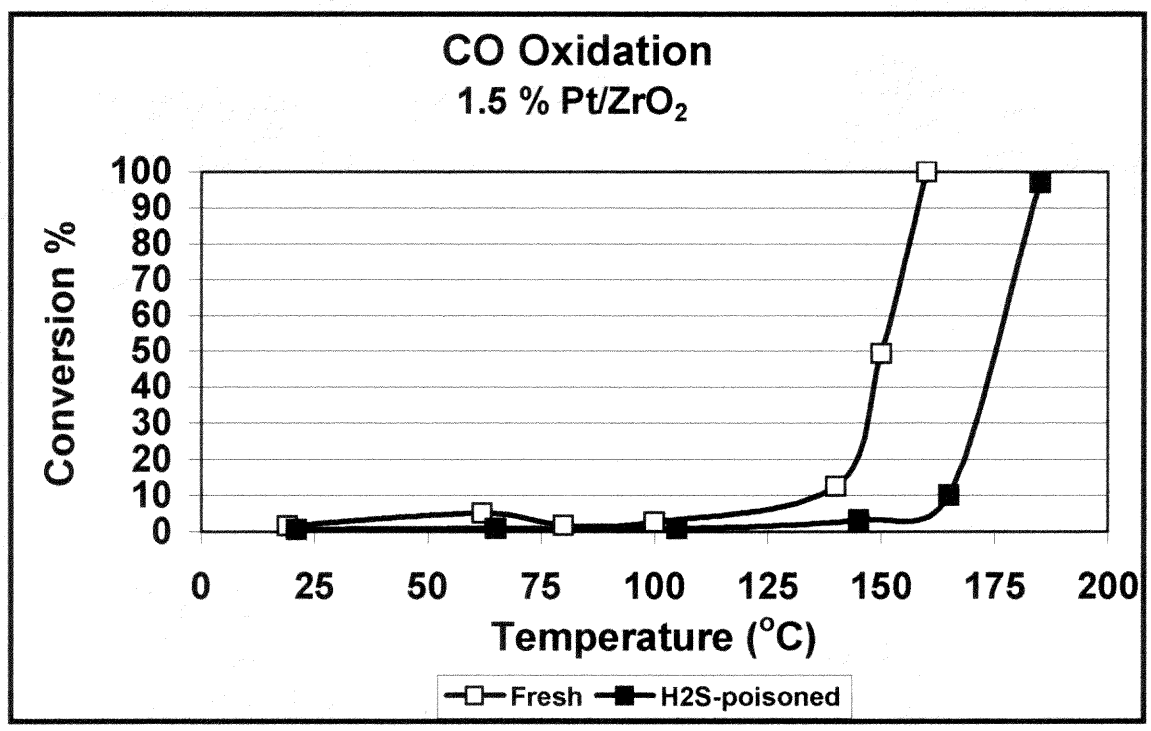

Figure 4.3: Fresh vs. H_2S-poisoned catalyst activity for the oxidation of 1 % CO in air on 1.5 % Pt/ZrO_2; GHSV = 85,320; (Poisoning: 200 ppm H_2S/Air @ 400°C for 24 hrs.; GHSV = 10,700)

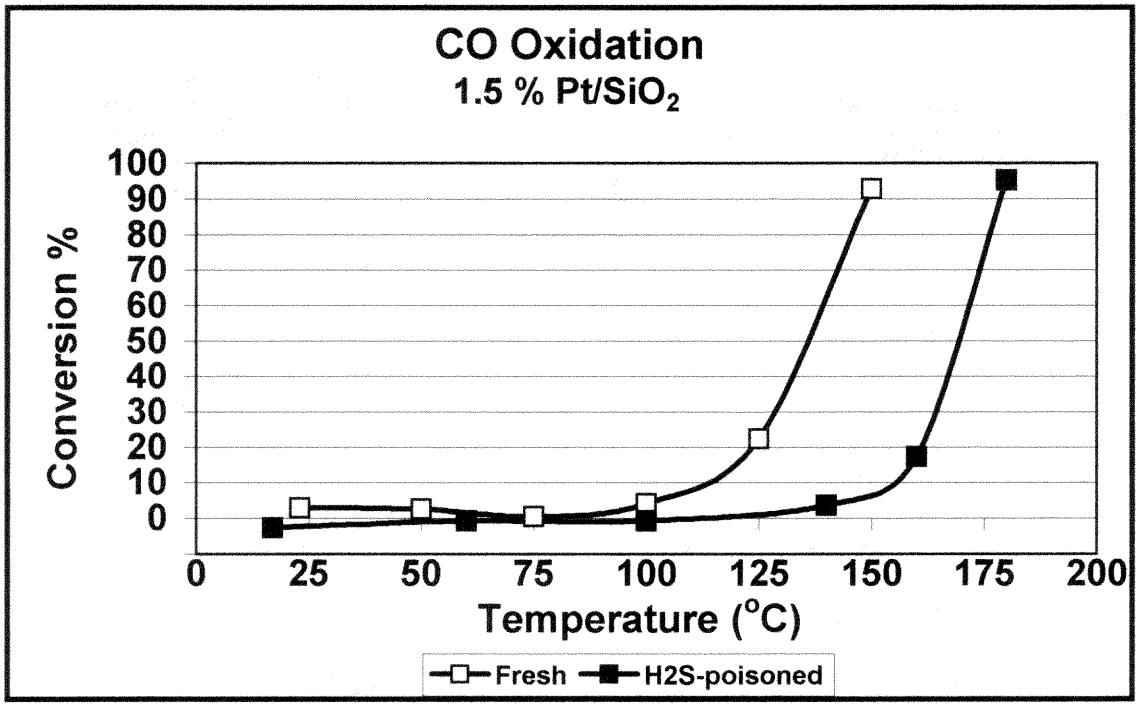

Figure 4.4: Fresh vs. H_2S-poisoned catalyst activity for the oxidation of 1 % CO in air on 1.5 % Pt/SiO_2; GHSV = 15,000; (Poisoning: 200 ppm H_2S/Air @ 400°C for 24 hrs.; GHSV = 1880)

Table 4.1: T_{50}[a] data for fresh, H_2S-poisoned, and SO_2-poisoned 1.5 % Pt/γ-Al_2O_3. All values are reported in °C.

Gas	Fresh	H_2S-poisoned	ΔT_{50}-H_2S[b]	SO_2-poisoned	ΔT_{50}-SO_2[c]
CO	133	196	+63	194	+61
CH_4	415	493	+78	489	+74
C_2H_6	367	341	-26		
C_2H_4	167	155	-12		
C_2H_2	239	250	+11		
C_3H_8	313	258	-55		
C_3H_6	166	183	+17		
C_4H_{10}	263	191	-72	224	-39

Notes: a) T_{50} is defined as the temperature at which 50 % conversion to CO_2 is achieved. These values were obtained from the conversion versus temperature plots.
b) ΔT_{50}-H_2S is the difference between 50 % conversion temperatures of the H_2S-poisoned catalyst and the fresh catalyst.
c) ΔT_{50}-SO_2 is the difference between 50 % conversion temperatures of the SO_2-poisoned catalyst and the fresh catalyst.

Table 4.2: T_{50}[a] data for fresh and H_2S-poisoned 1.5 % Pt/TiO_2. All values are reported in °C.

Gas	Fresh	H_2S-poisoned	ΔT_{50}-H_2S[b]
CO	90	165	+75
CH_4	374	389	+15
C_2H_6	346	336	-10
C_2H_4	177	184	+7
C_2H_2	254	253	-1
C_3H_8	308	287	-21
C_4H_{10}	258	216	-42

Notes: a) T_{50} is defined as the temperature at which 50 % conversion to CO_2 is achieved. These values were obtained from the conversion versus temperature plots.
b) ΔT_{50}-H_2S is the difference between 50 % conversion temperatures of the H_2S-poisoned catalyst and the fresh catalyst.

Table 4.3: T_{50}[a] data for fresh and H_2S-poisoned 1.5 % Pt/ZrO_2. All values are reported in °C.

Gas	Fresh	H_2S-poisoned	ΔT_{50}-H_2S[b]
CO	150	174	+24
CH_4	450	495	+45
C_2H_6	349	334	-15
C_2H_4	162	182	+20
C_2H_2	279	261	-18
C_3H_8	303	259	-44
C_4H_{10}	232	193	-39

Notes: a) T_{50} is defined as the temperature at which 50 % conversion to CO_2 is achieved. These values were obtained from the conversion versus temperature plots.
b) ΔT_{50}-H_2S is the difference between 50 % conversion temperatures of the H_2S-poisoned catalyst and the fresh catalyst.

Table 4.4: T_{50}[a] data for fresh, H_2S-poisoned, and SO_2-poisoned 1.5 % Pt/SiO_2. All values are reported in °C.

Gas	Fresh	H_2S-poisoned	ΔT_{50}-H_2S[b]	SO_2-poisoned	ΔT_{50}-SO_2[c]
CO	135	168	+33	168	+33
CH_4	599	592	-7	576	-23
C_2H_6	472	409	-63		
C_2H_4	120	134	+14		
C_2H_2	187	206	+19		
C_3H_8	385	315	-70		
C_4H_{10}	313	252	-61	244	-69

Notes: a) T_{50} is defined as the temperature at which 50 % conversion to CO_2 is achieved. These values were obtained from the conversion versus temperature plots.
b) ΔT_{50}-H_2S is the difference between 50 % conversion temperatures of the H_2S-poisoned catalyst and the fresh catalyst.
c) ΔT_{50}-SO_2 is the difference between 50 % conversion temperatures of the SO_2-poisoned catalyst and the fresh catalyst.

for H_2S-poisoned and fresh catalysts for each reaction. A positive value indicates deactivation while a negative value indicates activity enhancement.

An immediate observation of the CO oxidation activity curves and associated T_{50} data seems to indicate that H_2S poisoning caused the most severe deactivation for the Pt/TiO_2 catalyst. However, it is important to note that the space velocity used in the activity experiments was different for each catalyst and, thus, absolute comparisons of activity between the four catalysts based on the activity curves are not valid. The space velocities used for reactions on each catalyst are shown in Table 3.1.

4.1.2 CH_4 Oxidation

The oxidation of CH_4 was significantly deactivated following H_2S-poisoning of $Pt/\gamma\text{-}Al_2O_3$ and Pt/ZrO_2 as shown in Figures 4.5 and 4.7. In Figure 4.5, the activity curve for H_2S-poisoned $Pt/\gamma\text{-}Al_2O_3$ shows a kink in the curve at approximately 525°C. Repeated experiments showed that this was a real effect and it is likely due to some type of transformation occurring on the catalyst surface at this temperature. This effect was not seen in any of the other activity curves for $Pt/\gamma\text{-}Al_2O_3$ because all of the other oxidation reactions studied occurred at lower temperatures.

Figures 4.6 and 4.8 show that H_2S poisoning causes a slight deactivation for CH_4 oxidation at low conversions on Pt/TiO_2 and Pt/SiO_2. At high conversions, however, the effect is negligible.

The CH_4 oxidation results are in general agreement with results reported in the literature. Numerous studies have reported that deactivation of the CH_4 oxidation reaction occurs on Pt catalysts as a result of sulfur poisoning. The mechanism involves a

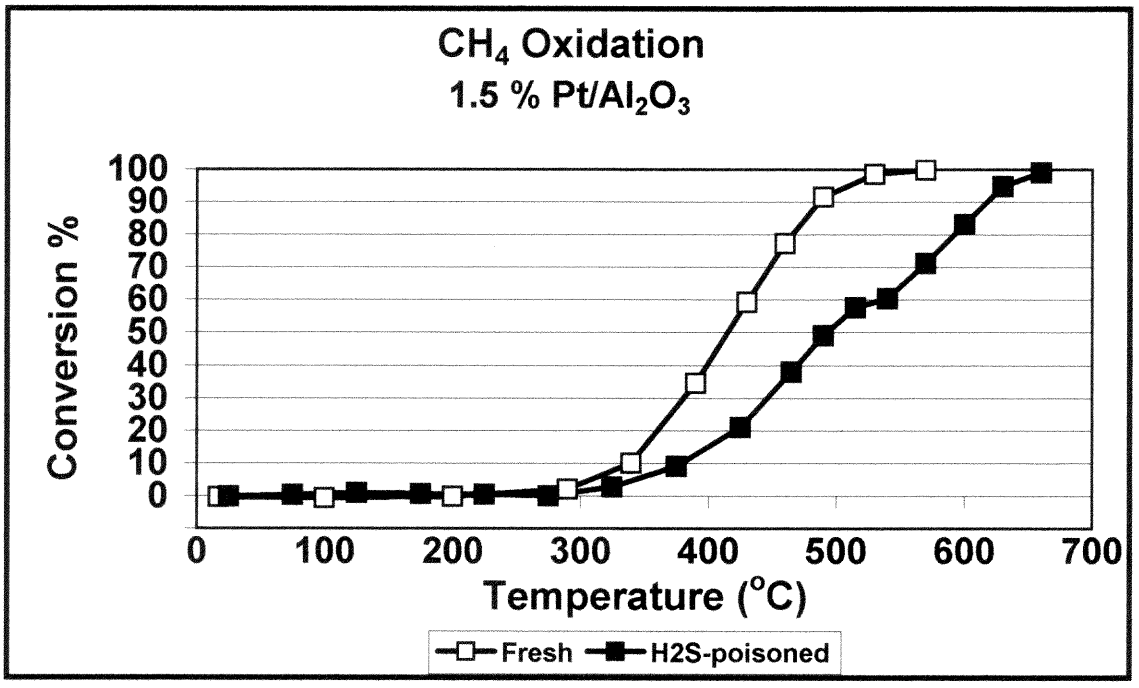

Figure 4.5: Fresh vs. H_2S-poisoned catalyst activity for the oxidation of 1 % CH_4 in air on 1.5 % Pt/γ-Al_2O_3; GHSV = 55,200. (Poisoning: 200 ppm H_2S/air @ 400°C for 24 hrs.; GHSV = 6900)

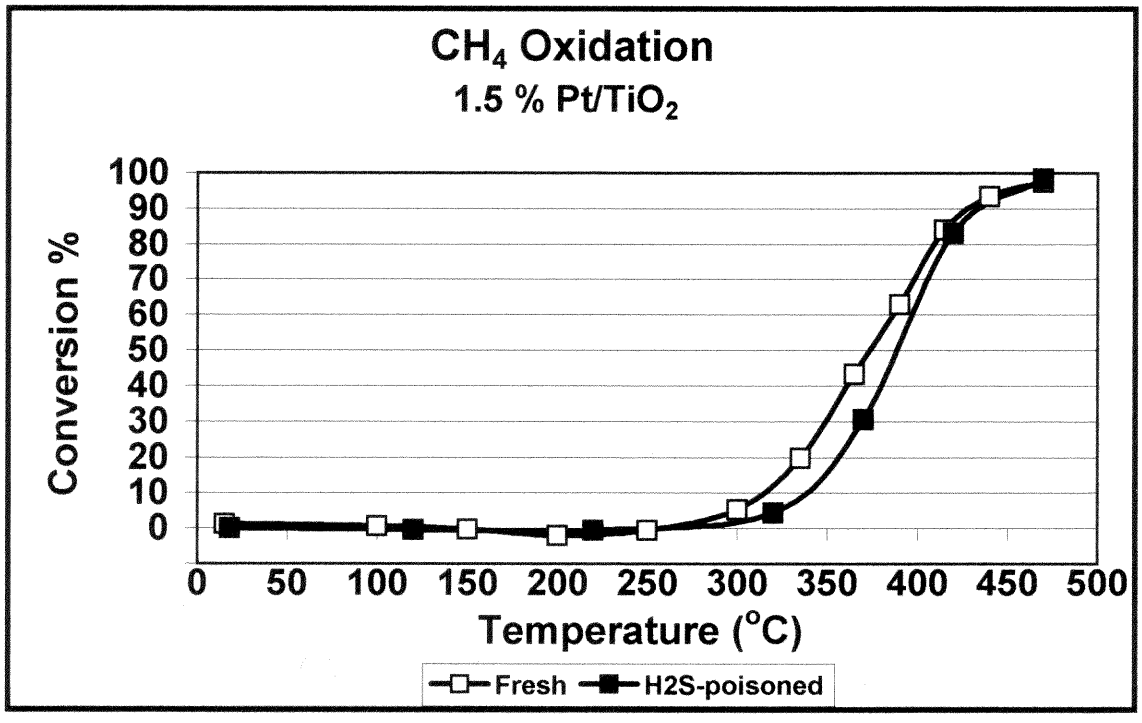

Figure 4.6: Fresh vs. H_2S-poisoned catalyst activity for the oxidation of 1 % CH_4 in air on 1.5 % Pt/TiO_2; GHSV = 52,380. (Poisoning: 200 ppm H_2S/air @ 400°C for 24 hrs.; GHSV = 6550)

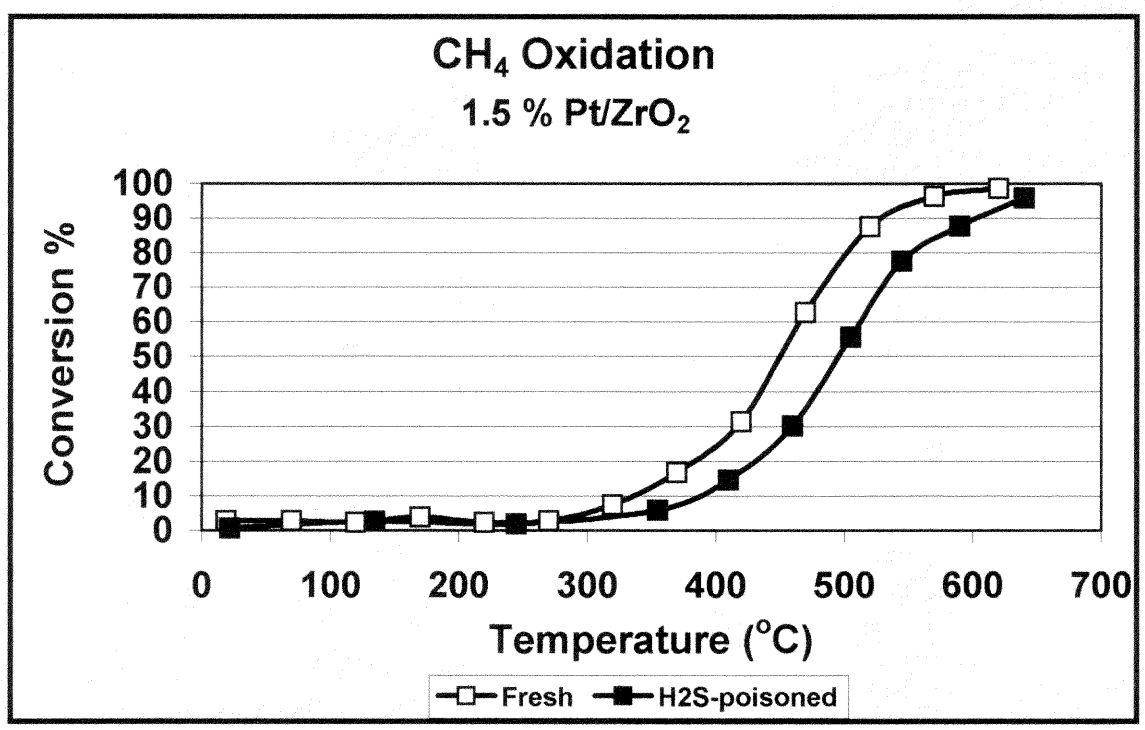

Figure 4.7: Fresh vs. H_2S-poisoned catalyst activity for the oxidation of 1 % CH_4 in air on 1.5 % Pt/ZrO_2; GHSV = 85,320. (Poisoning: 200 ppm H_2S/air @ 400°C for 24 hrs.; GHSV = 10,700)

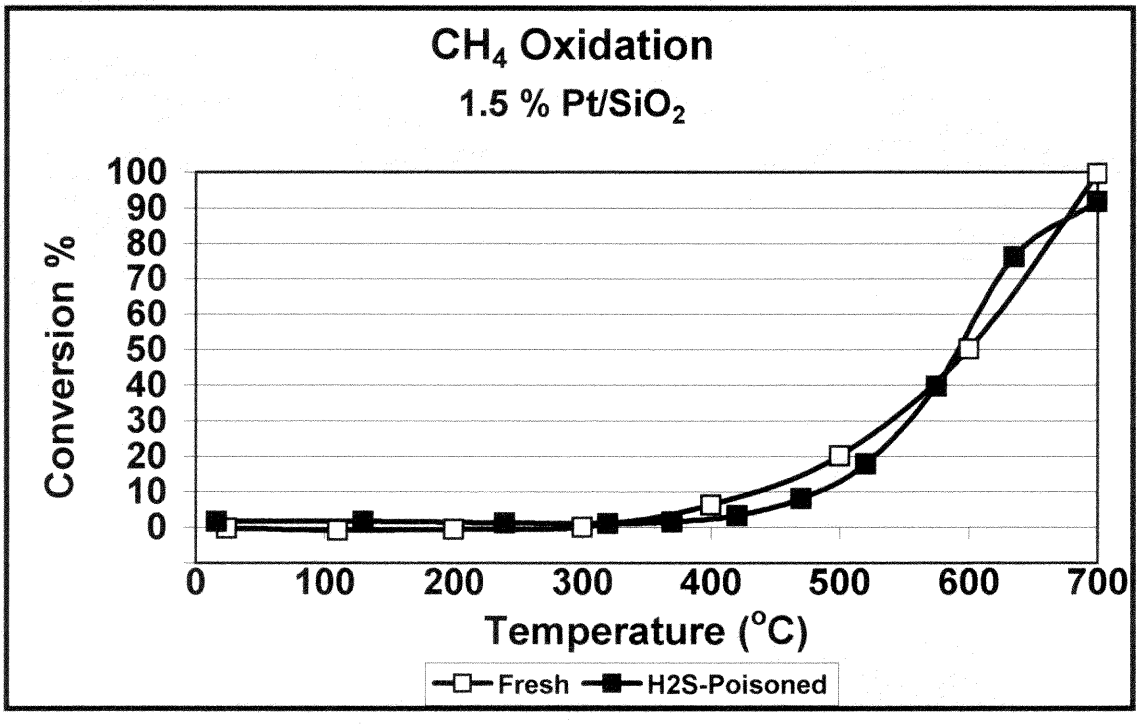

Figure 4.8: Fresh vs. H_2S-poisoned catalyst activity for the oxidation of 1 % CH_4 in air on 1.5 % Pt/SiO_2; GHSV = 15,000. (Poisoning: 200 ppm H_2S/air @ 400°C for 24 hrs.; GHSV = 1880)

loss of active sites due to pore blocking caused by the formation of sulfate on the support. However, sulfate is not known to form on SiO_2 surfaces and it is noteworthy that H_2S poisoning had a negligible effect for CH_4 oxidation on the Pt/SiO_2 catalyst in this study (Figure 4.8). Wang also observed deactivation for CH_4 oxidation on $Pt/\gamma\text{-}Al_2O_3$, Pt/TiO_2, and Pt/ZrO_2 following H_2S poisoning with a negligible effect shown on Pt/SiO_2 [31]. In other studies, Golunski et al. showed that the presence of SO_2 in an oxidizing exhaust stream had a negligible effect on CH_4 oxidation on a $Pt\text{-}Rh/CeO_2\text{-}Al_2O_3$ three-way catalyst [5]. Alternatively, Trimm et al. found that the addition of H_2S or SO_2 to the feedstream resulted in an activity ***increase*** for CH_4 oxidation on a 0.2 % Pt/Al_2O_3 catalyst [30]. This enhancement was attributed to the increased catalyst acidity due to the formation of aluminum sulfate. This observation may be due to the fact that low concentrations of sulfur (20 ppm) combined with the high dispersion of the 0.2 % Pt/Al_2O_3 catalyst were sufficient to prevent the effect of pore blocking on the catalyst surface.

4.1.3 Alkene and Alkyne Oxidation

The experimental results for C_2H_4, C_3H_6, and C_2H_2 oxidation are presented together since activity changes due to H_2S poisoning were small for each compound on each catalyst and may not be completely significant. Additionally, it has been assumed that each of these compounds is oxidized via a similar mechanism in which a gas-phase unsaturated hydrocarbon molecule reacts with a dissociatively adsorbed O atom. Compounds reacting by a similar mechanism would be expected to be affected by H_2S poisoning in a similar way and, for the most part, this is evident from the results.

Figure 4.9 shows that C_2H_4 oxidation is slightly enhanced on Pt/γ-Al_2O_3 following H_2S poisoning. This is in contrast to the same reaction on Pt/TiO_2, Pt/ZrO_2, and Pt/SiO_2 for which H_2S poisoning results in a slight deactivation as evident in Figures 4.10, 4.11, and 4.12. It is also in contrast to the results obtained by Kummer for C_2H_4 oxidation on a 0.15 % Pt/Al_2O_3 catalyst exposed to 66 ppm SO_2 in which significant deactivation was observed [19].

From Tables 4.1, 4.2, 4.3, and 4.4, ΔT_{50} values of –12, +7, +20, and +14 for C_2H_4 oxidation were found for Pt/γ-Al_2O_3, Pt/TiO_2, Pt/ZrO_2, and Pt/SiO_2, respectively. Although these values may seem significant considering that the reaction occurs between 125 and 200°C, limitations of the experimental apparatus resulted in an error on the order of ± 5°C for this reaction and the reactions of the other unsaturated hydrocarbon compounds. Thus, the activity changes observed are considered to be only slightly significant. On all four catalysts, including both fresh and H_2S-poisoned samples, the oxidation of C_2H_4 exhibits an extremely fast light-off. At this point on the activity curve (approximately 5-10 % conversion), the reaction produces enough heat to quickly accelerate to a conversion of 80-90 %. This activity change occurred over a temperature range of only 5-15°C. Consequently, it was difficult to obtain data points in the temperature range in which the rapid activity increase occurred. As a result of this rapid light-off behavior, the C_2H_4 oxidation experiments were much less reproducible than those for CO, CH_4, and alkane gases.

The oxidation of C_3H_6 was slightly deactivated on Pt/γ-Al_2O_3 due to H_2S poisoning as shown in Figure 4.13. This reaction exhibited similar behavior to the C_2H_4 reaction described above. In fact, Figures 4.9 and 4.13 show that the activity curves for

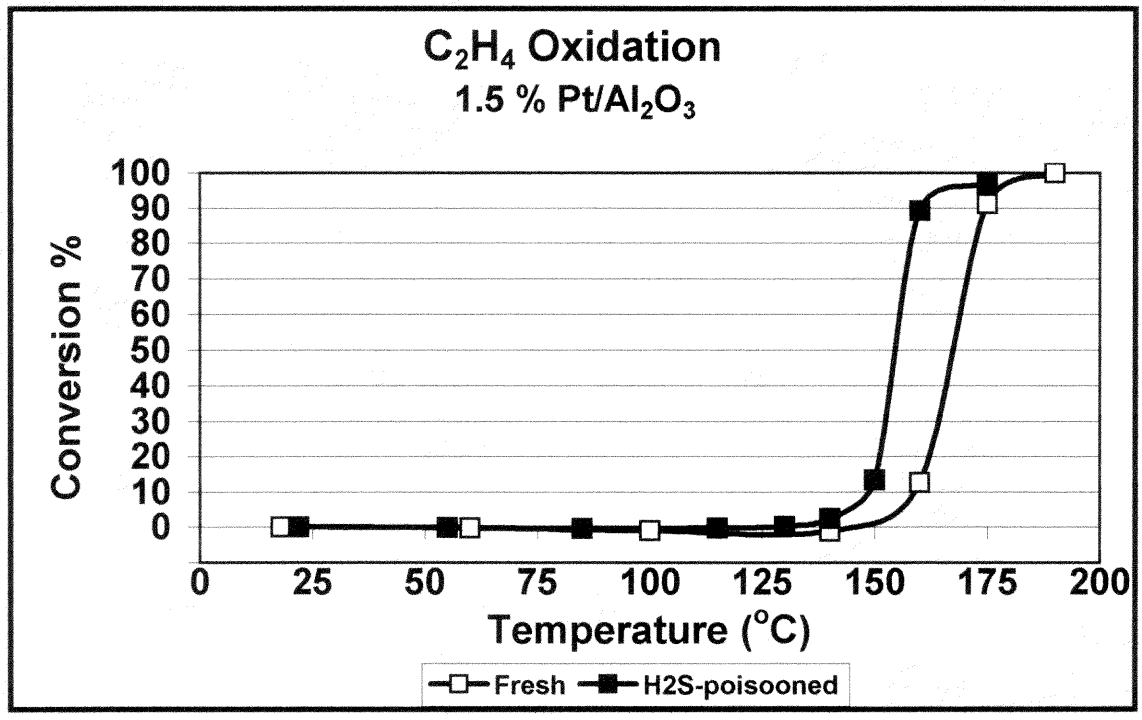

Figure 4.9: Fresh vs. H_2S-poisoned catalyst activity for the oxidation of 1 % C_2H_4 in air on 1.5 % Pt/γ-Al_2O_3; GHSV = 55,200. (Poisoning: 200 ppm H_2S/air @ 400°C for 24 hrs.; GHSV = 6900)

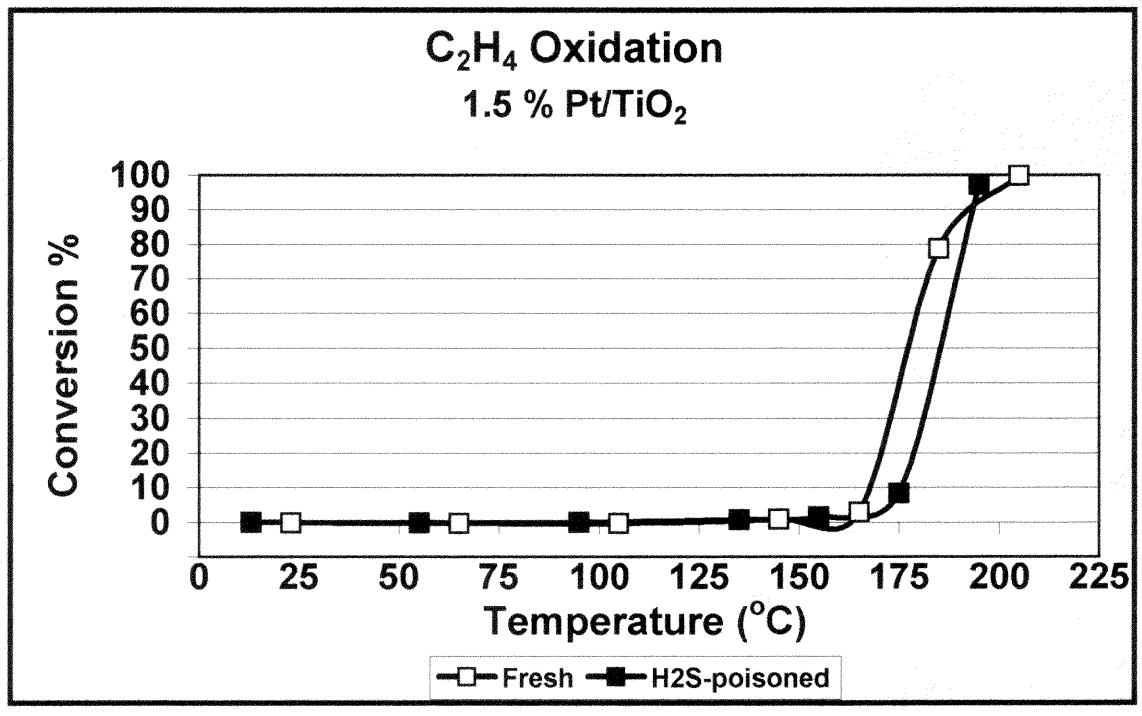

Figure 4.10: Fresh vs. H_2S-poisoned catalyst activity for the oxidation of 1 % C_2H_4 in air on 1.5 % Pt/TiO_2; GHSV = 52,380. (Poisoning: 200 ppm H_2S/air @ 400°C for 24 hrs.; GHSV = 6550)

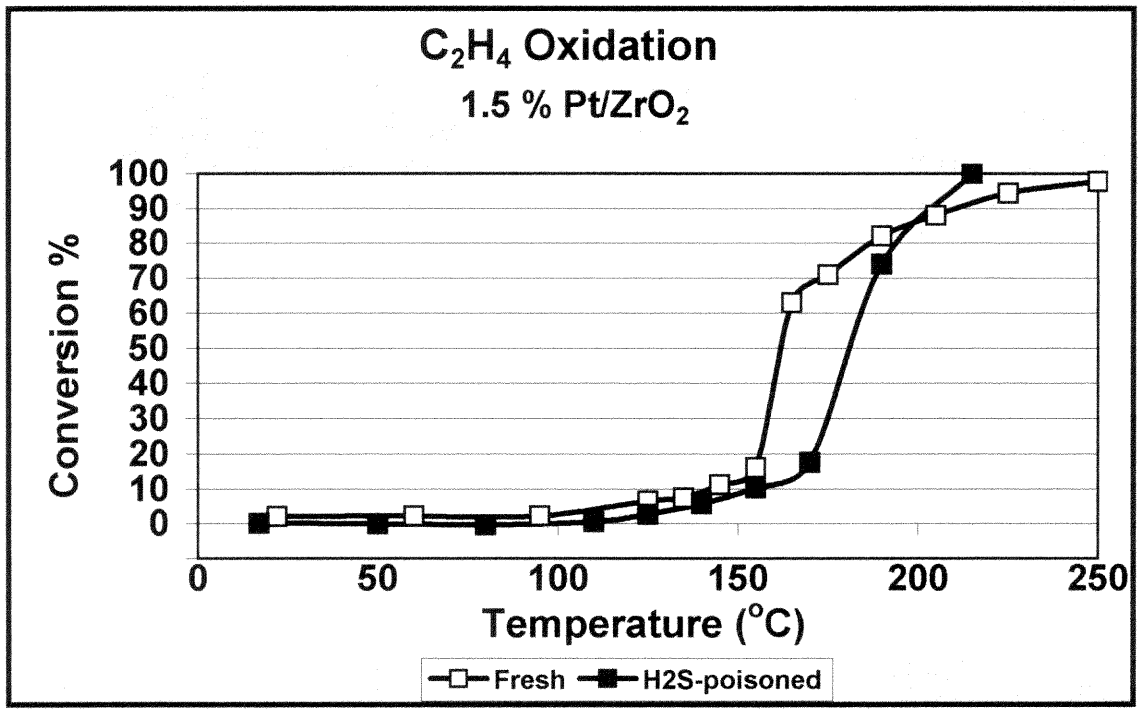

Figure 4.11: Fresh vs. H_2S-poisoned catalyst activity for the oxidation of 1 % C_2H_4 in air on 1.5 % Pt/ZrO_2; GHSV = 85,320. (Poisoning: 200 ppm H_2S/air @ 400°C for 24 hrs.; GHSV = 10,700)

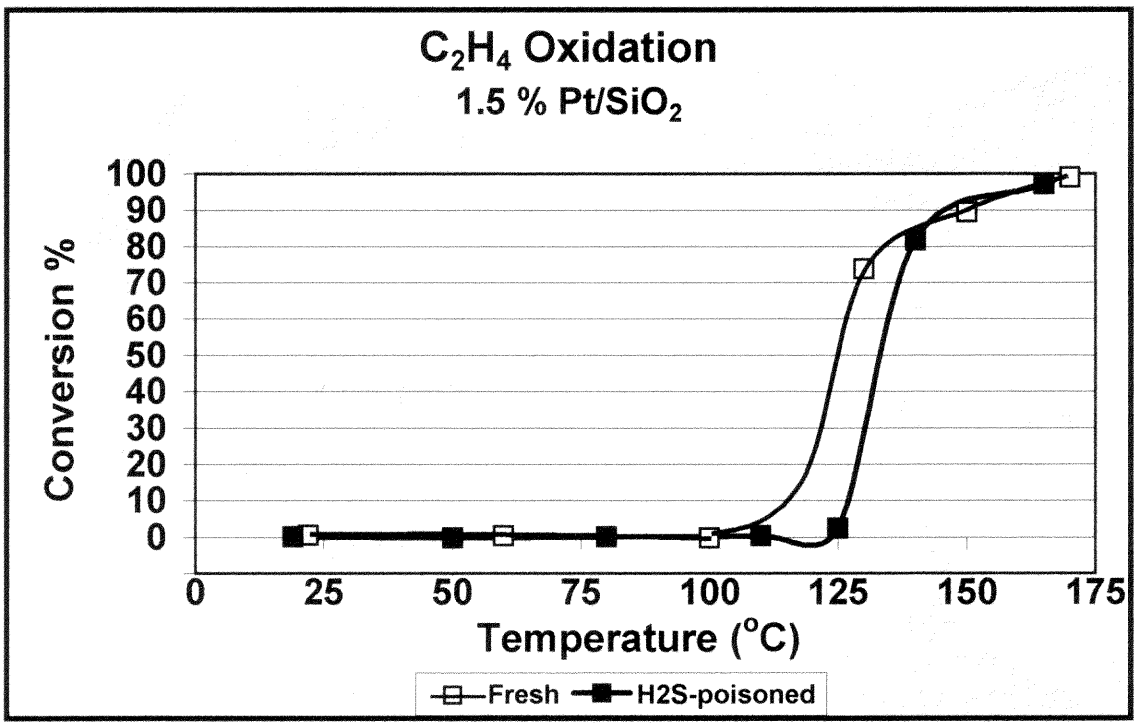

Figure 4.12: Fresh vs. H_2S-poisoned catalyst activity for the oxidation of 1 % C_2H_4 in air on 1.5 % Pt/SiO_2; GHSV = 15,000. (Poisoning: 200 ppm H_2S/air @ 400°C for 24 hrs.; GHSV = 1880)

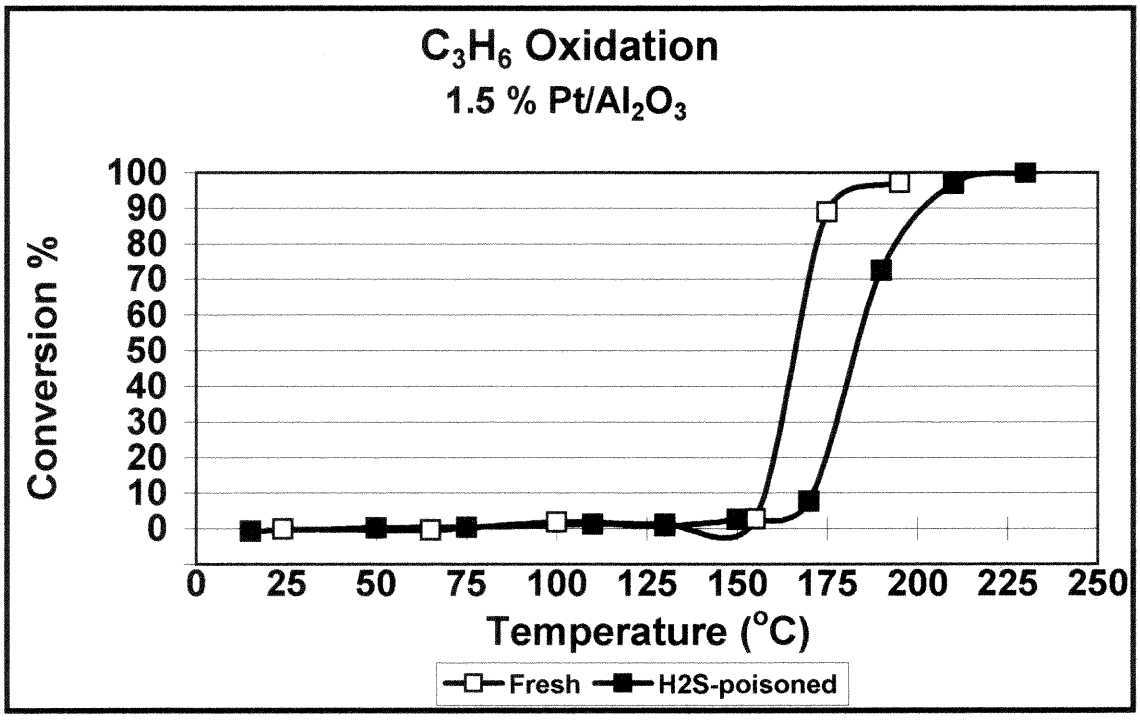

Figure 4.13: Fresh vs. H_2S-poisoned catalyst activity for the oxidation of 1 % C_3H_6 in air on 1.5 % Pt/γ-Al_2O_3; GHSV = 55,200. (Poisoning: 200 ppm H_2S/air @ 400°C for 24 hrs.; GHSV = 6900)

the oxidation of C_2H_4 and C_3H_6 on fresh Pt/γ-Al_2O_3 are almost identical, leading to the speculation that the reactions occur by a similar mechanism. However, the fact that C_2H_4 oxidation is slightly enhanced by H_2S poisoning and C_3H_6 oxidation is slightly deactivated may be an indication that the reaction mechanisms are slightly different or, that the observed changes in activity are insignificant.

Burch et al. [39] studied the C_3H_6-NO-O_2 reaction on 1 % Pt/Al_2O_3 and found that the addition of SO_2 to the feedstream resulted in a slight reversible deactivation and that the original catalyst activity was restored when SO_2 was removed from the gas stream. However, when the catalyst was pre-sulfated, no effect on activity was observed. Under the conditions employed, it was found that the sulfation procedure resulted in the formation of sulfate entirely on the catalyst support. Thus, it was concluded that sulfate located on the support had no effect on the C_3H_6-NO-O_2 reaction due to the fact that this reaction occurred entirely on the Pt surface in contrast to the C_3H_8-NO-O_2 reaction which occurs on both Pt and the Al_2O_3 surface. This reaction was observed to be deactivated by support sulfation.

Results for C_2H_4 and C_3H_6 oxidation can be explained in a similar fashion. It is assumed that sulfur poisoning of Pt/γ-Al_2O_3, Pt/TiO_2, and Pt/ZrO_2 results in the formation of sulfate primarily on the support surface. If the alkene reactions occur on the Pt surface only, then, it would seem probable that the H_2S poisoning procedure would have little effect on the activity. As noted, the changes in observed activity are relatively small and seem to substantiate this hypothesis. However, the formation of sulfate on the support was accompanied by significant pore blockage and Pt crystal growth as shown in experiments discussed below. These effects would be expected to inhibit the dissociative

chemisorption of O_2 on Pt site, which is a key step in the proposed reaction mechanism. Thus, an inhibition of the overall oxidation reactions of C_2H_4 and C_2H_2 would also be expected in contrast to the observed results. It is possible that significant inhibition effects due to H_2S poisoning were not observed as a result of the excess amount of O_2 in the system (~20 %).

The experimental results for C_2H_2 oxidation were mixed, although changes in activity due to H_2S poisoning on all four catalysts were extremely small. This reaction behaves in a similar fashion to the C_2H_4 and C_3H_6 reactions in that measurements in the activity range between 20 and 80 % conversion were difficult. Figures 4.14 and 4.17 show that the C_2H_2 reaction on Pt/γ-Al_2O_3 and Pt/SiO_2 were slightly deactivated following H_2S poisoning. A slight enhancement of activity is shown in Figure 4.16 for Pt/ZrO_2 while Figure 4.15 shows a negligible effect on Pt/TiO_2. The proposed explanation for alkene oxidation results presented above also applies to the C_2H_2 reaction results.

4.1.4 Alkane Oxidation

Unlike the experiments described above for the oxidation of unsaturated hydrocarbons, the results obtained for the oxidation of saturated hydrocarbons were uniform among the four different catalysts studied. These experiments were also shown to be highly reproducible.

Figures 4.18, 4.19, 4.20, and 4.21 show that H_2S poisoning resulted in an activity enhancement for C_2H_6 oxidation on all four catalysts. H_2S poisoning also caused an enhancement of activity for C_3H_8 oxidation on all four catalysts as shown in Figures 4.22,

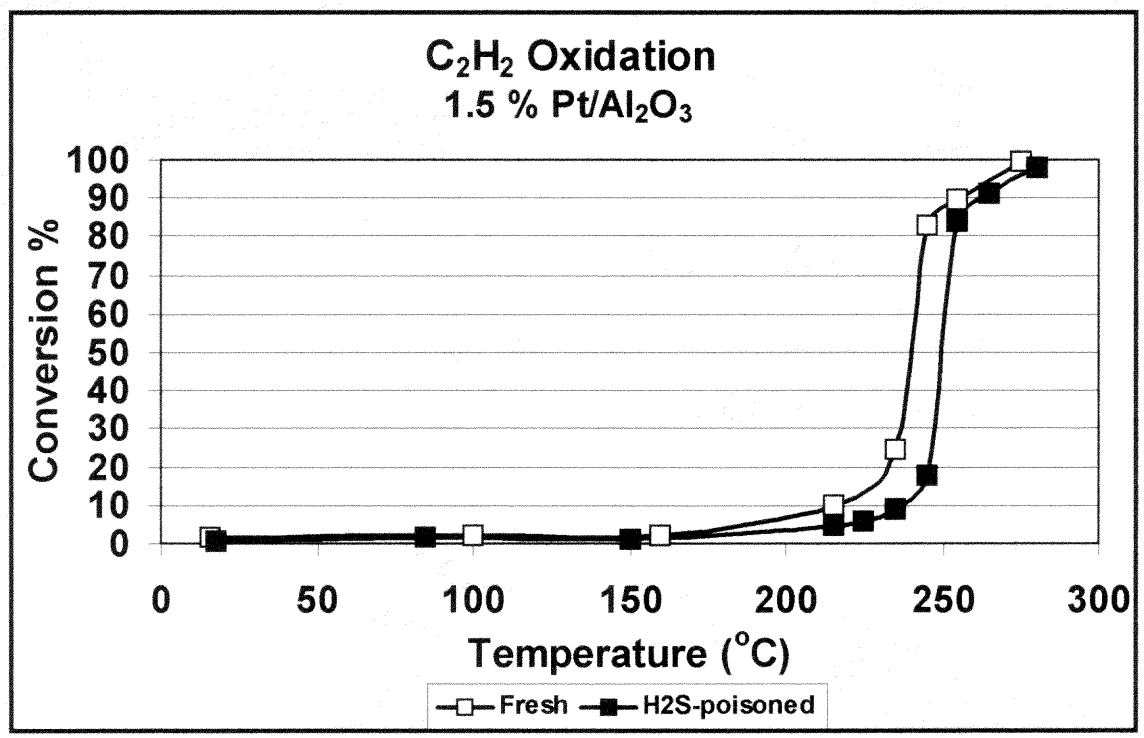

Figure 4.14: Fresh vs. H_2S-poisoned catalyst activity for the oxidation of 1 % C_2H_2 in air on 1.5 % Pt/γ-Al_2O_3; GHSV = 55,200. (Poisoning: 200 ppm H_2S/air @ 400°C for 24 hrs.; GHSV = 6900)

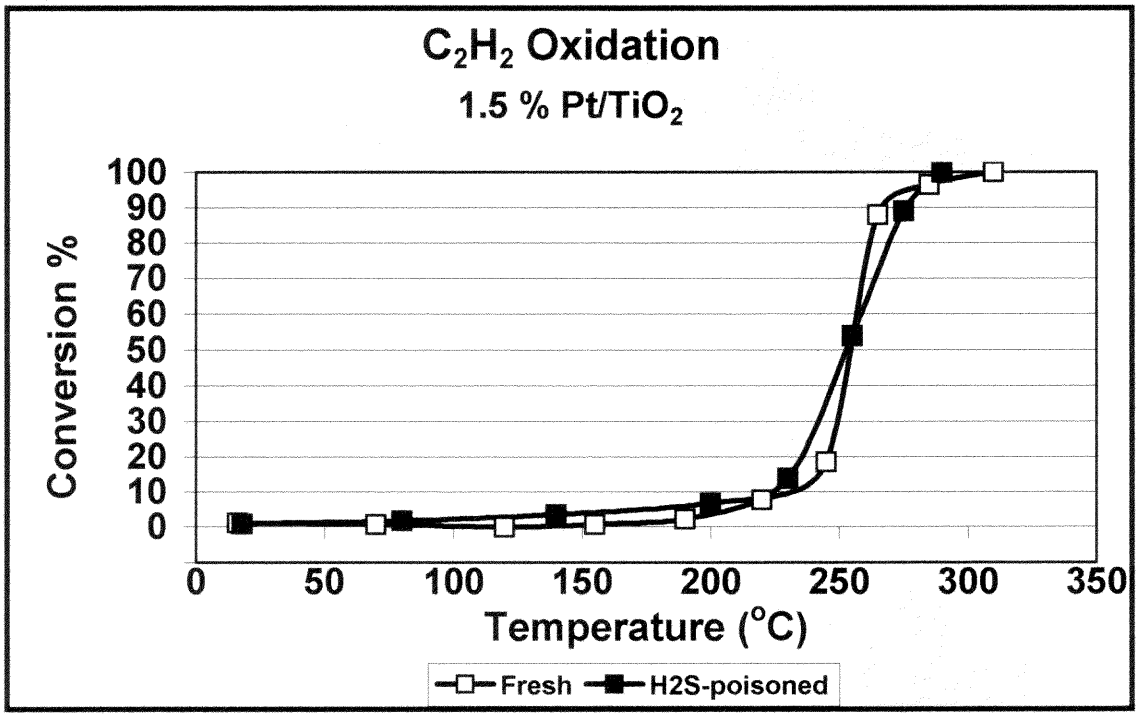

Figure 4.15: Fresh vs. H_2S-poisoned catalyst activity for the oxidation of 1 % C_2H_2 in air on 1.5 % Pt/TiO_2; GHSV = 52,380. (Poisoning: 200 ppm H_2S/air @ 400°C for 24 hrs.; GHSV = 6550)

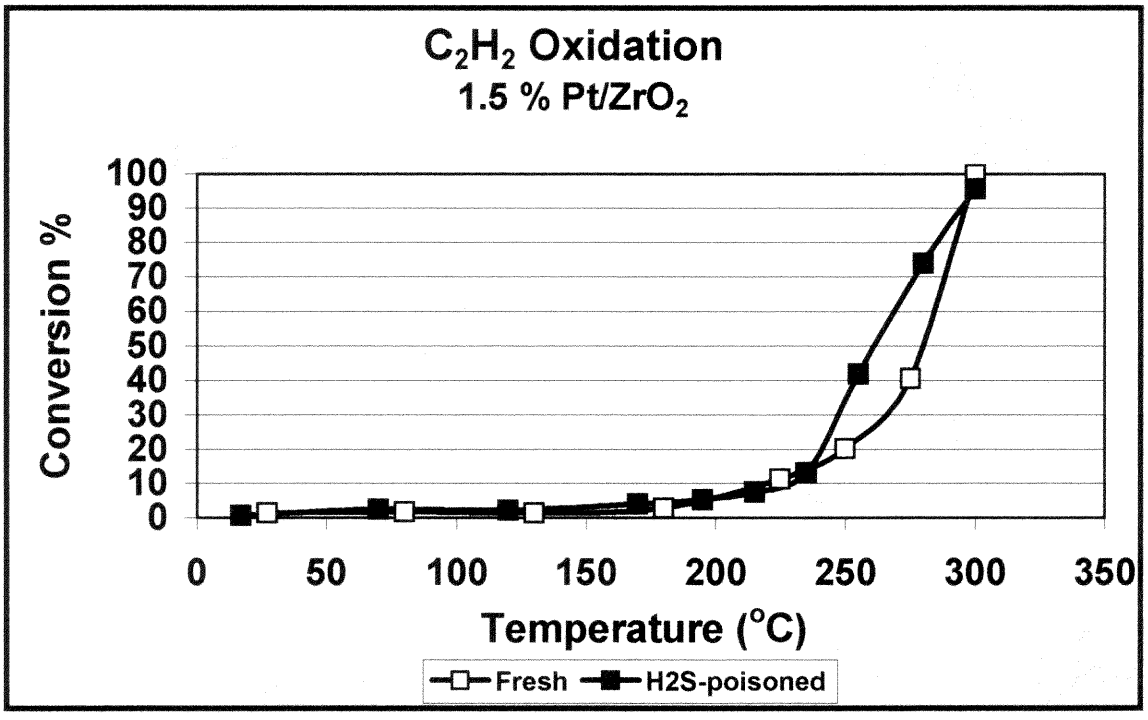

Figure 4.16: Fresh vs. H_2S-poisoned catalyst activity for the oxidation of 1 % C_2H_2 in air on 1.5 % Pt/ZrO_2; GHSV = 85,320. (Poisoning: 200 ppm H_2S/air @ 400°C for 24 hrs.; GHSV = 10,700)

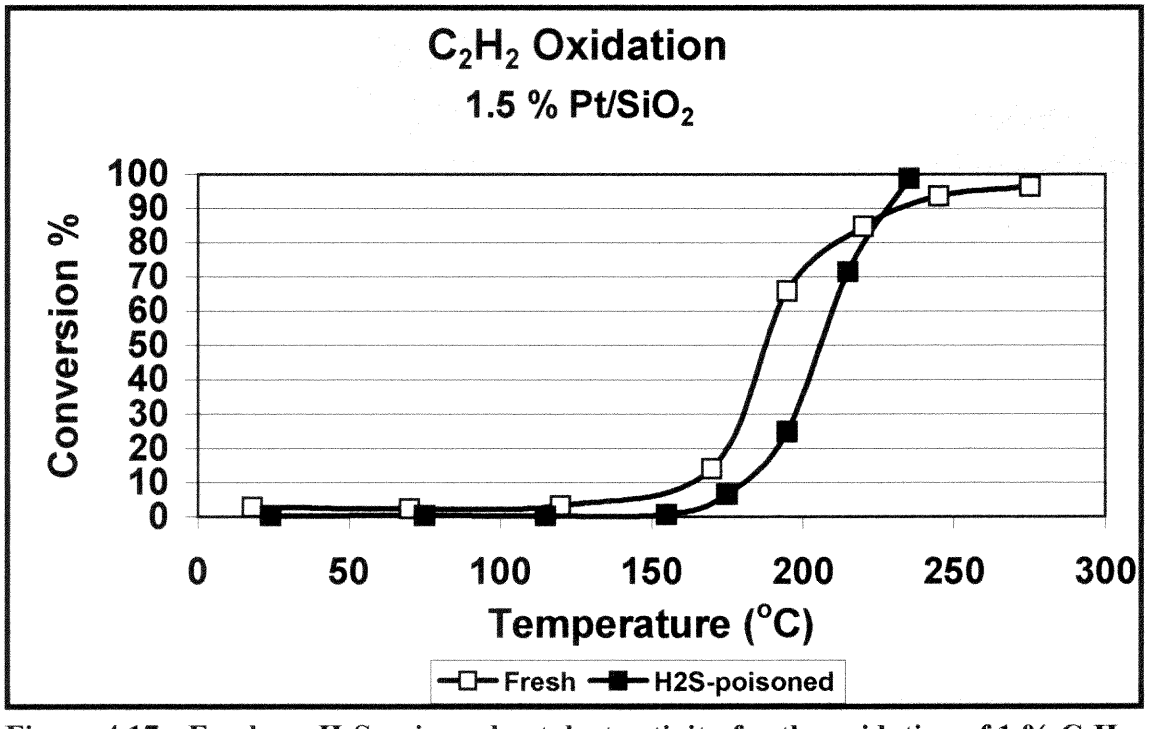

Figure 4.17: Fresh vs. H_2S-poisoned catalyst activity for the oxidation of 1 % C_2H_2 in air on 1.5 % Pt/SiO_2; GHSV = 15,000. (Poisoning: 200 ppm H_2S/air @ 400°C for 24 hrs.; GHSV = 1880)

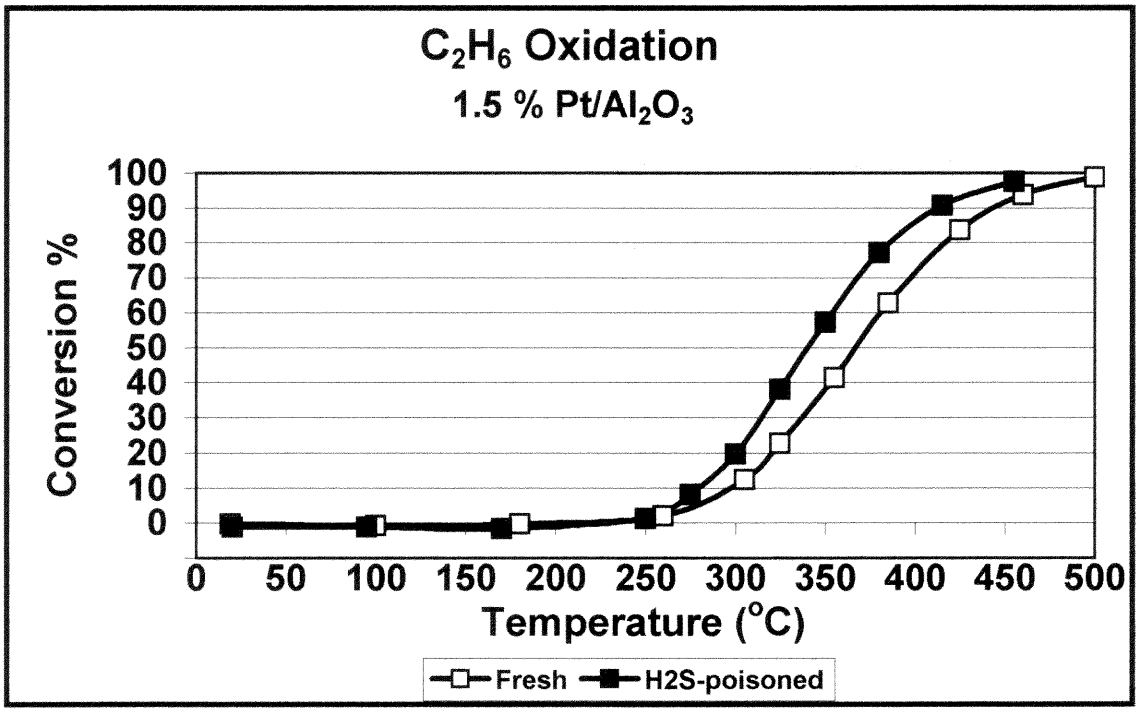

Figure 4.18: Fresh vs. H_2S-poisoned catalyst activity for the oxidation of 1 % C_2H_6 in air on 1.5 % $Pt/\gamma\text{-}Al_2O_3$; GHSV = 55,200. (Poisoning: 200 ppm H_2S/air @ 400°C for 24 hrs.; GHSV = 6900)

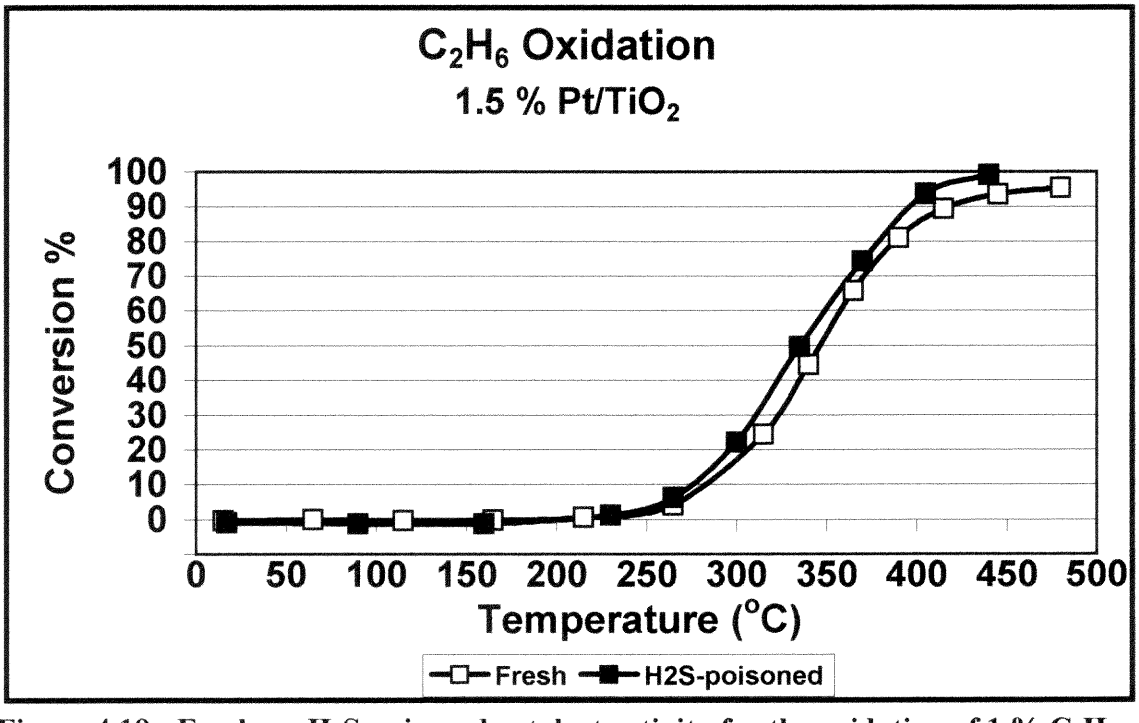

Figure 4.19: Fresh vs. H_2S-poisoned catalyst activity for the oxidation of 1 % C_2H_6 in air on 1.5 % Pt/TiO_2; GHSV = 52,380. (Poisoning: 200 ppm H_2S/air @ 400°C for 24 hrs.; GHSV = 6550)

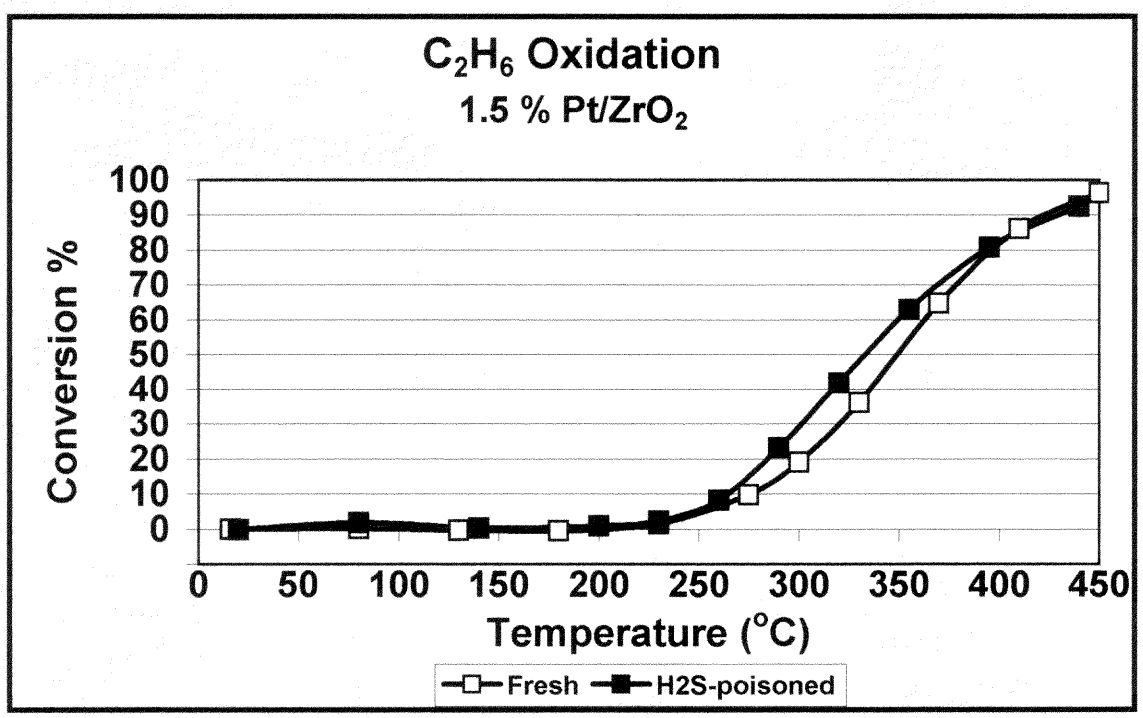

Figure 4.20: Fresh vs. H_2S-poisoned catalyst activity for the oxidation of 1 % C_2H_6 in air on 1.5 % Pt/ZrO_2; GHSV = 85,320. (Poisoning: 200 ppm H_2S/air @ 400°C for 24 hrs.; GHSV = 10,700)

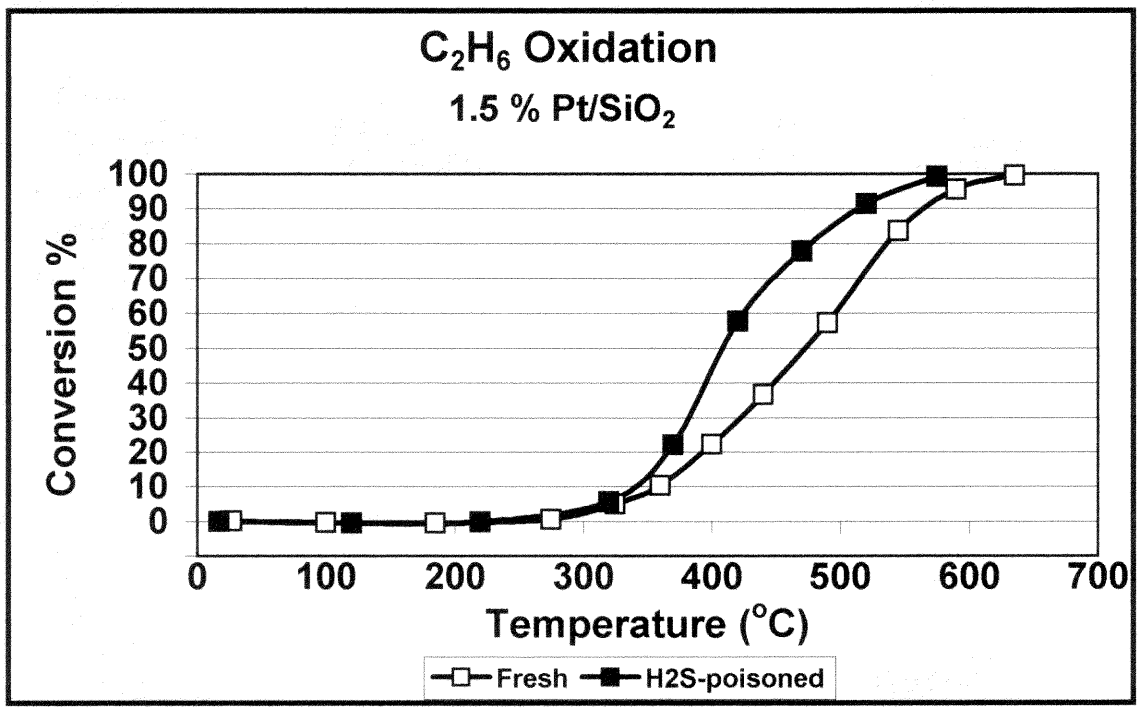

Figure 4.21: Fresh vs. H_2S-poisoned catalyst activity for the oxidation of 1 % C_2H_6 in air on 1.5 % Pt/SiO_2; GHSV = 15,000. (Poisoning: 200 ppm H_2S/air @ 400°C for 24 hrs.; GHSV = 1880)

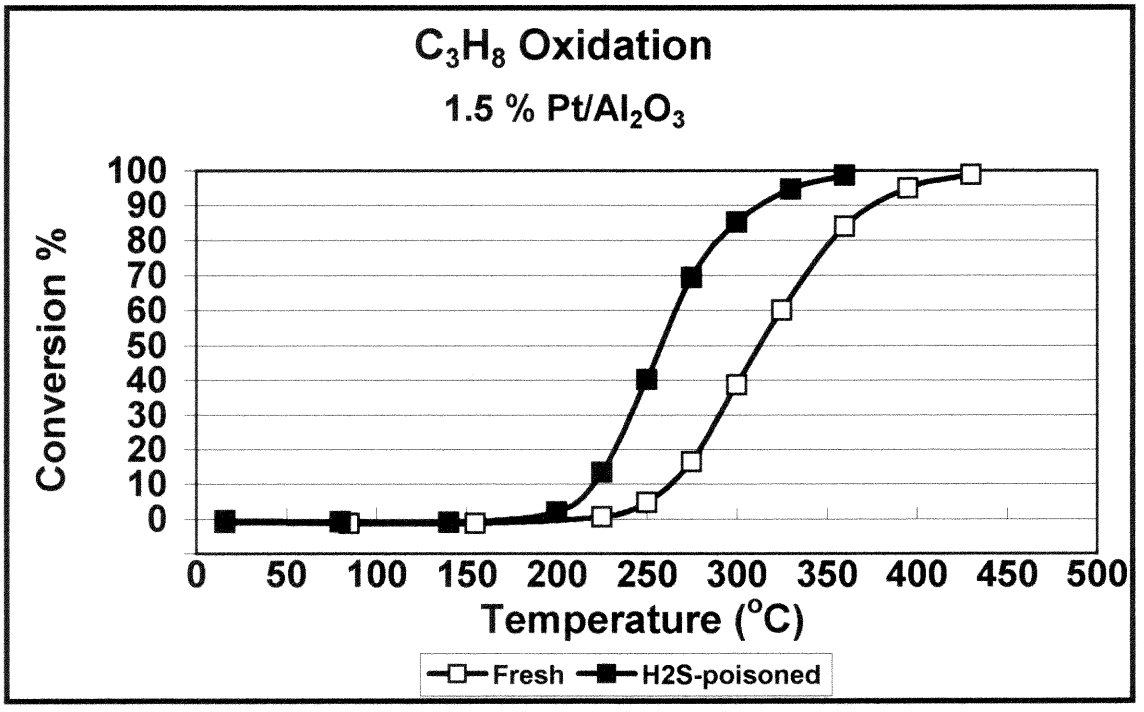

Figure 4.22: Fresh vs. H_2S-poisoned catalyst activity for the oxidation of 1 % C_3H_8 in air on 1.5 % Pt/γ-Al_2O_3; GHSV = 55,200. (Poisoning: 200 ppm H_2S/air @ 400°C for 24 hrs.; GHSV = 6900)

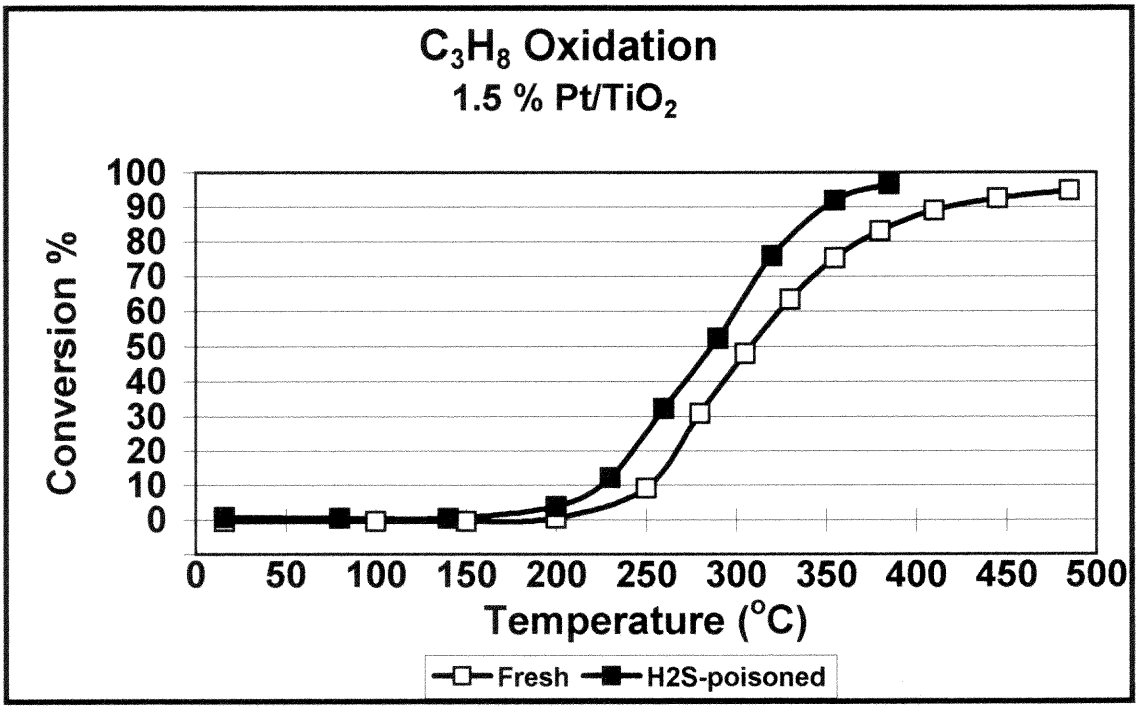

Figure 4.23: Fresh vs. H_2S-poisoned catalyst activity for the oxidation of 1 % C_3H_8 in air on 1.5 % Pt/TiO_2; GHSV = 52,380. (Poisoning: 200 ppm H_2S/air @ 400°C for 24 hrs.; GHSV = 6550)

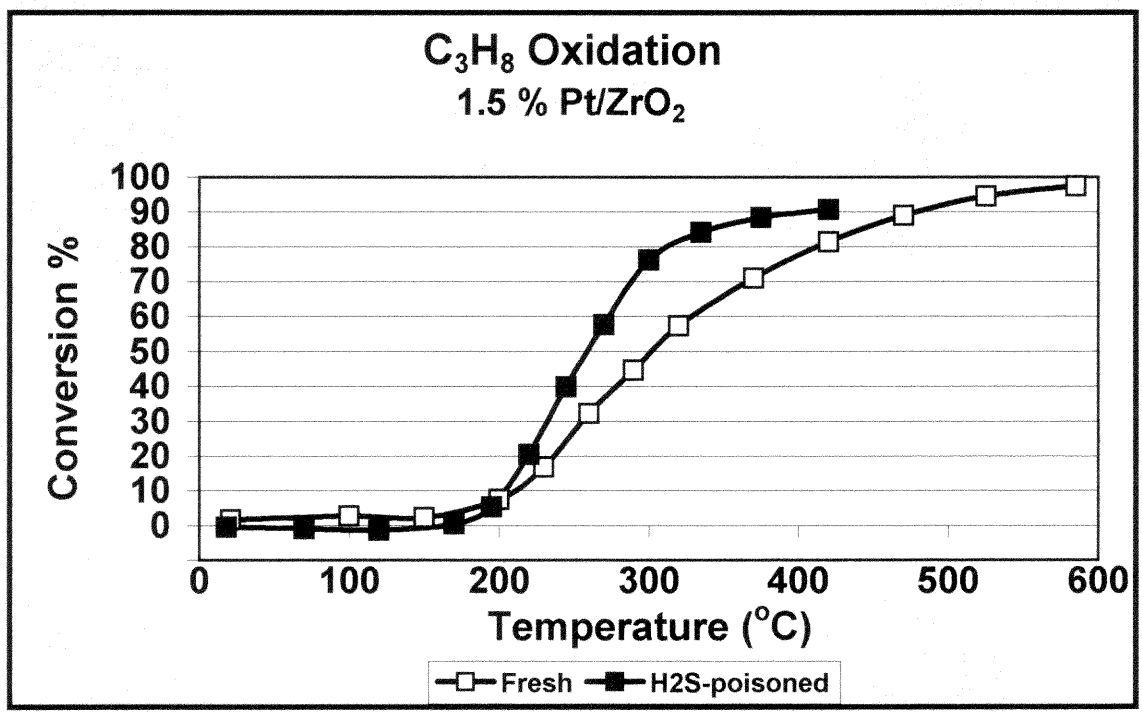

Figure 4.24: Fresh vs. H_2S-poisoned catalyst activity for the oxidation of 1 % C_3H_8 in air on 1.5 % Pt/ZrO_2; GHSV = 85,320. (Poisoning: 200 ppm H_2S/air @ 400°C for 24 hrs.; GHSV = 10,700)

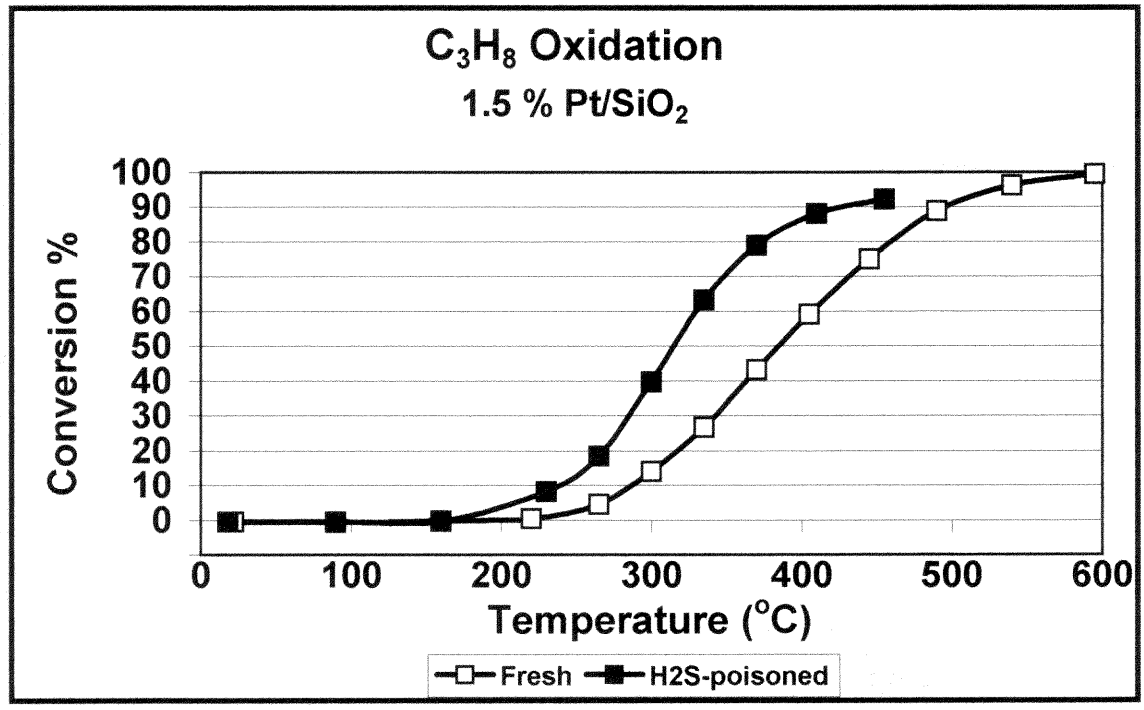

Figure 4.25: Fresh vs. H_2S-poisoned catalyst activity for the oxidation of 1 % C_3H_8 in air on 1.5 % Pt/SiO_2; GHSV = 15,000. (Poisoning: 200 ppm H_2S/air @ 400°C for 24 hrs.; GHSV = 1880)

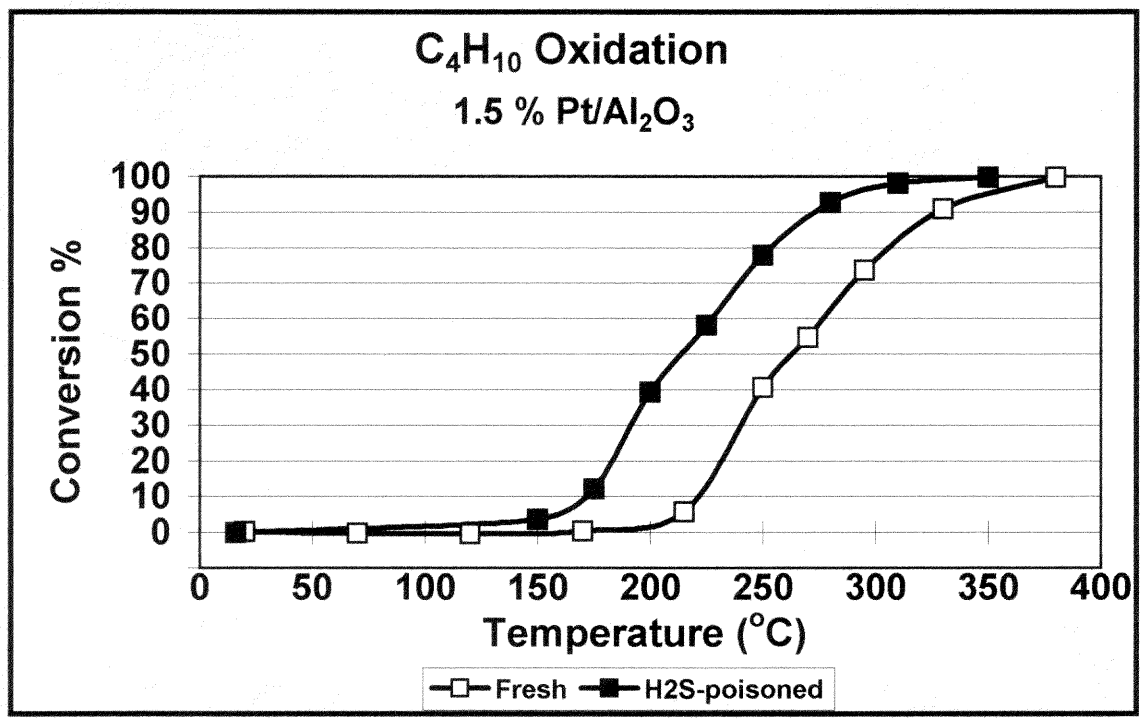

Figure 4.26: Fresh vs. H_2S-poisoned catalyst activity for the oxidation of 1 % C_4H_{10} in air on 1.5 % Pt/γ-Al_2O_3; GHSV = 55,200. (Poisoning: 200 ppm H_2S/air @ 400°C for 24 hrs.; GHSV = 6900)

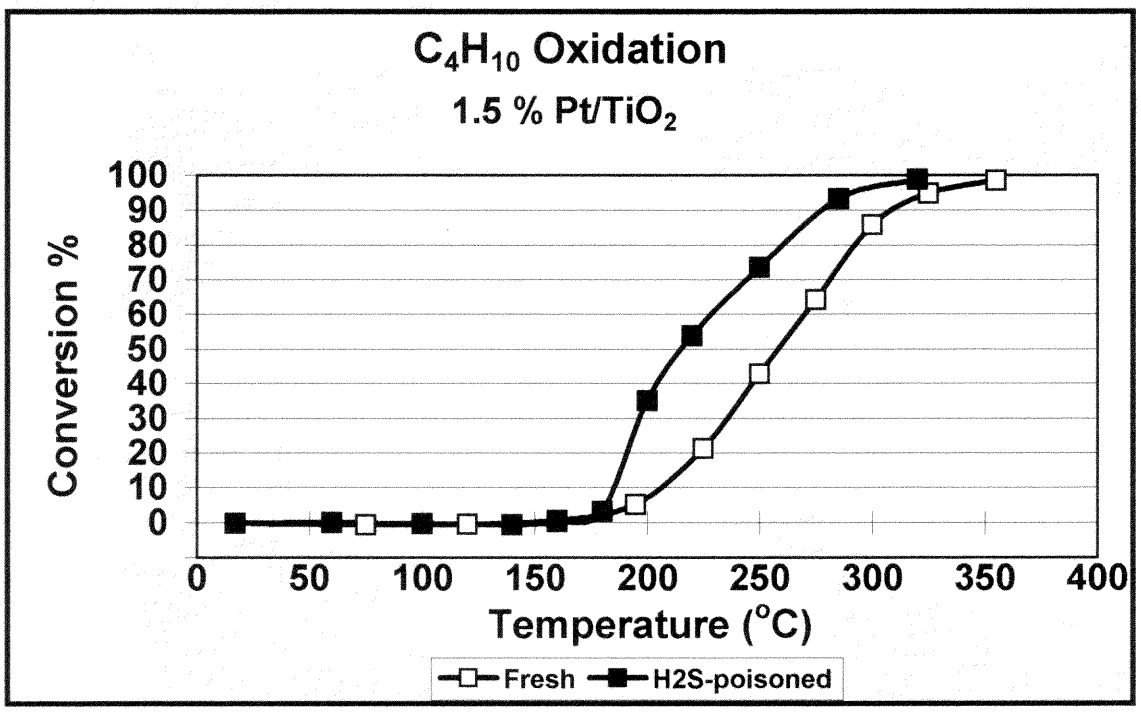

Figure 4.27: Fresh vs. H_2S-poisoned catalyst activity for the oxidation of 1 % C_4H_{10} in air on 1.5 % Pt/TiO_2; GHSV = 52,380. (Poisoning: 200 ppm H_2S/air @ 400°C for 24 hrs.; GHSV = 6550)

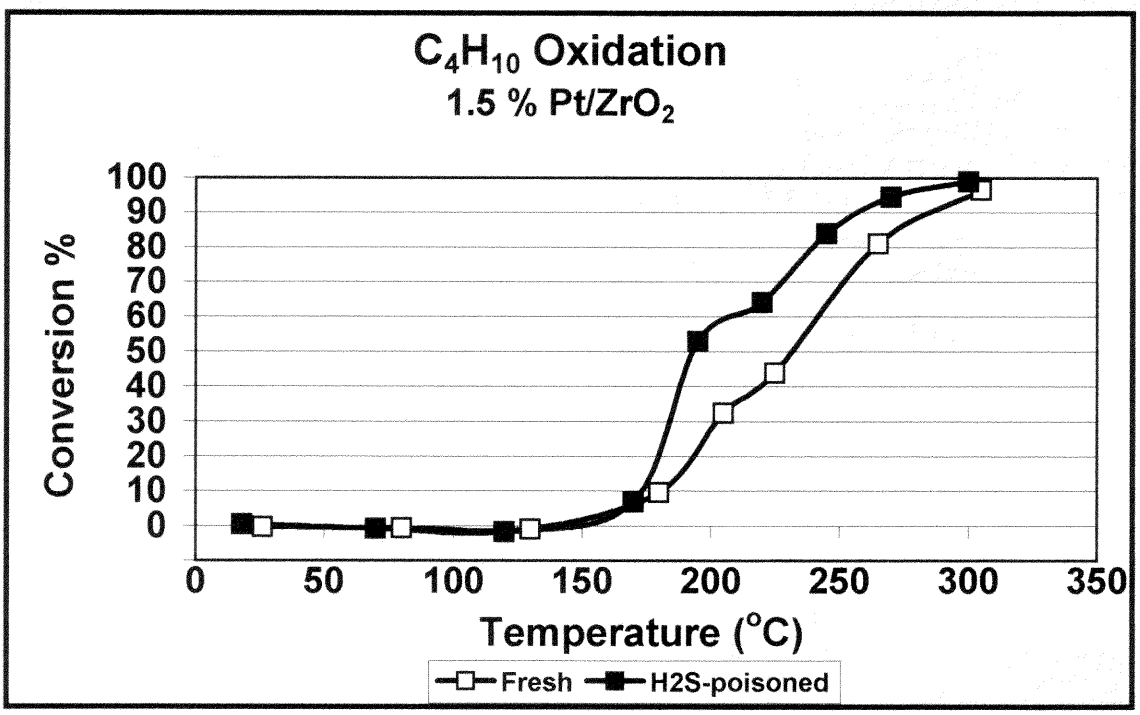

Figure 4.28: Fresh vs. H_2S-poisoned catalyst activity for the oxidation of 1 % C_4H_{10} in air on 1.5 % Pt/ZrO_2; GHSV = 85,320. (Poisoning: 200 ppm H_2S/air @ 400°C for 24 hrs.; GHSV = 10,700)

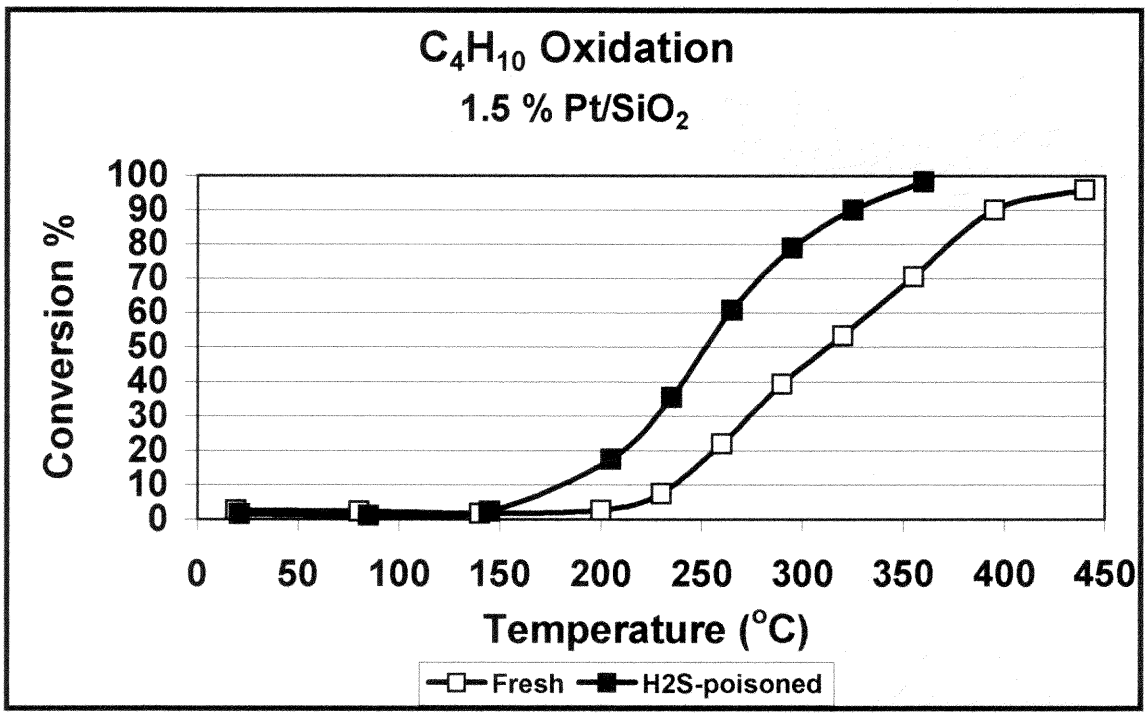

Figure 4.29: Fresh vs. H_2S-poisoned catalyst activity for the oxidation of 1 % C_4H_{10} in air on 1.5 % Pt/SiO_2; GHSV = 15,000. (Poisoning: 200 ppm H_2S/air @ 400°C for 24 hrs.; GHSV = 1880)

4.23, 4.24, and 4.25. Additionally, experiments showed that C_4H_{10} oxidation activity was enhanced by H_2S poisoning on all four catalysts and results are presented in Figures 4.26, 4.27, 4.28, and 4.29. Figure 4.28 shows kinks in the activity curves for C_4H_{10} oxidation on both fresh and H_2S-poisoned Pt/ZrO_2 catalysts occurring in a temperature range of 200-225°C on both curves. The effect is similar to that found in the activity curve for CH_4 oxidation on H_2S-poisoned $Pt/\gamma\text{-}Al_2O_3$ shown in Figure 4.5. Most likely, this is a result of some type of surface transformation occurring in this temperature range. The effect was not observed on other Pt/ZrO_2 activity curves since all of the other reactions studied occurred at significantly lower temperatures or significantly higher temperatures.

The enhancement of C_3H_8 oxidation on $Pt/\gamma\text{-}Al_2O_3$ due to sulfur poisoning has been observed by numerous researchers including Golunski et al. [5], Burch et al. [25], Lambert et al. [27,28,29], and Wang [31]. Burch et al. [26] also observed enhanced C_3H_8 oxidation due to sulfur poisoning of Pt/TiO_2. Wang [31] found enhanced activity for C_3H_8 oxidation on Pt/Al_2O_3, Pt/TiO_2, and Pt/ZrO_2 which had each been poisoned by 100 ppm H_2S in air at 400°C. Contrary to the results presented above in Figure 4.25 however, Wang [31] did not observe an activity enhancement on H_2S-poisoned Pt/SiO_2. Wang's results are in agreement with numerous reports in the literature showing no change in the C_3H_8 oxidation activity of Pt/SiO_2 due to sulfur poisoning, including the work of Burch et al. [25]. Nevertheless, Figure 4.25 clearly shows an enhancement for C_3H_8 oxidation activity on Pt/SiO_2. This result is supported by similar effects observed in Figures 4.21 and 4.29 for C_2H_6 and C_4H_{10} oxidation on Pt/SiO_2. At present, no examples of enhanced alkane activity due to sulfur poisoning of Pt/SiO_2 have been found in the literature.

Very few studies have been reported on the effects of sulfur poisoning on Pt catalyst activity for alkane oxidation for compounds other than C_3H_8. Lambert et al. [7,24] did not observe sulfate-induced enhancement for C_2H_6 oxidation even though enhancement ***was*** observed for C_3H_8 oxidation. These researchers have suggested, in agreement with others, that hydrocarbon oxidation on Pt catalysts is initiated by hydrogen abstraction and that this initial step is enhanced by sulfate on Pt sites or on the support surface. Their conclusion is that enhancement is observed for C_3H_8 rather than C_2H_6 due to the presence of a weaker C-H bond present on the secondary carbon atom of C_3H_8.Although results shown in Figures 4.18, 4.19, 4.20, and 4.21 show enhanced C_2H_6 oxidation activity, Lambert et al.'s explanation may still be valid. Comparing the oxidation of C_2H_6, C_3H_8, and C_4H_{10} on each catalyst, it is clear that the enhancement of the C_2H_6 reaction is much less pronounced than the enhancements observed for the C_3H_8 or the C_4H_{10} oxidation reactions. This seems to substantiate the theory that sulfur poisoning enhances the hydrogen abstraction initialization step. It is then expected that C_2H_6 oxidation enhancement would occur to a lesser degree than that of the larger hydrocarbons since C_2H_6 contains only primary carbon atoms containing stronger C-H bonds then the secondary carbon atoms present in C_3H_8 and C_4H_{10}.

4.1.5 γ-Al_2O_3 Oxidation Activity

As described in Ch. 3, γ-Al_2O_3 was physically mixed with each of the catalysts when conducting the activity experiments. In order to show that the activity observed in the experiments described above did not result from the γ-Al_2O_3 diluent, several activity experiments were carried out using γ-Al_2O_3 only. These activity curves are shown in

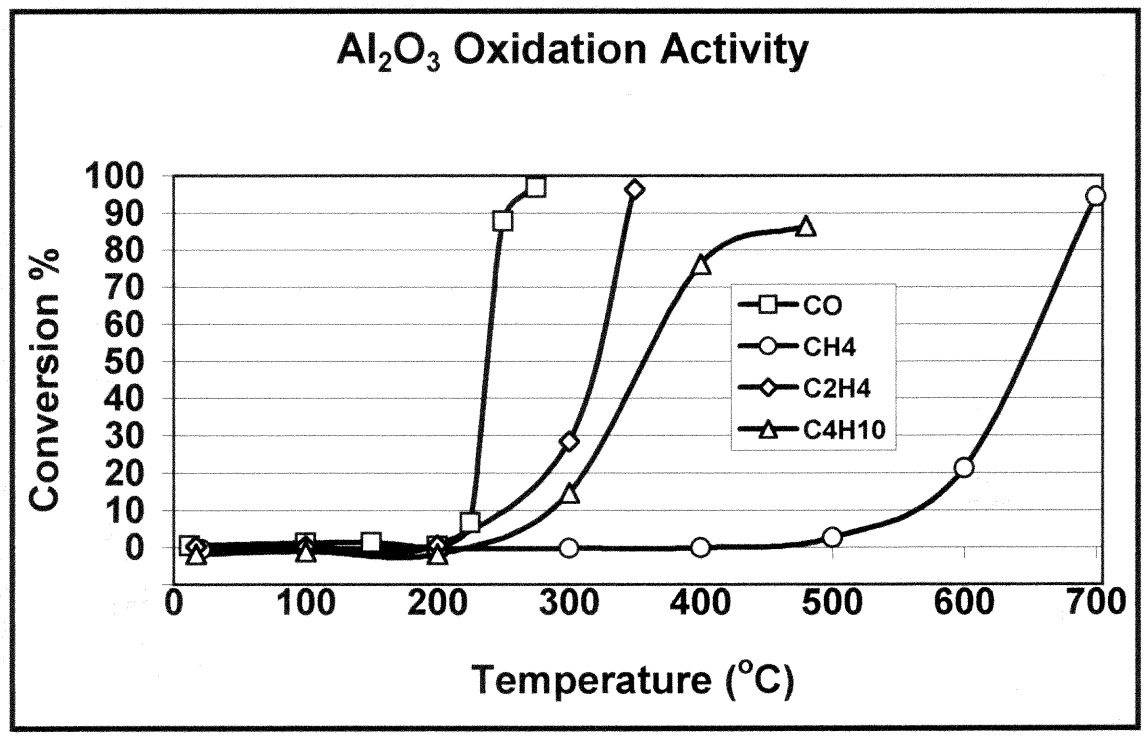

Figure 4.30: Activity of γ-Al_2O_3 for the oxidation of 1 % CO, CH_4, C_2H_4, and C_4H_{10} in air; GHSV = 6800.

Figure 4.30. The oxidation of CO begins on γ-Al_2O_3 at temperatures greater than 200°C. For the each of the four catalysts, both fresh and H_2S-poisoned, the CO oxidation reaction is complete below this temperature and, thus, γ-Al_2O_3 does not contribute to the observed activity of the supported Pt catalysts. A similar analysis of CH_4 oxidation shows that the reaction on most of the supported Pt catalyst samples occurs at lower temperatures than the reaction on γ-Al_2O_3 alone, with the exceptions of H_2S-poisoned Pt/ γ-Al_2O_3 and both fresh and H_2S-poisoned Pt/SiO_2. Even in these cases however, γ-Al_2O_3 probably doesn't contribute to the reaction at conversions lower than 50 %. The oxidation of C_2H_4 occurred on γ-Al_2O_3 at higher temperatures than any of the four Pt catalysts studied and thus, γ-Al_2O_3 did not contribute to the measured catalytic activity of the Pt-containing catalysts. It was assumed that the C_3H_6 and C_2H_2 reactions exhibited similar behavior. Finally, the activity of γ-Al_2O_3 for C_4H_{10} oxidation occurred at a temperature sufficiently high, that only the activity of the fresh Pt/SiO_2 catalyst was appreciably affected by the presence of γ-Al_2O_3. Again, it was assumed, based on the similarity of the reactions, that C_2H_6 and C_3H_8 oxidation activity was not affected by the γ-Al_2O_3 diluent.

4.2 H_2 Chemisorption Measurements

Sulfur poisoning is known to cause significant losses in Pt dispersion on supported Pt catalysts. Often, this loss of dispersion can be directly linked to the loss of catalyst activity associated with sulfur poisoning. Pt dispersion for fresh and H_2S-poisoned catalysts was determined by H_2 chemisorption and results are shown in Table 4.5. A brief discussion of H_2 chemisorption and the experimental procedures are provided in

Ch 3, section 3.4. The experimental data used to calculate each dispersion value is shown in Figures 1-8 in Appendix B.

Table 4.5: H_2 chemisorption data for fresh and H_2S-poisoned Pt catalysts

Catalyst	Fresh	H_2S-poisoned[a]
1.5 % Pt/γ-Al_2O_3	53.6 %	19.6 %
1.5 % Pt/TiO_2	58.0 %	21.9 %
1.5 % Pt/ZrO_2	20.8 %	10.9 %
1.5 % Pt/SiO_2	20.8 %	15.2 %

Note: a) Each catalyst was poisoned with a 200 ppm H_2S/air mixture at 400°C for 24 hrs.

The results show that Pt/γ-Al_2O_3, Pt/TiO_2, and Pt/ZrO_2 experienced significant losses of dispersion due to H_2S poisoning. The dispersion values for H_2S-poisoned Pt/γ-Al_2O_3 and Pt/TiO_2 catalysts were much less than half of the original fresh catalyst values. Pt dispersion on the Pt/ZrO_2 catalyst was reduced by approximately 1/2 following H_2S poisoning while the Pt/SiO_2 catalyst dispersion was reduced by about 1/4. It is important to note that the dispersion loss was the least on Pt/SiO_2, for which the formation of sulfate on the support has not been previously observed.

Although H_2 chemisorption results can directly determine changes in the number of active sites present, the mechanism for such changes is not always evident. In this particular series of experiments, there are at least two possible explanations for the observed losses in dispersion resulting from H_2S poisoning and both explanations are illustrated by the conceptual model presented in Figure 4.31. In this model, the fresh supported Pt catalyst at the top of Figure 4.31 has 9 Pt sites exposed at the surface. Schemes (a) and (b) both show a decrease in the number of exposed Pt sites from 9 to 5, but the mechanisms for the decrease are different. Scheme (a) shows a loss of Pt

Figure 4.31: Schematic showing two alternative pathways for Pt dispersion loss as determined by H_2 chemisorption. The solid line represents the support surface and the gray circles and ellipses are representative of Pt crystals.

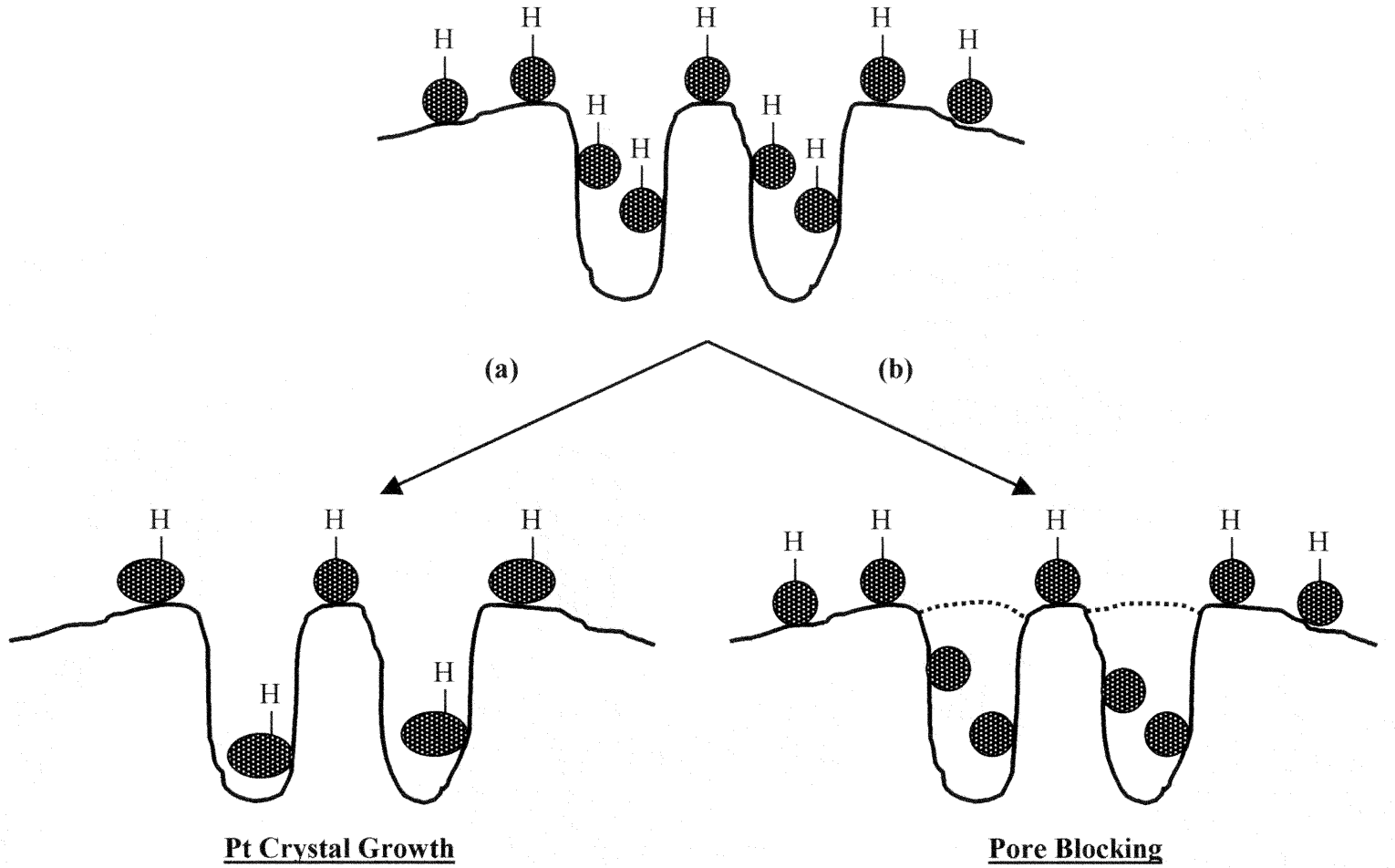

dispersion as a result of Pt crystal growth in which mobile Pt particles coalesce to form larger Pt particles on the support surface with less exposed Pt sites. Alternatively, scheme (b) shows a loss of Pt dispersion cause by the blockage of pores on the support material. In this case the Pt particles to not change size, but reactants are unable to contact with the exposed Pt sites located in the blocked pores.

An additional explanation for the loss of dispersion on sulfur-poisoned catalysts involves the formation of sulfate on exposed Pt sites. Adsorbed sulfate groups could alter the chemisorption of H_2 on exposed Pt sites and, thus, lead to a loss of Pt dispersion as determined by H_2 chemisorption experiments. However, this effect is expected to be small since sulfate groups are known to be more stable on the support surfaces than on Pt sites.

It is possible and extremely likely that H_2S-poisoning causes a combination of Pt crystal growth, sulfate formation on Pt sites, and pore blocking due to sulfate formation on γAl_2O_3, TiO_2, ZrO_2 surfaces. SiO_2 is not observed to form surface sulfates, so it is likely that the observed loss of dispersion is a result of Pt crystal growth and sulfate formation on Pt sites. As noted previously, the loss of dispersion on Pt/SiO_2 was less than that observed on the other catalyst samples presumably due to the absence of pore blocking effects of support sulfate formation. BET surface area analysis can be employed to clarify H_2 chemisorption results. The BET method measures the overall surface area of the metal/support surface while chemisorption experiments essentially measure the area of exposed metal atoms only. If the loss of dispersion is primarily a result of Pt crystal growth, it is expected that the BET surface area would not change much. Conversely, severe dispersion loss due to pore blockage by sulfate formation

would be expected to be accompanied by a large decrease in the BET surface area. BET surface area results are discussed in section 4.3.

The H_2 chemisorption experiments were conducted using a method slightly different from methods commonly used by other researchers. In typical hydrogen chemisorption experiments, the catalyst sample is reduced in hydrogen at an elevated temperature prior to performing the chemisorption step. This is done to provide a clean, reduced surface for metal dispersion determination. However, experiments revealed that Pt dispersion values increased continuously as the hydrogen reduction temperature was increased. After reducing the 1.5 % Pt/γ-Al_2O_3 catalyst sample at 600°C for 2 hours, a dispersion of 90.0 % was obtained. A similar treatment on the H_2S-poisoned 1.5 % Pt/γ-Al_2O_3 catalyst yielded a dispersion of 87.7 %. Thus, it seems that hydrogen treatment caused a re-dispersion of the Pt particles on the γ-Al_2O_3 support yielding a highly dispersed catalyst. However, this highly dispersed state did not exist in the conditions at which the activity experiments were conducted. Consequently, experiments in this study were performed by heating the catalyst samples in N_2 at 600°C in order to remove any adsorbed compounds. In effect, no reduction procedure was performed. This procedure produced dispersion results, which reflected the actual dispersion of the Pt catalysts during activity and poisoning experiments. An important observation is that the H_2S-poisoned Pt/γ-Al_2O_3 catalyst gave a dispersion of 87.7 % following a reduction at 600°C. This is comparable to the value of 90.0 % found for a similarly treated fresh Pt/γ-Al_2O_3 catalyst and appears to indicate that the reduction procedure may have been sufficient to regenerate the H_2S-poisoned catalyst. No regeneration studies were performed in this study, however.

4.3 BET Surface Area Measurements

The overall surface areas of fresh and H_2S-poisoned Pt catalysts were determined using the BET method as described in Ch. 3, section 3.5, and results are present in Table 4.6. The results show a small decrease in surface area for Pt/γ-Al_2O_3 and a larger decrease on Pt/TiO_2 and Pt/ZrO_2 after H_2S poisoning. The effect of H_2S poisoning on Pt/SiO_2 was negligible.

Table 4.6: BET surface area data for fresh and H_2S-poisoned Pt catalysts. All values are reported in m^2/g.

Catalyst	Fresh	H_2S-poisoned[a]
1.5 % Pt/γ-Al_2O_3	77	65
1.5 % Pt/TiO_2	40	31
1.5 % Pt/ZrO_2	64	48
1.5 % Pt/SiO_2	132	134

Notes: a) Each catalyst was poisoned with a 200 ppm H_2S/air mixture at 400°C for 24 hrs.

The small change in surface area on Pt/γ-Al_2O_3, combined with the large decrease in Pt dispersion seen in Table 4.5, clearly indicates that H_2S-poisoning resulted in a significant amount of Pt crystal growth and a relatively smaller amount of pore blockage due to sulfate formation on the γ-Al_2O_3 support surface. This has important implications for sulfur-induced activity effects on Pt/γ-Al_2O_3 since Pt crystal growth causes an increase in the mean particle size and associated changes in activity. Some evidence exists in the literature suggesting that larger Pt particle sizes are more active for alkane oxidation reactions. Specifically, Lambert et al. [29] suggest that larger Pt particles may be more active for hydrogen abstraction or C-H bond scission, the initial step in alkane oxidation. Thus, the enhancement of alkane oxidation observed on Pt/γ-Al_2O_3, as well as

on the other H_2S-poisoned catalysts, can be partially explained by the increase in Pt particle size resulting from the agglomeration of Pt particles.

The decreases in surface area caused by H_2S-poisoning of Pt/TiO_2 and Pt/ZrO_2 were relatively large and seem to indicate a substantial amount of pore blocking due to sulfate formation on the support surface. However, this information, combined with the decreases in Pt dispersion shown in Table 4.5, is not sufficient to determine the relative amounts of Pt crystal growth and sulfate formation that have occurred due to H_2S-poisoning. Most likely a combination of both has occurred.

The negligible effect of H_2S-poisoning on Pt/SiO_2 surface area was expected since sulfate has not been observed to form on SiO_2 surfaces. Thus, the decrease in dispersion from 20.8 % to 15.2 % can be primarily attributed to Pt crystal growth on the catalyst surface. Pt crystal growth results in an increase in the mean Pt particle size which is likely to be responsible for the enhanced oxidation activity of H_2S-poisoned Pt/SiO_2 for alkane oxidation. The mechanism for this effect is described above.

4.4 FTIR Analysis

FTIR spectroscopy was used to determine the existence and composition of sulfur compounds residing on the catalyst surfaces following H_2S poisoning. For each catalyst the absorbance spectrum of a fresh sample was subtracted from the absorbance spectrum of an H_2S-poisoned sample to obtain a difference spectrum. These spectra are shown in Figures 4.32, 4.33, 4.34, and 4.35 for 1.5% Pt/γ-Al_2O_3, 1.5 % Pt/TiO_2, 1.5 % Pt/ZrO_2 and 1.5 % Pt/SiO_2, respectively.

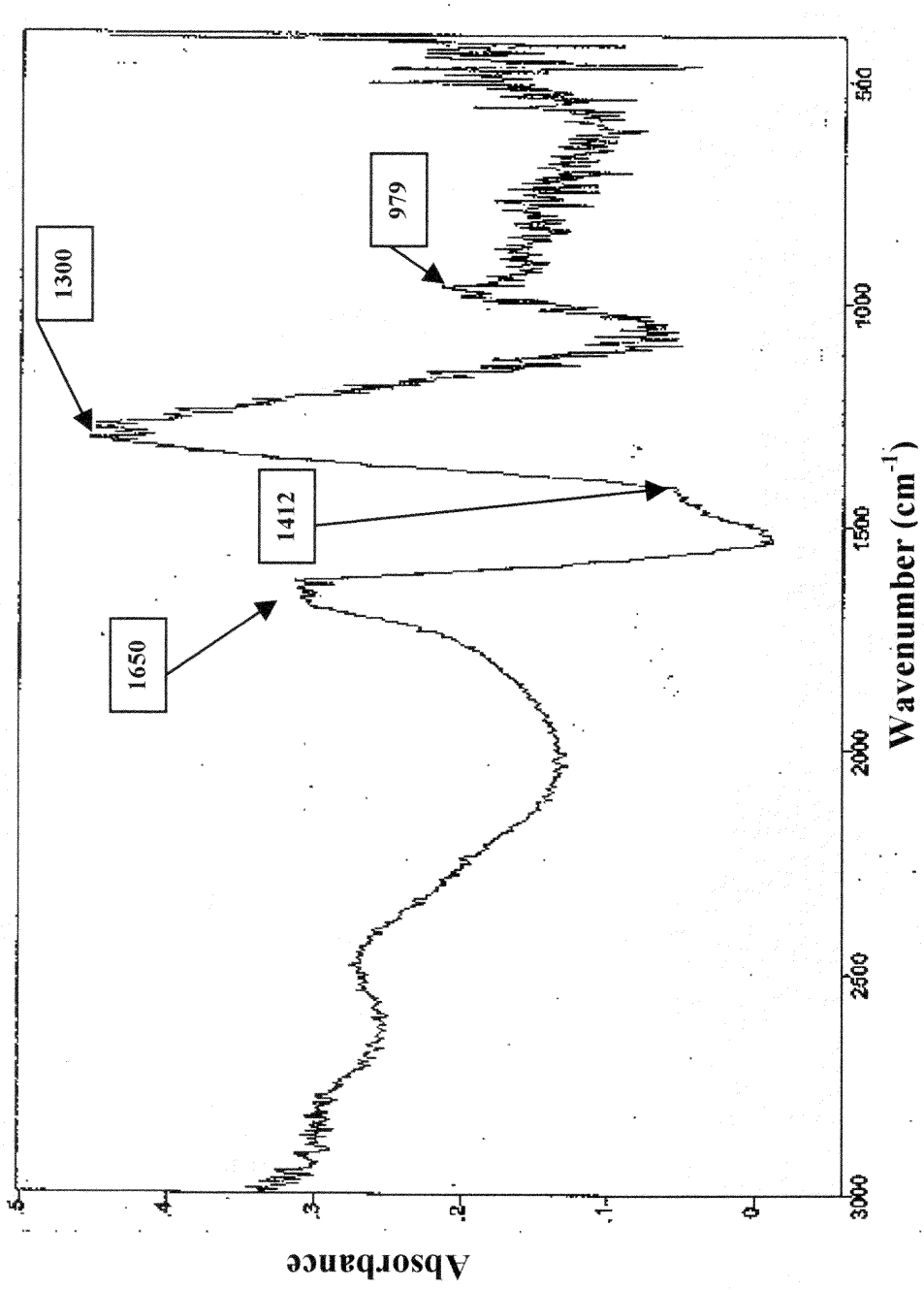

Figure 4.32: FTIR spectrum resulting from the subtraction of the fresh 1.5 % Pt/γ-Al_2O_3 spectrum from the H_2S-poisoned 1.5 % Pt/γ-Al_2O_3 spectrum.

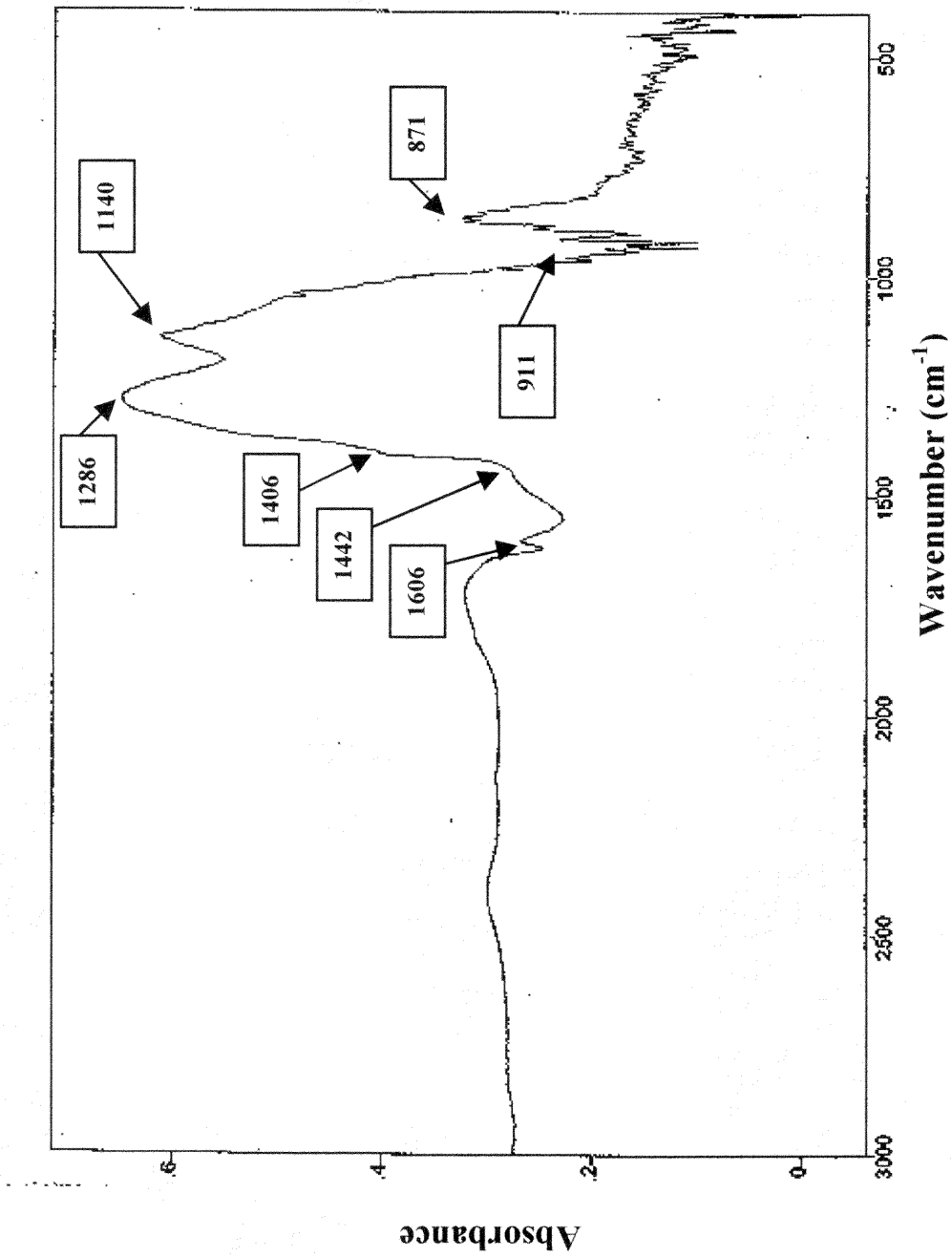

Figure 4.33: FTIR spectrum resulting from the subtraction of the fresh 1.5 % Pt/TiO_2 spectrum from the H_2S-poisoned 1.5 % Pt/TiO_2 spectrum.

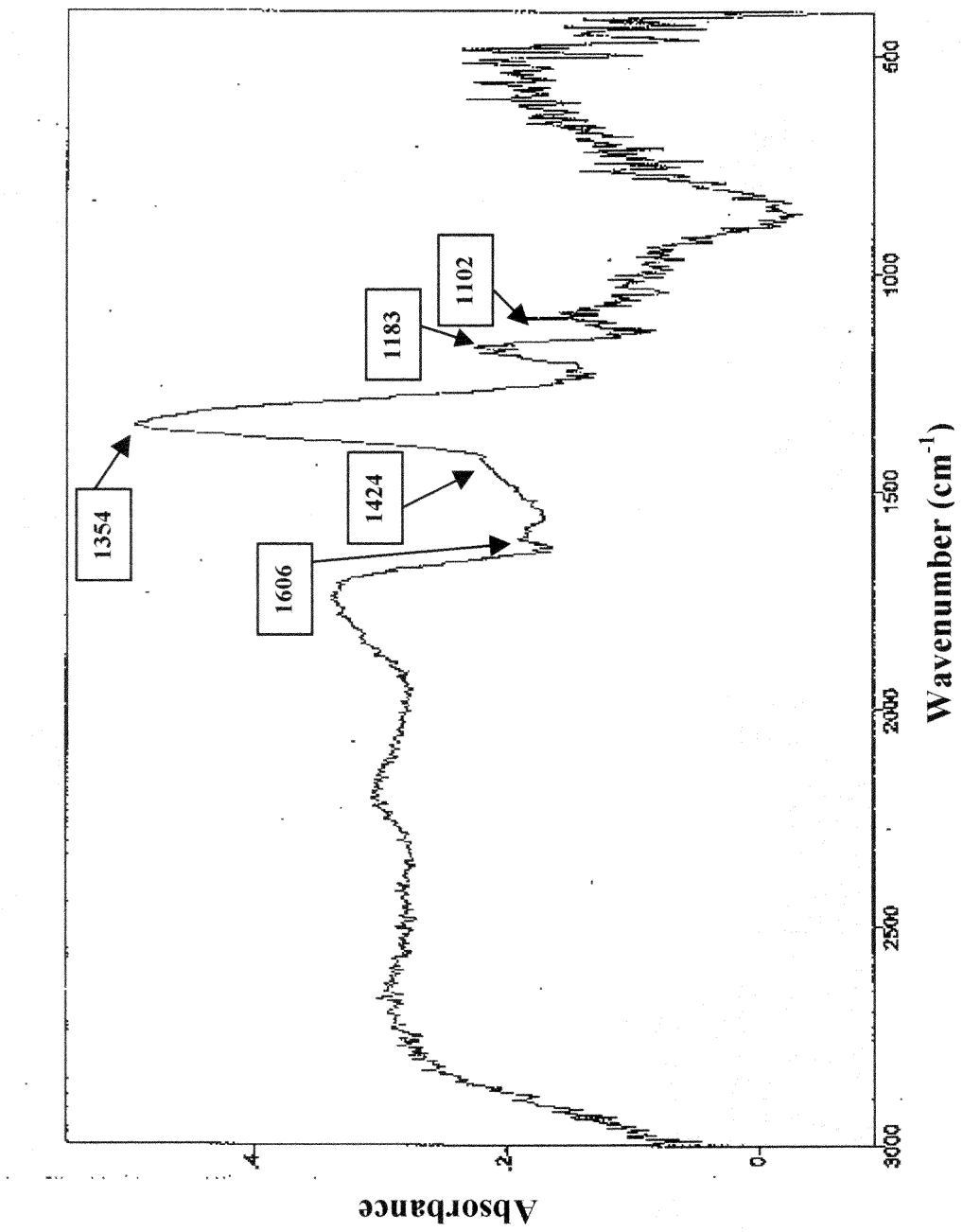

Figure 4.34: FTIR spectrum resulting from the subtraction of the fresh 1.5 % Pt/ZrO_2 spectrum from the H_2S-poisoned 1.5 % Pt/ZrO_2 spectrum.

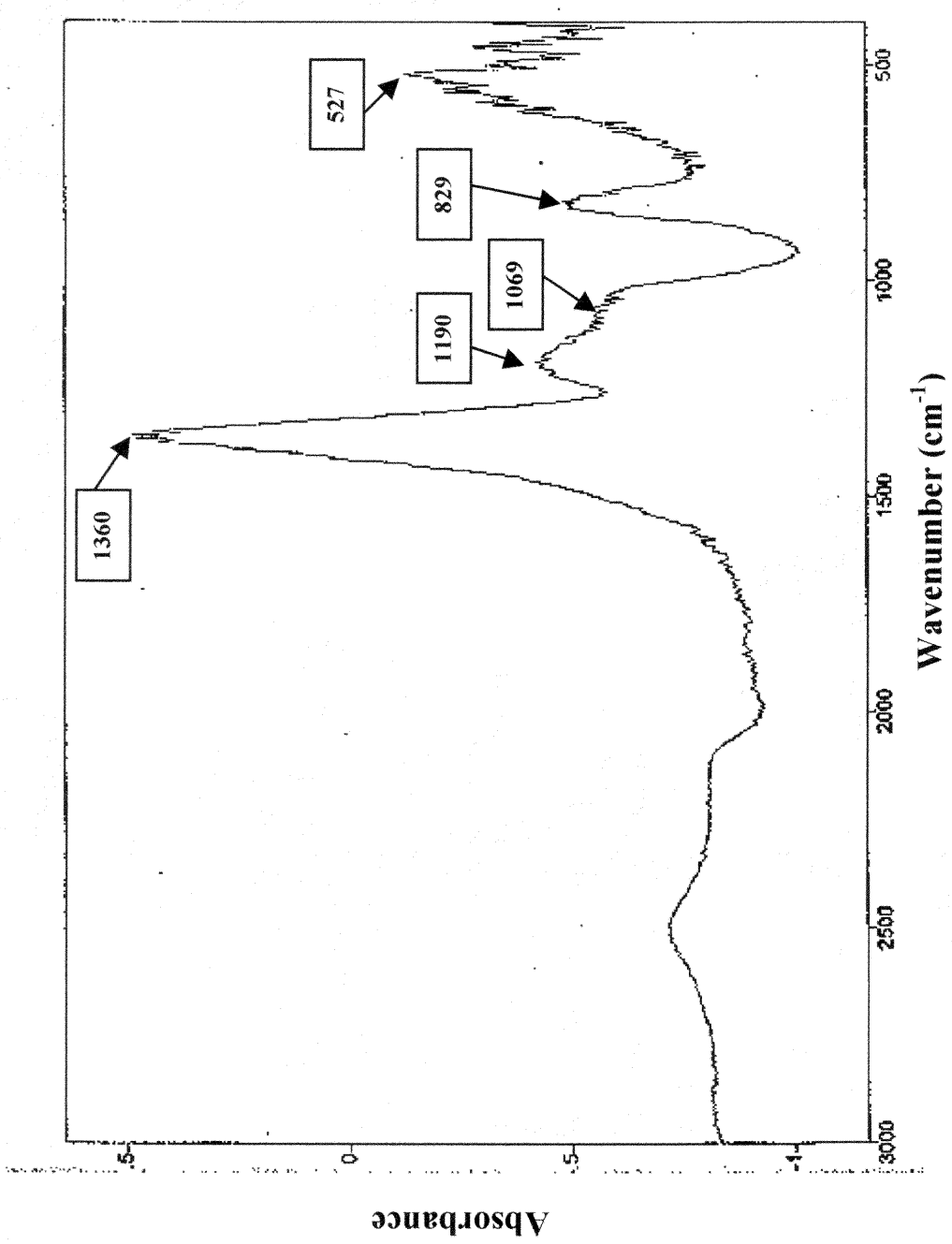

Figure 4.35: FTIR spectrum resulting from the subtraction of the fresh 1.5 % Pt/SiO_2 spectrum from the H_2S-poisoned 1.5 % Pt/SiO_2 spectrum.

A general description of expected IR absorption frequencies for various sulfite and sulfate ions and coordinated complexes is presented in Figure 4.36 [14]. Structures (a), (b), and (c) show the expected absorption frequencies for the free sulfite ion, sulfur-coordinated sulfite ion, and oxygen-coordinated sulfite ion, respectively. Structures (d), (e), and (f) show absorption frequencies for a unidentate oxygen-coordinated sulfate ion, a chelating bidentate oxygen-coordinated sulfate ion, and a bridged bidentate oxygen-coordinated sulfate ion, respectively. Finally, structure (g) lists the absorption frequencies for molecular sulfate compounds.

For molecular sulfate compounds, the IR bands at 1440-1350 cm^{-1} and 1230-1150 cm^{-1} are generally quite strong, corresponding to the asymmetric and symmetric S=O stretching frequencies. Many researchers have observed these bands following sulfur oxidation on Al_2O_3 surfaces including Deo et al. [10], Chang [11], and Okamoto et al. [12].

FTIR results for the four H_2S-poisoned catalysts studied show a variety of overlapping absorbance peaks in the 1400-900 cm^{-1} range which are all indicative of the presence of sulfur compounds on the catalyst surfaces. Most likely, sulfur exists in several different forms on each catalyst, including all three types of coordinated sulfate ions and molecular sulfate compounds. This may be the reason for the poor resolution observed for peaks found in this region. The existence of sulfite ions was not expected but could not be ruled out based on FTIR results.

The FTIR spectrum for H_2S-poisoned Pt/γ-Al_2O_3 shown in Figure 4.32 shows an absorption band at 1650 cm^{-1} (corresponding to adsorbed water), a strong band at 1300 cm^{-1} and a small peak at 979 cm^{-1}. The absorption band at 1300 cm^{-1} probably

Figure 4.36: IR absorption frequencies and symmetry groups for selected sulfite and sulfate groups [14]

Sulfite ions:

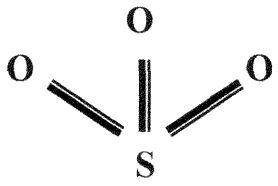

(a) C_{3v}

1010 cm^{-1}
961 cm^{-1}

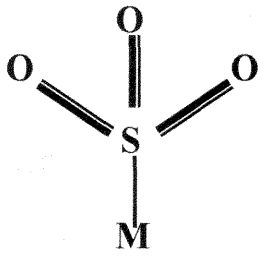

(b) C_{3v}

1120-1050 cm^{-1}
985-940 cm^{-1}

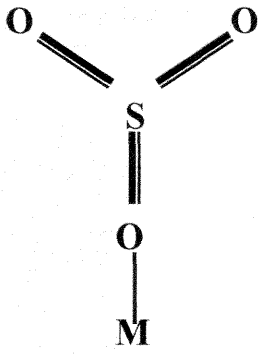

(c) C_s

985-940 cm^{-1}
902 cm^{-1}
862 cm^{-1}

Sulfate ions:

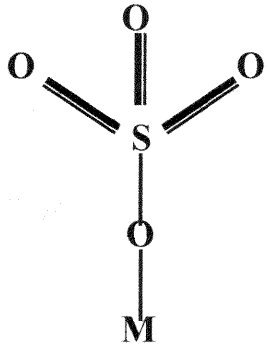

(d) C_{3v}

1147-1117 cm^{-1}
1044-1032 cm^{-1}
970 cm^{-1}

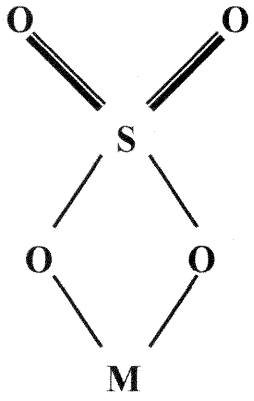

(e) C_{2v}

1240-1230 cm^{-1}
1125-1090 cm^{-1}
1035-995 cm^{-1}
960-940 cm^{-1}

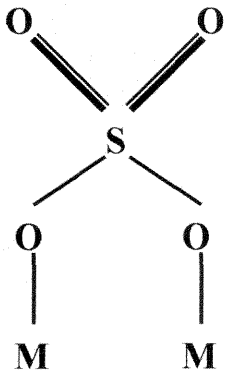

(f) C_{2v}

1195-1160 cm^{-1}
1110-1105 cm^{-1}
1035-1030 cm^{-1}
990-960 cm^{-1}

Sulfate compounds and molecular sulfuric acid:

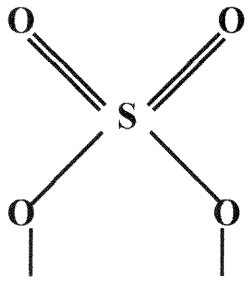

(g) C_{2v}

1440-1350 cm^{-1}
1230-1150 cm^{-1}
1000-960 cm^{-1}
910 cm^{-1}

indicates the formation of molecular sulfate, although it occurs slightly below the expected range of 1440-1350 cm^{-1}. This peak is strong and may obscure smaller peaks at lower wavelengths that correspond to adsorbed sulfate ions. The peak at 979 cm^{-1} may be a result of molecular sulfate or coordinated sulfate ions.

The results for Pt/TiO_2, shown in Figure 4.33, show a small band at 1606 cm^{-1}, which is an indication of adsorbed H_2O. A shoulder at 1406 cm^{-1} may be a result of molecular sulfate formation. However, this peak is partially obscured by two strong, overlapping absorption bands at 1286 and 1140 cm^{-1}, which appear to suggest that sulfur exists mostly as coordinated sulfate ions on the Pt/TiO_2 catalyst surface. A sharp peak at 911 cm^{-1}, however also reveals the presence of molecular sulfate and the sharp peak at 871 cm^{-1} may be an indication of the presence of adsorbed sulfite ions.

Figure 4.34 shows the typical H_2O absorption band at 1606 cm^{-1} as well as a strong absorption band at 1354 cm^{-1} resulting from the formation of molecular sulfate on Pt/ZrO_2. Smaller peaks at 1183 and 1102 cm^{-1} may correspond to molecular sulfate and/or coordinated sulfate ions.

A surprising result was found for the H_2S-poisoned Pt/SiO_2 catalyst shown in Figure 4.35. A strong absorption band is present at 1360 cm^{-1}, which is indicative of molecular sulfate formation. Two smaller bands at 1190 and 1069 also suggest the presence of molecular sulfate or adsorbed sulfate ions. Sulfur compounds and ions are not known to form on SiO_2 catalyst supports, so it is proposed that the observed sulfur species are present on the Pt metal sites only.

This raises the question of whether the sulfur compounds found on $Pt/\gamma\text{-}Al_2O_3$, Pt/TiO_2, and Pt/ZrO_2 are present on the support surface or Pt metal sites. On these

catalysts, sulfur compounds are thought to be more stable on the support surface. However, the presence of small amounts of sulfur compounds on active Pt sites cannot be ruled out.

4.5 Temperature-Programmed Reduction Results

Further evidence for the formation of sulfate on the catalyst surfaces is provided by temperature-programmed reduction (TPR) studies. TPR profiles for fresh and H_2S-poisoned catalysts are compared in Figures 4.37, 4.38, 4.39, and 4.40. Each figure shows TPR plots for both fresh and H_2S-poisoned catalysts on the same graph for easy comparison.

Figure 4.37 reveals a huge difference in the TPR profile between fresh and H_2S-poisoned Pt/γ-Al_2O_3. In fact, Pt/γ-Al_2O_3 showed the largest change in TPR profile due to H_2S-poisoning of all four catalysts studied, indicating that it is the most heavily sulfated catalyst of the group. The detector signal for the H_2S-poisoned Pt/γ-Al_2O_3 reduction peak is so much larger than the signal maxima observed on the fresh sample that the fresh Pt/γ-Al_2O_3 TPR plot cannot be observed on the same y-scale. Thus, the insert in Figure 4.37 shows the TPR plot for the fresh catalyst with a much expanded signal axis. Fresh Pt/γ-Al_2O_3 shows several overlapping peaks including two similar sized peaks at 216°C and 298°C as well as two larger peaks at 419°C and 475°C. The peaks at 419°C and 475°C closely match peaks found for the fresh Pt/TiO_2 and Pt/SiO_2 catalysts (see Figures 4.38 and 4.40) and may correspond to the reduction of oxidic Pt particles. The TPR plot for H_2S-poisoned Pt/γ-Al_2O_3 is characterized by a strong hydrogen uptake peak

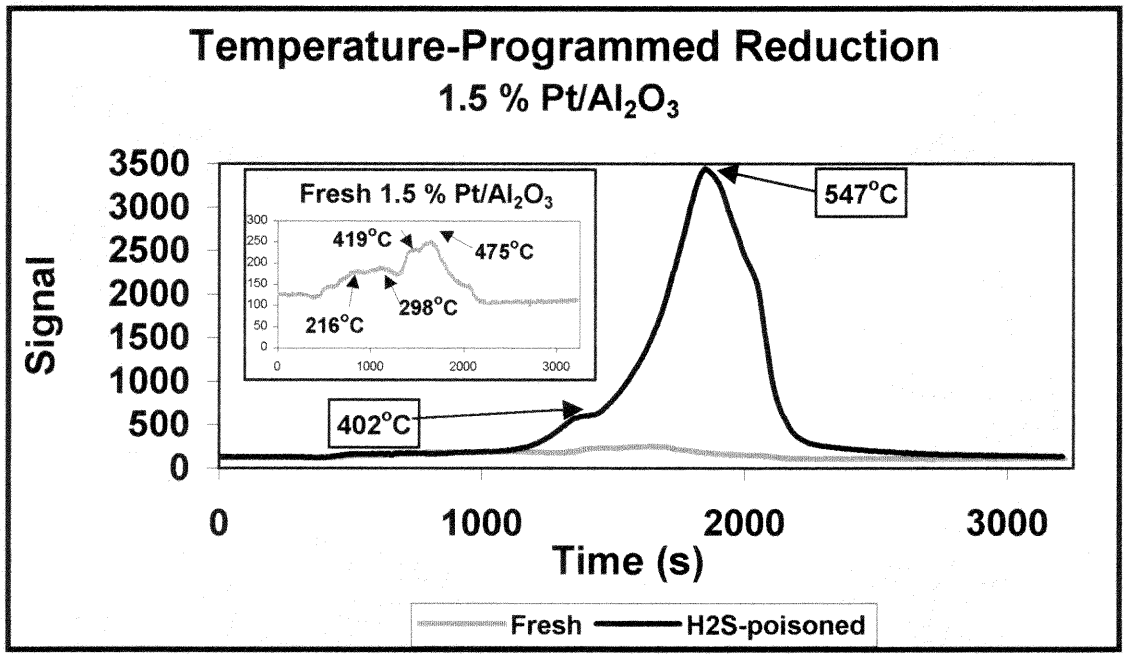

Figure 4.37: Temperature-programmed reduction plots for fresh and H_2S-poisoned 1.5 % Pt/γ-Al_2O_3

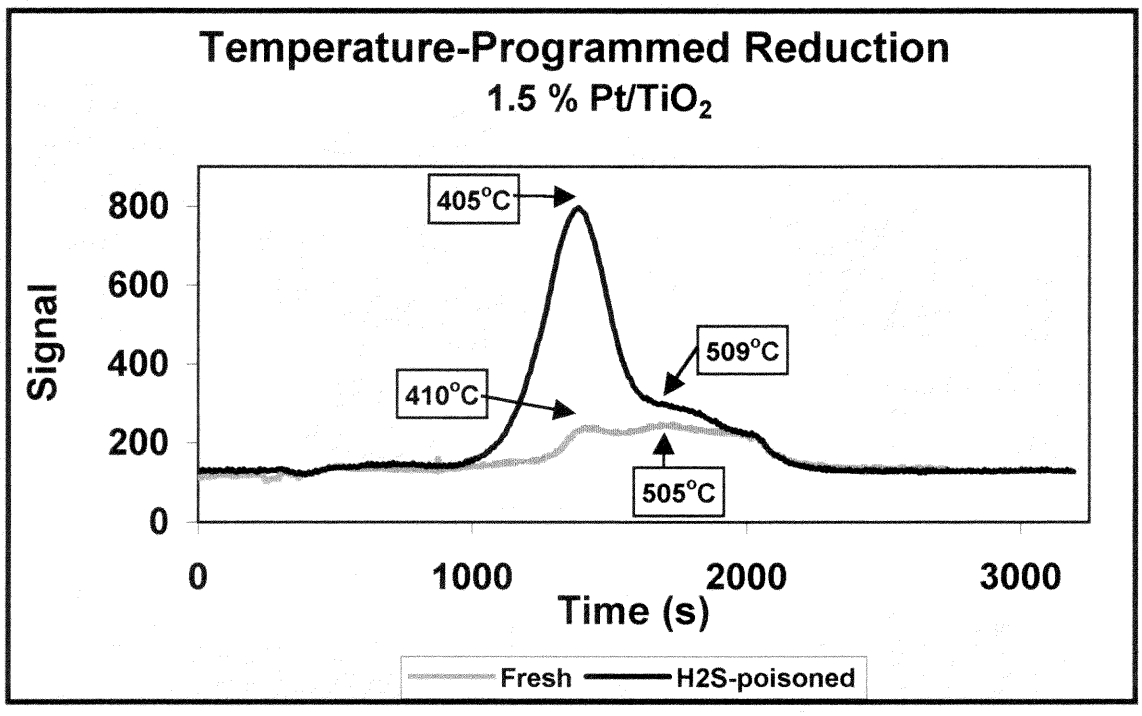

Figure 4.38: Temperature-programmed reduction plots for fresh and H_2S-poisoned 1.5 % Pt/TiO_2

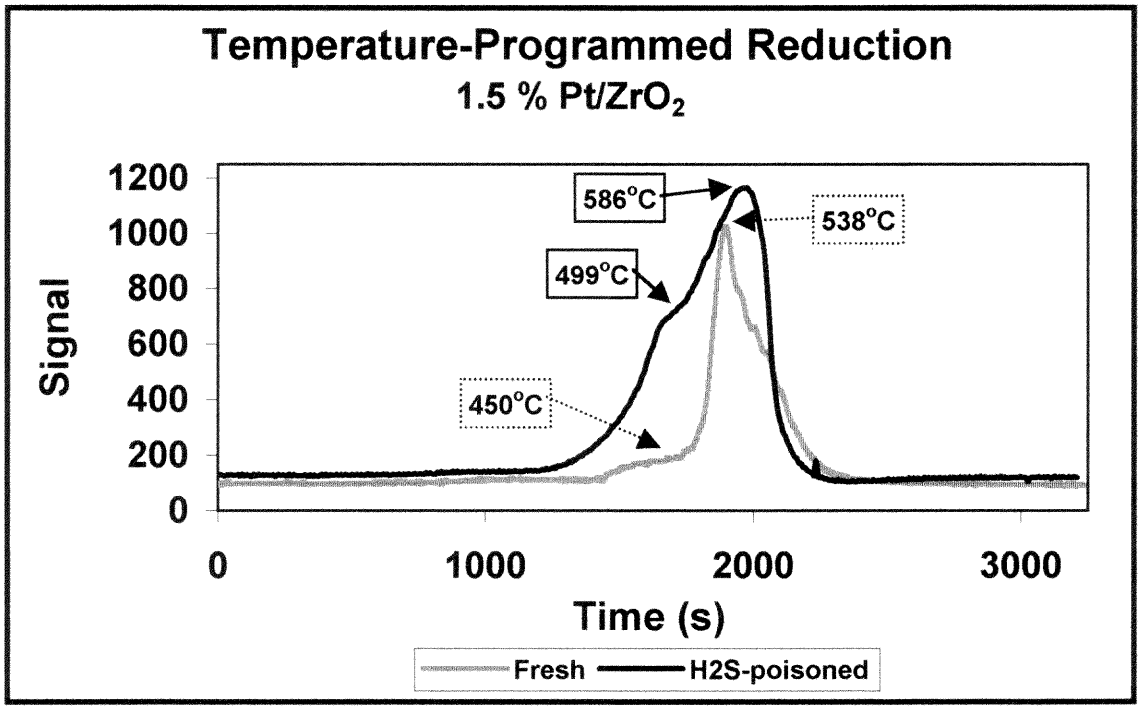

Figure 4.39: Temperature-programmed reduction plots for fresh and H_2S-poisoned 1.5 % Pt/ZrO_2

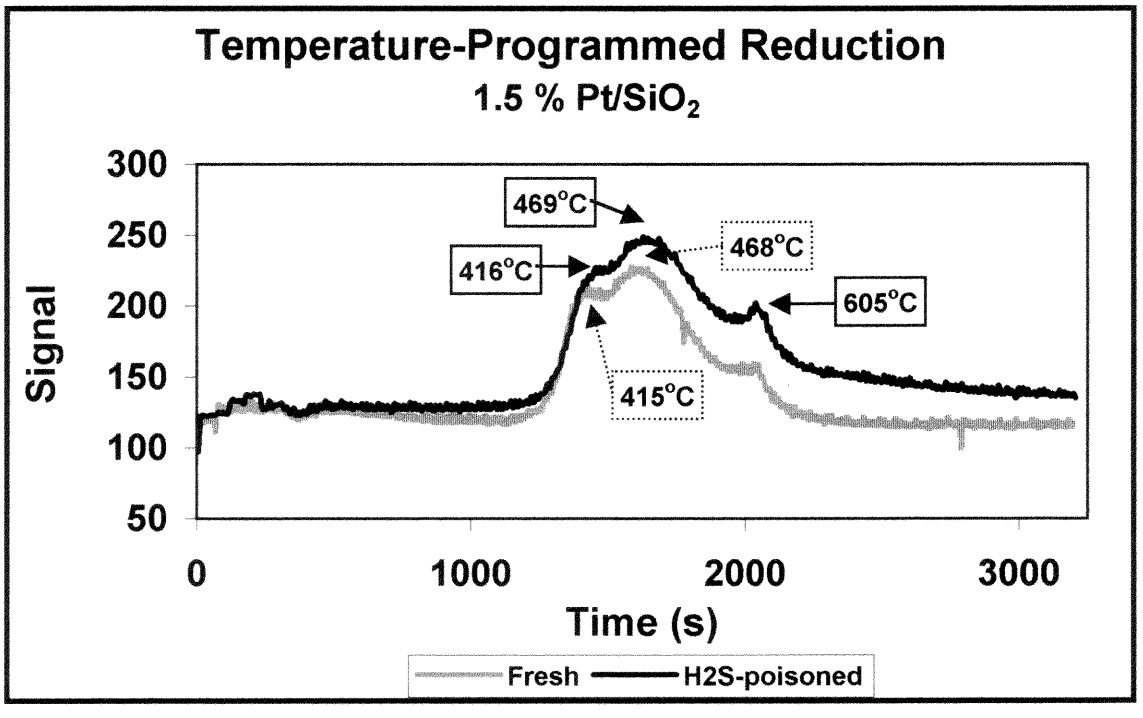

Figure 4.40: Temperature-programmed reduction plots for fresh and H_2S-poisoned 1.5 % Pt/SiO_2

centered at 547°C with a much smaller shoulder at 402°C. This large peak at 547°C probably corresponds to the reduction of aluminum sulfate on the catalyst surface.

TPR plots for fresh and H_2S-poisoned Pt/TiO_2 shown in Figure 4.38 also show a large change in TPR profile following H_2S-poisoning. Fresh Pt/TiO_2 yields two overlapping reduction peaks at 410°C and 505°C, which are similar in appearance and location to the peaks found for fresh $Pt/\gamma\text{-}Al_2O_3$ and Pt/SiO_2. As postulated in the preceding paragraph, these peaks probably result from the reduction of oxidic Pt particles. The TPR profile for H_2S-poisoned Pt/TiO_2 exhibits a strong reduction peak at 405°C with a shoulder at 509°C. This is in marked contrast to the TPR profile shown in Figure 4.37 for $Pt/\gamma\text{-}Al_2O_3$ where the positions of the peak and shoulder are reversed. The results are consistent with the FTIR analysis for H_2S-poisoned Pt/TiO_2 in which it was suggested that sulfate exists mainly as coordinated sulfate ions on the TiO_2 surface. The reduction peak at 405°C is most likely attributable to these coordinated sulfate ions and the shoulder present at 509°C may indicate a small amount of titanium sulfate. However, the signal for this shoulder is not that much greater than that of a similar peak observed for fresh Pt/TiO_2 and the presence of titanium sulfate should be considered minimal. In the previous paragraph, the reduction peak at 547°C on $Pt/\gamma\text{-}Al_2O_3$ was assigned to the reduction of aluminum sulfate. No assignment was made for the shoulder at 402°C, however, and it is likely that this peak is also a result of coordinated sulfate ions on the $\gamma\text{-}Al_2O_3$ surface.

The TPR plot for fresh Pt/ZrO_2 (Figure 4.39) is characterized by a strong reduction peak centered at 538°C and a smaller, partially obscured shoulder at 450°C. Pt/ZrO_2 is the most highly reducible of the four catalysts studied. Although the detector

signal heights for the TPR peaks for fresh and H_2S-poisoned Pt/ZrO_2 appear smaller than the peak observed for H_2S-poisoned $Pt/\gamma\text{-}Al_2O_3$, this is only because it was necessary to decrease the detector current for the Pt/ZrO_2 experiments in order to prevent the peaks from going off-scale. Both fresh and H_2S-poisoned Pt/ZrO_2 TPR peaks are, in fact, larger than the H_2S-poisoned $Pt/\gamma\text{-}Al_2O_3$ peak. In the TPR plot for H_2S-poisoned Pt/ZrO_2, it appears as if the shoulder observed on the fresh catalyst has shifted to 499°C and is much stronger on the H_2S-poisoned catalyst. Additionally, the original peak at 538°C may be obscured by a larger peak centered at 586°C, which probably corresponds to the reduction of sulfate on the catalyst support. This large peak with a low temperature-side shoulder is comparable in appearance to a similar peak and shoulder shown in the TPR plots for $Pt/\gamma\text{-}Al_2O_3$ and probably result from the reduction of zirconium sulfate and coordinated sulfate ions, respectively.

The TPR results for Pt/SiO_2 confirm the presence of a small amount of sulfate on the catalyst surface as found in the FTIR studies. This is evident in Figure 4.40 as the small peak at 605°C for H_2S-poisoned Pt/SiO_2. A kink in the plot occurs at a similar point for fresh Pt/SiO_2 but this is most likely an effect of the experimental procedure. In the TPR experiments, the furnace temperature was programmed to increase to 600°C and the furnace was then held at this temperature for 20 minutes. The point on the TPR plot at which the furnace stops heating is characterized by a small, but rapid decrease in the detector signal. Thus, it was concluded that the apparent shoulder present at approximately 600°C in the TPR plot of for fresh Pt/SiO_2 is not significant. However, the H_2S-poisoned Pt/SiO_2 sample clearly shows a signal increase at 605°C as well as a broad H_2 uptake over the course of the 20 minute temperature-hold. Other peaks on the plots

are almost identical for the fresh and H_2S-poisoned Pt/SiO_2 catalysts. As proposed above in section 4.4, the TPR results seem to support the contention that a small amount of sulfate exists on the Pt surface and this adsorbed sulfate may also contribute to the enhancement of alkane oxidation observed on H_2S-poisoned Pt/SiO_2 catalysts.

4.6 Temperature-Programmed Desorption Experiments

Heterogeneous catalytic reactions generally proceed through the following steps: bulk diffusion of gaseous reactants to the catalyst surface; diffusion of the reactants through the pore structure of the catalyst; adsorption of reactants on the active sites; reaction at the active sites; desorption of the products from the active sites; diffusion of the products through the pore network; and diffusion into the bulk gas. Temperature-programmed desorption (TPD) experiments were conducted in order to determine the role that the third step (adsorption of reactants) plays in the activity changes observed for H_2S-poisoned Pt catalysts.

4.6.1 C_3H_8 Adsorption

The adsorption and temperature-programmed desorption of C_3H_8 was investigated on fresh and H_2S-poisoned catalysts. C_3H_8 was chosen as an adsorbate since many researchers have attributed an enhanced interaction between C_3H_8 and the catalyst surface as a mechanism for the enhancement of C_3H_8 oxidation on sulfur-poisoned Pt catalysts. Lambert et al. [29] concluded that sulfate formation on both Pt metal sites and on the Al_2O_3 surface results in enhanced C-H bond activation and a subsequent enhancement of oxidation activity. Burch e. al. [25] also conclude that sulfate formation on Al_2O_3 in close proximity to Pt sites yields surface sites active for C-H bond activation.

The TPD plots for C_3H_8 on fresh and H_2S-poisoned Pt catalysts are shown in Figures 4.41, 4.42, 4.43, and 4.44, and several observations can be made from these results.

H_2S-poisoning appears to have a large effect on the adsorption characteristics for C_3H_8 on $Pt/\gamma\text{-}Al_2O_3$ and Pt/ZrO_2. For both catalysts, H_2S-poisoning results in a substantial increase in the total C_3H_8 adsorbed as shown by the peak areas given in Figures 4.41 and 4.43. Additionally, the desorption peak maxima for H_2S-poisoned catalysts are shifted to lower temperatures and, the temperatures at which desorption initially occurs are also shifted to lower temperatures. These effects indicate an increase in reactivity for C_3H_8 adsorbed on H_2S-poisoned Pt/Al_2O_3 and Pt/ZrO_2. This increase in reactivity, as determined by the TPD plots, must be related to sulfate formed on the support surface. Although C_3H_8 activity may also be enhanced due to the formation of sulfate on Pt sites, this additional activity is not likely to be detected by this technique. The Pt is present in a small amount (1.5 % by weight) and adsorption of C_3H_8 on Pt sites is probably beyond the detection limits of the experimental apparatus.

The results for Pt/TiO_2 are shown in Figure 4.42 and indicate only a very small increase in C_3H_8 adsorption following H_2S-poisoning. In fact the adsorption of C_3H_8 was very low on both fresh and H_2S-poisoned Pt/TiO_2 and close to the detection limit of the instrument. The noisy signal evident in Figure 4.42 is partially a result of the expanded signal axis. Results for Pt/TiO_2 indicate that the activity enhancement for alkane oxidation due to H_2S-poisoning is primarily associated with reactivity changes on the Pt metal sites only.

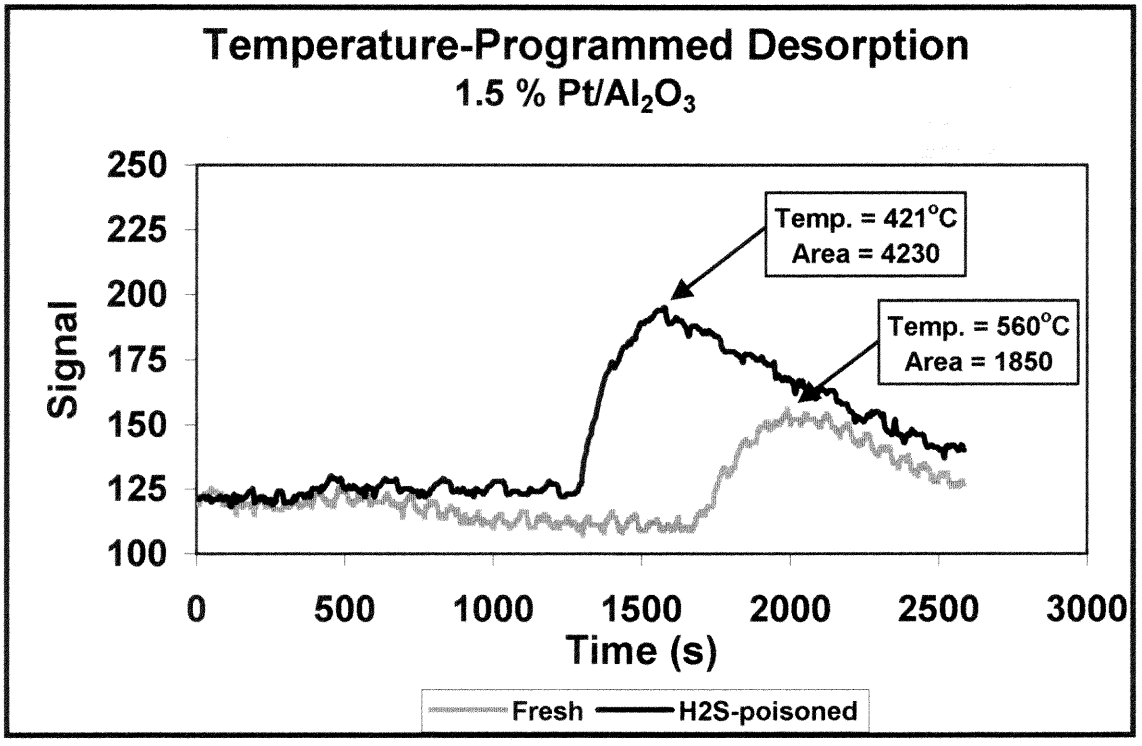

Figure 4.41: Temperature-programmed desorption curves for fresh and H_2S-poisoned 1.5 % Pt/γ-Al_2O_3 following C_3H_8 adsorption at 100°C

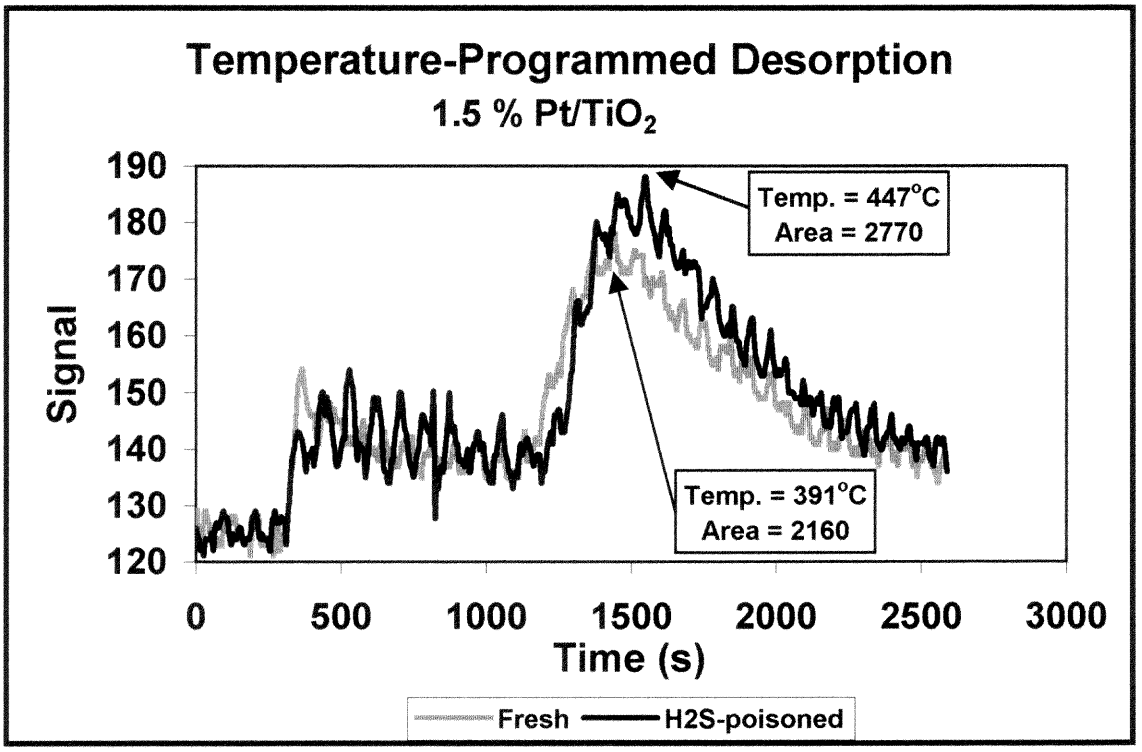

Figure 4.42: Temperature programmed desorption curves for fresh and H_2S-poisoned 1.5 % Pt/TiO_2 following C_3H_8 adsorption at 150°C

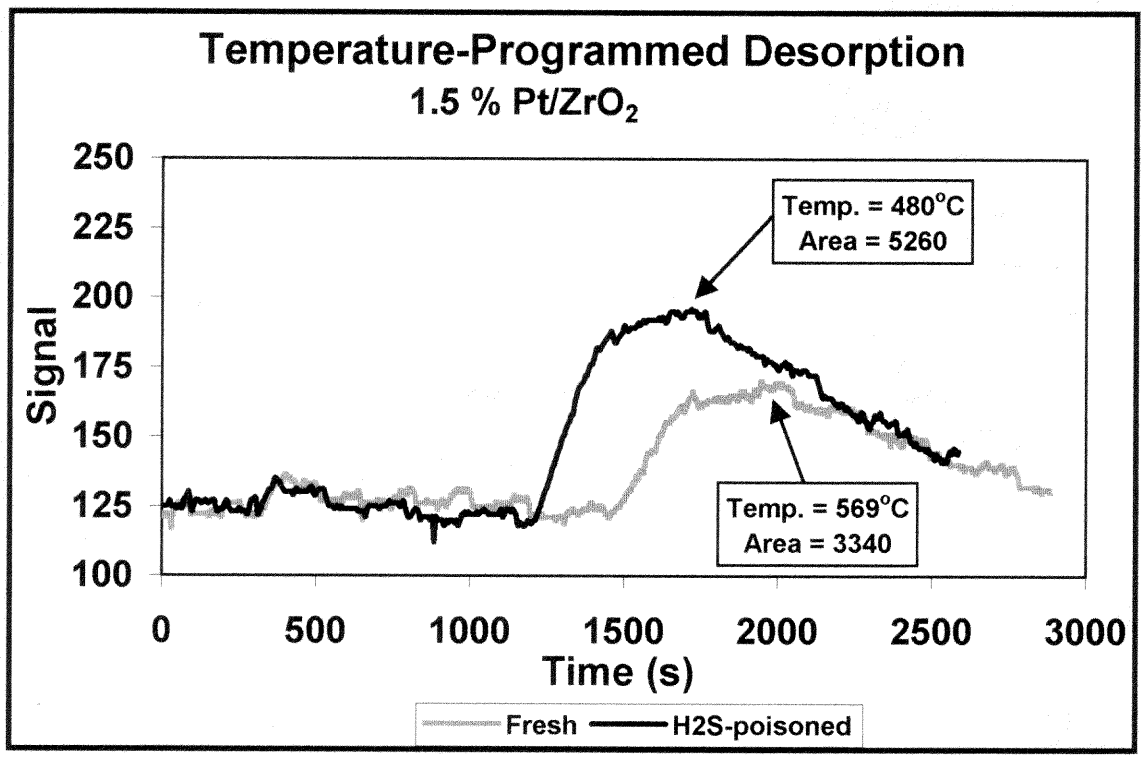

Figure 4.43: Temperature programmed desorption curves for fresh and H_2S-poisoned 1.5 % Pt/ZrO_2 following C_3H_8 adsorption at 150°C

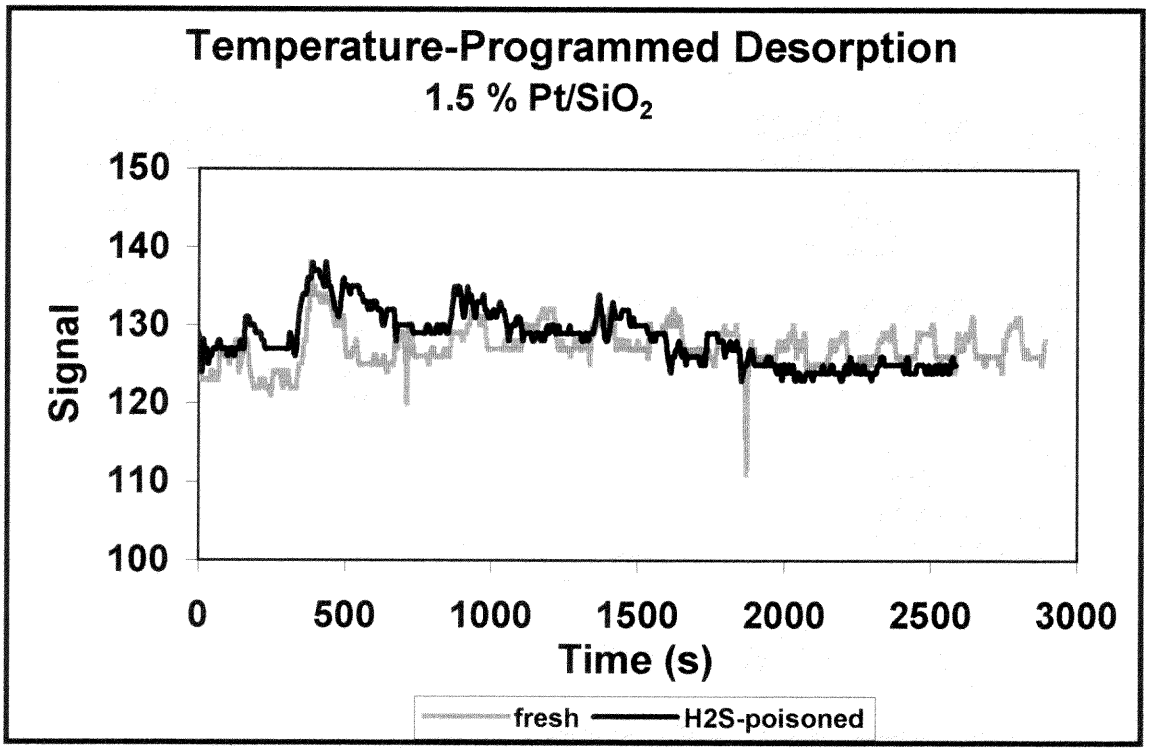

Figure 4.44: Temperature programmed desorption curves for fresh and H_2S-poisoned 1.5 % Pt/SiO_2 following C_3H_8 adsorption at 150°C

No desorption peaks were found for C_3H_8 adsorption on fresh or H_2S-poisoned Pt/SiO_2. Figure 4.44 shows the TPD plots for both samples with a largely expanded detector signal axis. Like Pt/TiO_2 these results show that activity changes associated with H_2S-poisoning are related to changes occurring in the activity of the Pt metal sites only.

4.6.2 CO Adsorption

CO oxidation on Pt catalysts occurs by reaction of Pt-adsorbed CO with dissociatively adsorbed O atoms on Pt sites. Sulfur poisoning is expected to deactivate this reaction by inhibiting both CO adsorption and dissociative O_2 adsorption. This inhibition can be the additive result of Pt crystal growth, pore blockage, and sulfur-mediated electronic effects on Pt metal sites. Although CO does not adsorb appreciably on the support materials, it adsorbs on Pt sites to a much greater extent than C_3H_8 and could be detected by the experimental apparatus. TPD plots for CO adsorption on fresh and H_2S-poisoned catalysts are shown in Figures 4.45, 4.46, 4.47, and 4.48.

Figures 4.45 and 4.47 show virtually no effect of H_2S poisoning for CO adsorption on $Pt/\gamma\text{-}Al_2O_3$ or Pt/ZrO_2. These results were unexpected and it may indicate that the deactivation of both catalysts by H_2S poisoning may be related to changes in the competitive adsorption process between CO and O_2 on active Pt sites. In the TPD experiments, O_2 was not present in the system so, these experiments may not reflect the true activity of CO under reaction conditions.

On the other hand, Figure 4.46 shows a substantial loss in CO adsorption capacity for H_2S-poisoned Pt/TiO_2. In fact, Pt/TiO_2 adsorbed more CO than any of the other catalysts studied, and this is supported by the fact that Pt/TiO_2 was the most active for

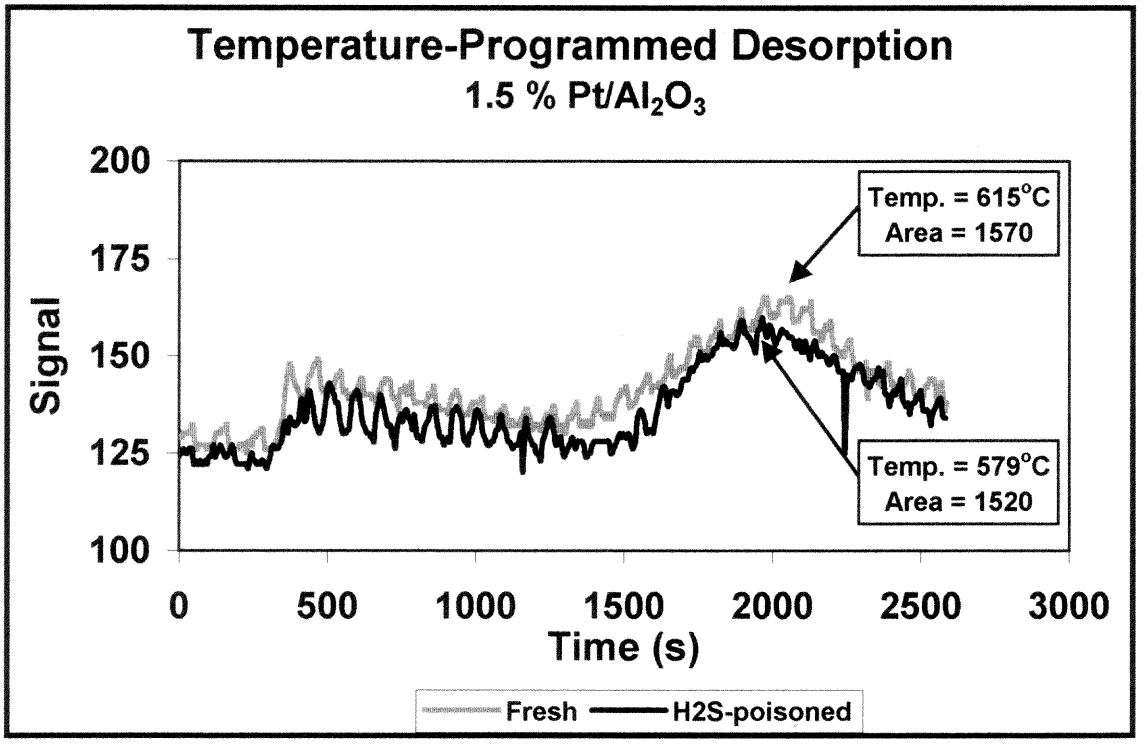

Figure 4.45: Temperature-programmed desorption curves for fresh and H_2S-poisoned 1.5 % Pt/γ-Al_2O_3 following CO adsorption at 50°C

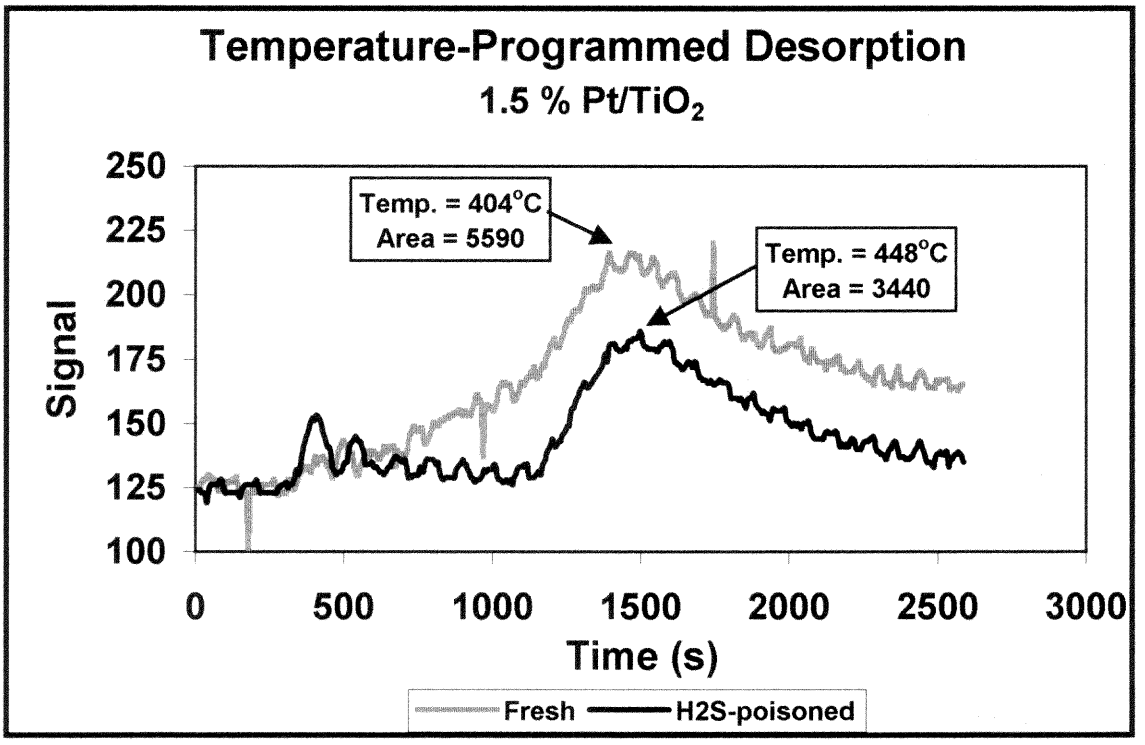

Figure 4.46: Temperature-programmed desorption curves for fresh and H_2S-poisoned 1.5 % Pt/TiO_2 following CO adsorption at 50°C

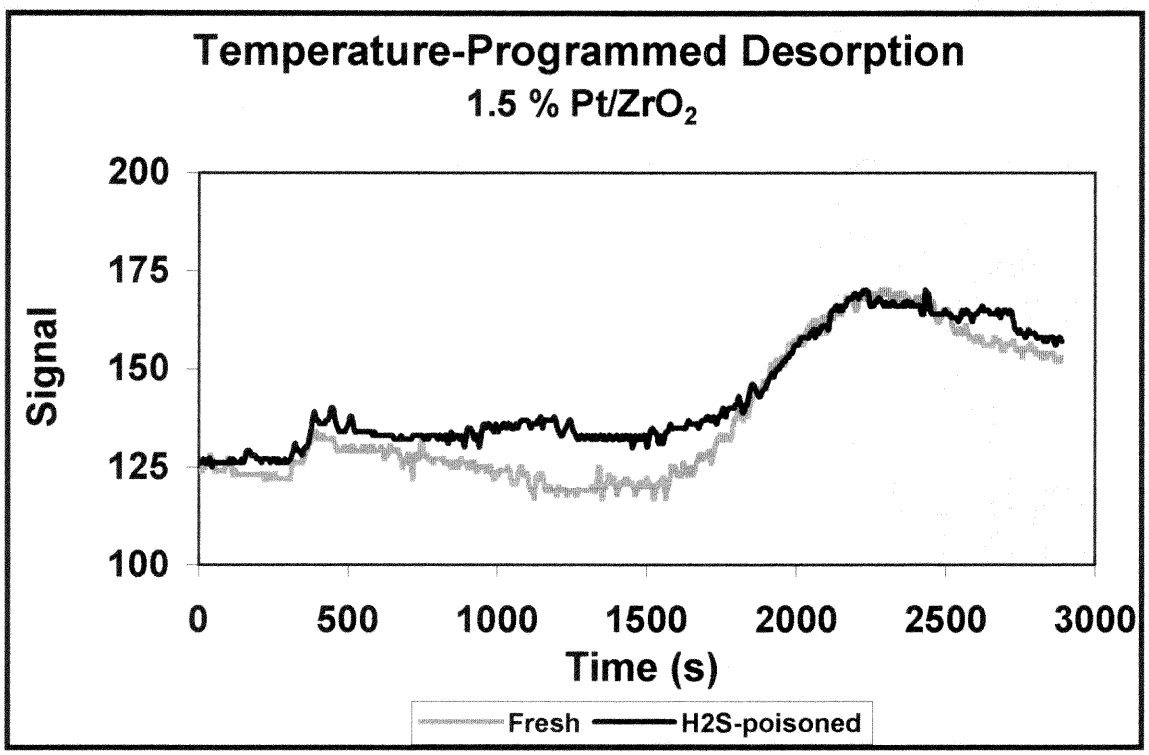

Figure 4.47: Temperature-programmed desorption curves for fresh and H_2S-poisoned 1.5 % Pt/ZrO_2 following CO adsorption at 75°C

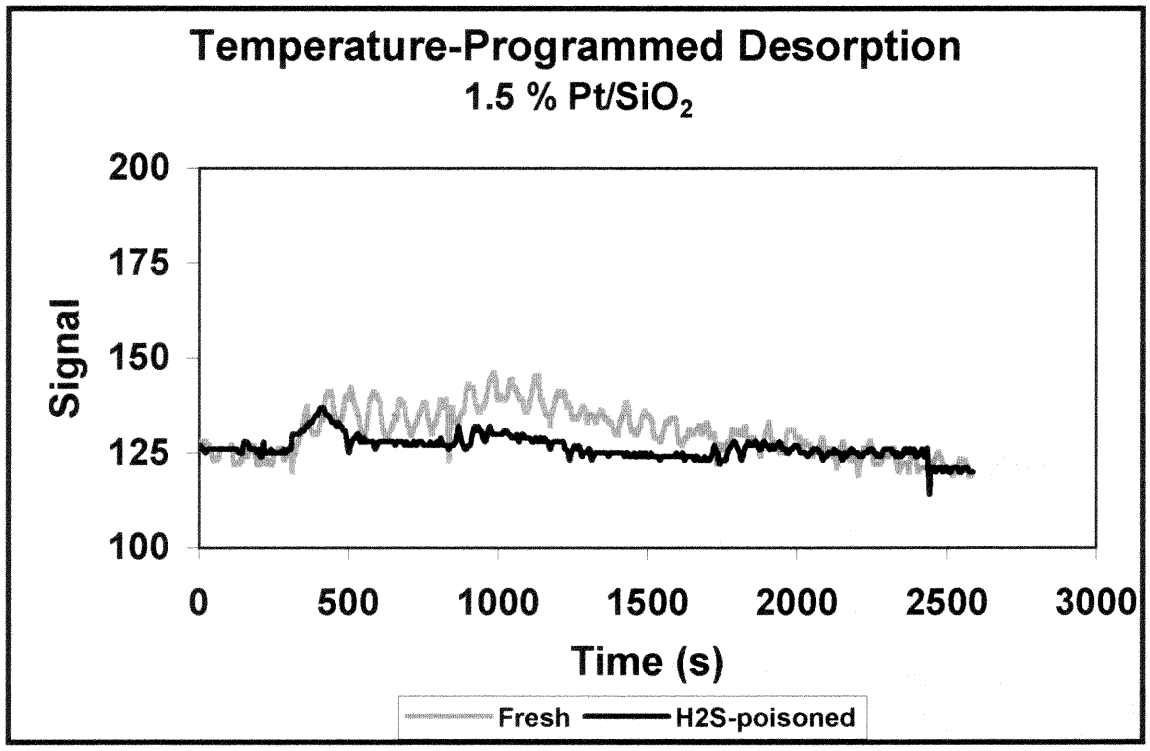

Figure 4.48: Temperature-programmed desorption curves for fresh and H_2S-poisoned 1.5 % Pt/SiO_2 following CO adsorption at 50°C

CO oxidation. Pt/TiO_2 appears to be deactivated by H_2S poisoning for CO oxidation as a result of decreased CO adsorption capacity.

The fresh Pt/SiO_2 catalyst (Figure 4.48) shows a broad and barely detectable CO desorption peak while the TPD plot for the H_2S-poisoned sample was essentially flat, indicating no CO adsorption. However, these observations are not truly significant since CO adsorption on Pt/SiO_2 appears to be beyond the sensitivity of the experimental apparatus used to conduct these experiments.

4.7 Effects of H_2O on Catalyst Poisoning and Activity

Several reports in the literature have suggested that water plays an important role in the sulfur poisoning of noble metal catalysts on oxide supports. As mentioned earlier, the catalysts used in this study probably contained significant amounts of adsorbed H_2O during the activity and poisoning experiments. Also, during the poisoning procedure, the oxidation of H_2S results in the production of significant amounts of H_2O, which may interact with sulfur compounds and alter the effects of sulfur on the catalyst surface. An additional source of H_2O is derived from the oxidation of hydrocarbon compounds during the activity experiments. Consequently, experiments were performed using SO_2 as the poisoning gas in order to determine the effect, if any, that H_2O had on catalyst poisoning and subsequent activity.

Experiments were conducted with 1.5 % $Pt/\gamma\text{-}Al_2O_3$ and 1.5 % Pt/SiO_2 and a poisoning gas mixture of 200 ppm SO_2 in air. Further experimental details are provided in Ch 3, section 3.9. The activity for both poisoned catalysts was determined for the oxidation of CO, CH_4, and C_4H_{10} and compared to the corresponding fresh and H_2S-

poisoned activity presented in section 4.1. Plots showing the activity curves for fresh, SO_2-poisoned, and H_2S-poisoned catalysts are shown in Figures 4.49, 4.50, 4.51, 4.52, 4.53, and 4.54. T_{50} and ΔT_{50} data are presented in Tables 4.1 and 4.4.

Experiments showed no difference in activity for CO oxidation on Pt/γ-Al_2O_3 for either H_2S or SO_2 poisoning (Figure 4.49). The same behavior was also observed for CO oxidation on the H_2S and SO_2 poisoned Pt/SiO_2 catalysts (Figure 4.50). Similarly, the CH_4 oxidation activity was equal regardless of the sulfur poisoning compound on both Pt/γ-Al_2O_3 and Pt/SiO_2 catalysts (Figures 4.51 and 4.52). A difference in activity was found, however, for the oxidation of C_4H_{10} on H_2S and SO_2 poisoned Pt/γ-Al_2O_3 catalysts. As shown in Figure 4.53, C_4H_{10} oxidation activity was enhanced to a lesser extent on the SO_2-poisoned sample as opposed to the H_2S-poisoned sample. However, Figure 4.54 shows similar activity for C_4H_{10} oxidation on both poisoned Pt/SiO_2 samples.

In a study on PdO/Al_2O_3 catalysts used for lean-burn natural gas engine emission abatement, McCormick et al. [40] found that H_2O and SO_2 have a synergistic poisoning effect that is enhanced at higher temperatures (~520°C). These researchers found that the combination of H_2O and SO_2 resulted in the deactivation of a PdO/Al_2O_3 catalyst for methane oxidation. The deactivation was greater than that observed for either H_2O or SO_2 poisoning alone. The authors suggest that H_2O inhibits the adsorption of SO_3 on Al_2O_3. In general, sulfate formation occurs on catayst supports like Al_2O_3 when a metal catalyst (Pt or Pd) oxidizes H_2S and SO_2 to SO_3, which can spillover to the support and react to form sulfate. McCormick et al. propose that H_2O causes a reverse spillover of

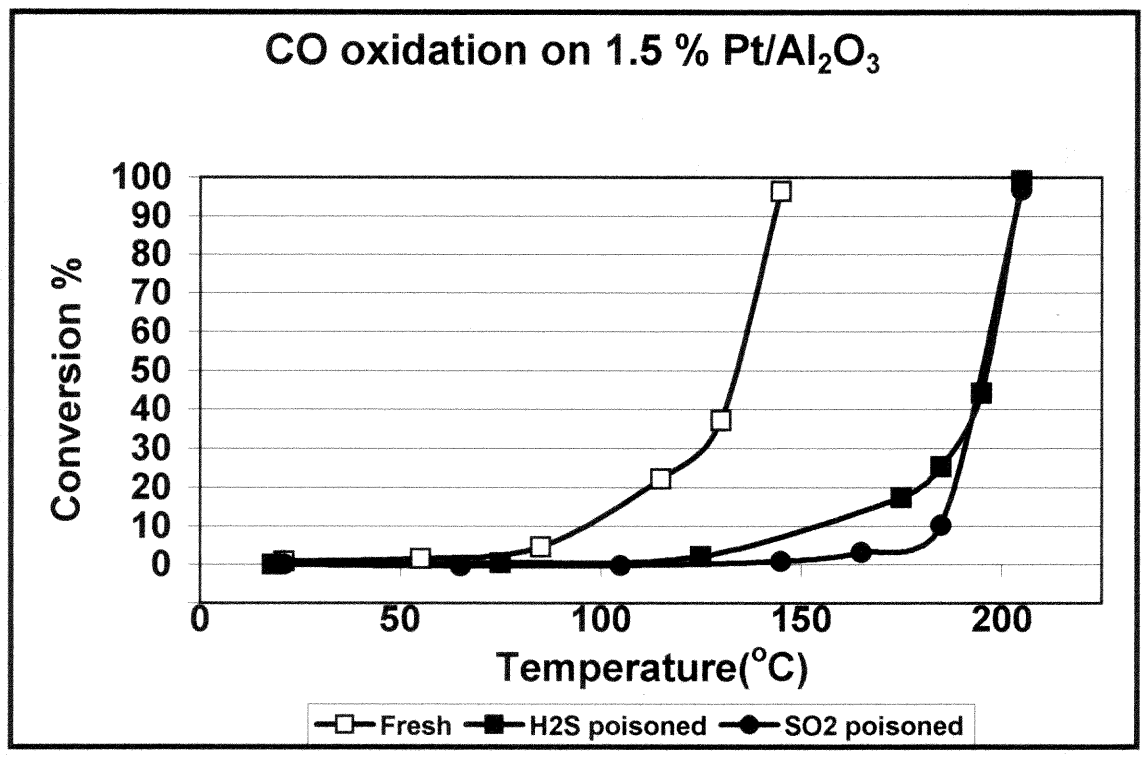

Figure 4.49: Comparison of CO oxidation activity for fresh, H_2S-poisoned, and SO_2-poisoned 1.5 % Pt/γ-Al_2O_3; GHSV = 55,200. (Poisoning: 200 ppm H_2S/air or SO_2/air @ 400°C for 24 hrs.; GHSV = 6,900)

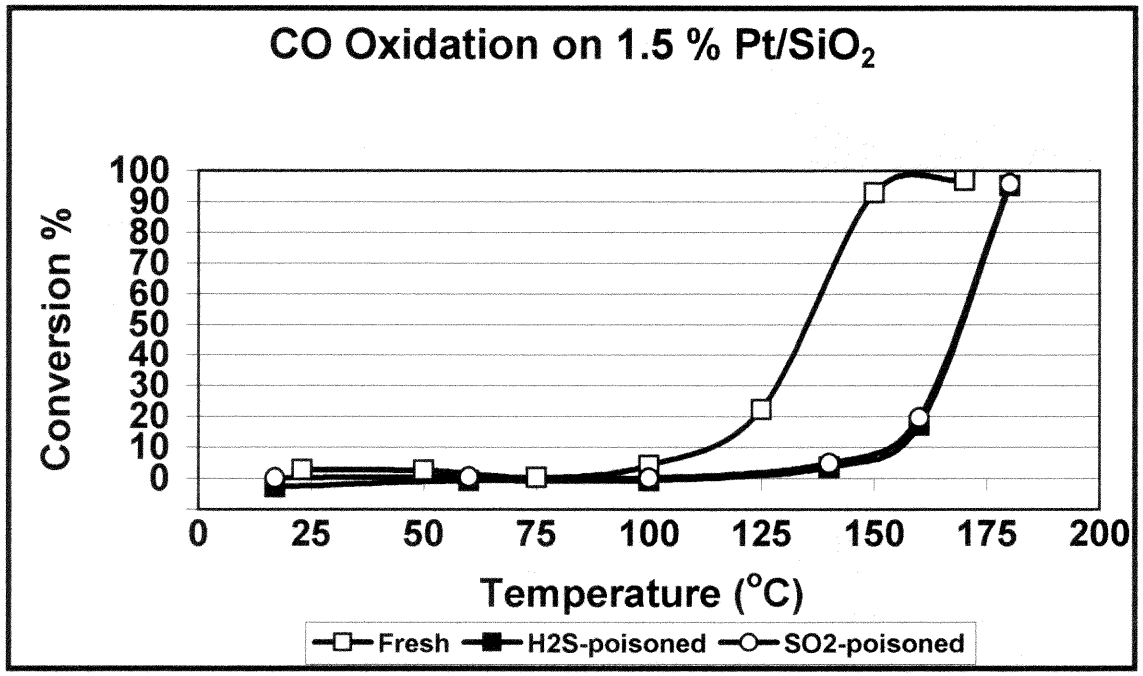

Figure 4.50: Comparison of CO oxidation activity for fresh, H_2S-poisoned, and SO_2-poisoned 1.5 % Pt/SiO_2; GHSV = 15,000. (Poisoning: 200 ppm H_2S/air or SO_2/air @ 400°C for 24 hrs.; GHSV = 1880)

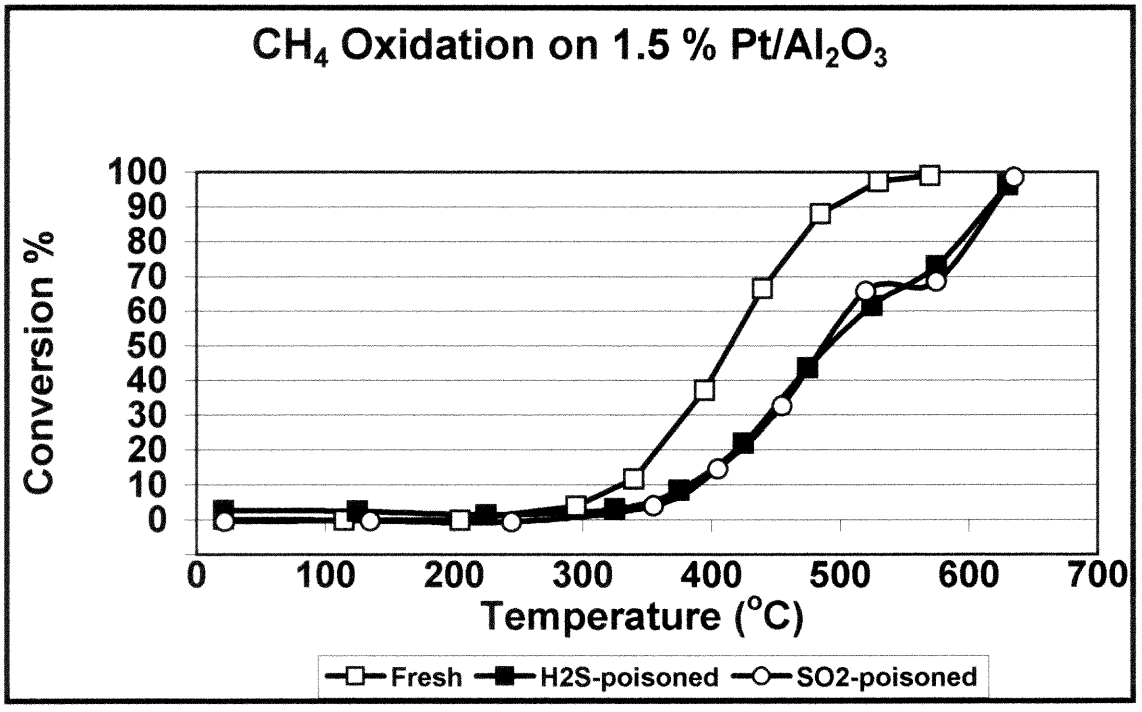

Figure 4.51: Comparison of CH_4 oxidation activity for fresh, H_2S-poisoned, and SO_2-poisoned 1.5 % Pt/γ-Al_2O_3; GHSV = 55,200. (Poisoning: 200 ppm H_2S/air or SO_2/air @ 400°C for 24 hrs.; GHSV = 6,900)

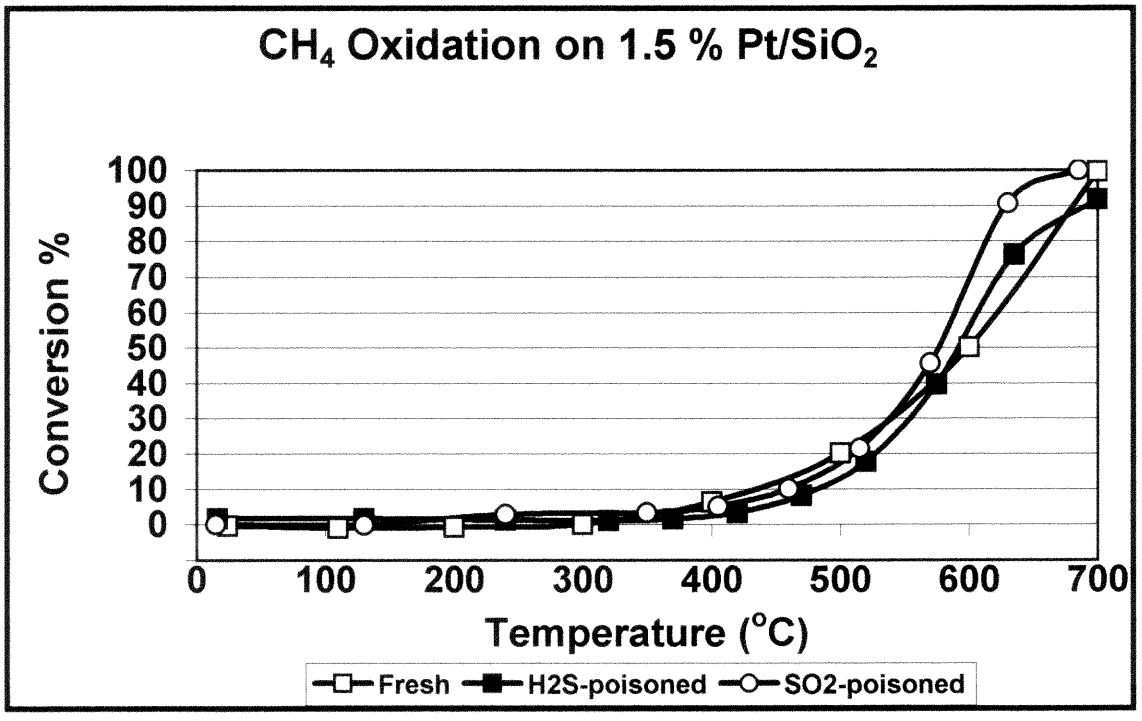

Figure 4.52: Comparison of CH_4 oxidation activity for fresh, H_2S-poisoned, and SO_2-poisoned 1.5 % Pt/SiO_2; GHSV = 15,000. (Poisoning: 200 ppm H_2S/air or SO_2/air @ 400°C for 24 hrs.; GHSV = 1880)

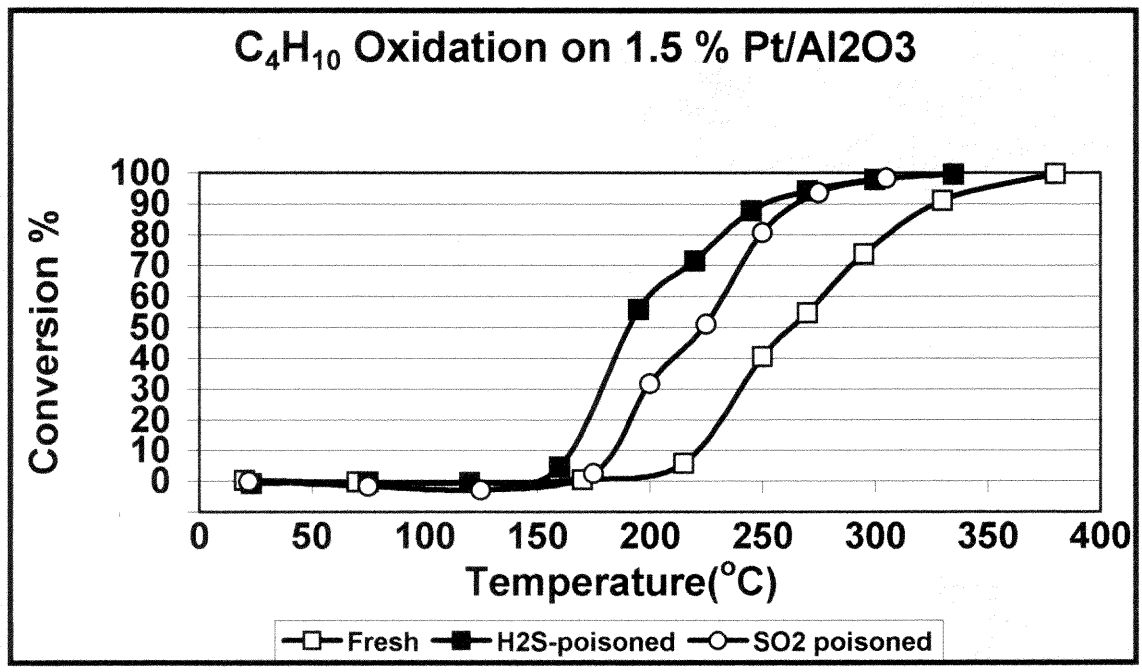

Figure 4.53: Comparison of C_4H_{10} oxidation activity for fresh, H_2S-poisoned, and SO_2-poisoned 1.5 % Pt/γ-Al_2O_3; GHSV = 55,200. (Poisoning: 200 ppm H_2S/air or SO_2/air @ 400°C for 24 hrs.; GHSV = 6,900)

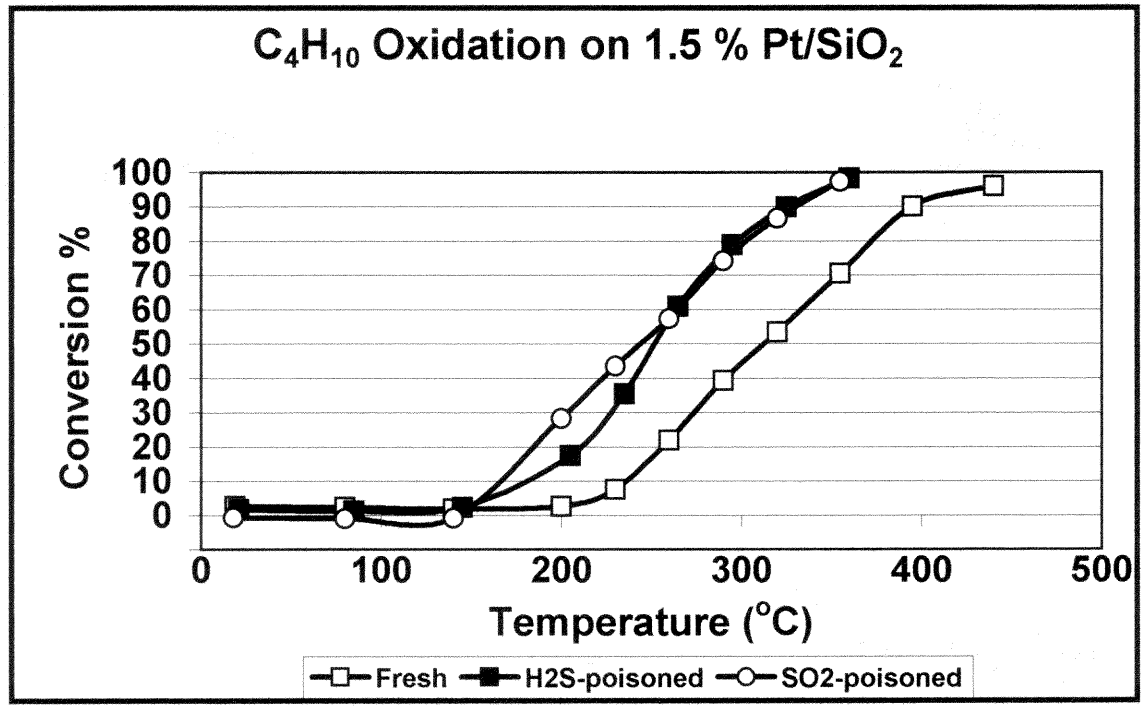

Figure 4.54: Comparison of C_4H_{10} oxidation activity for fresh, H_2S-poisoned, and SO_2-poisoned 1.5 % Pt/SiO_2; GHSV = 15,000. (Poisoning: 200 ppm H_2S/air or SO_2/air @ 400°C for 24 hrs.; GHSV = 1880)

SO_3 from the support to the PdO active sites leading to the formation of $PdSO_4$ and subsequent deactivation for CH_4 oxidation.

A similar mechanism can be proposed for the results found in this work. The adsorption of H_2O on γ-Al_2O_3 may prevent SO_3 from migrating far from the Pt metal sites. This, in turn, could result in the formation of sulfate on either the Pt surface or at the Pt-γ-Al_2O_3 interface. Many researchers have suggested that sulfate sites are active for C-H bond activation in alkanes. The presence of H_2O would, therefore, cause the formation of sites with enhanced alkane oxidation activity. This is confirmed by the results shown in Figure 4.53, in which C_4H_{10} oxidation on Pt/γ-Al_2O_3 was enhanced to a greater extent for H_2S poisoning than SO_2-poisoning relative to fresh catalyst activity. This mechanism is further supported by the fact that the Pt/SiO_2 catalyst was enhanced equally by H_2S or SO_2 poisoning for C_4H_{10} oxidation. Sulfur compounds are not known to interact with SiO_2 surfaces and the effect of H_2O is expected to be minimal.

CHAPTER 5

CONCLUSION

A series of oxidation activity experiments were conducted for fresh, H_2S-poisoned, and SO_2-poisoned Pt catalysts supported on γ-Al_2O_3, TiO_2, ZrO_2 and SiO_2 surfaces. The experiments included the complete oxidation of CO and several light hydrocarbons including CH_4, C_2H_6, C_2H_4, C_2H_2, C_3H_8, C_3H_6, and n-C_4H_{10}. A summary of the results is presented in Tables 5.1 and 5.2 showing changes in the 50 % conversion temperatures (ΔT_{50}) resulting from both forms of sulfur poisoning on each catalyst. Positive values are indicative of reaction deactivation and negative values indicate reaction enhancement. A summary of changes in Pt dispersion and BET surface area resulting from H_2S poisoning of each Pt catalyst is shown in Table 5.3. The mechanisms responsible for the observed effects of sulfur poisoning are discussed for each catalyst in the sections presented below.

Table 5.1: A summary of ΔT_{50}[a] values obtained for each oxidation reaction on H_2S-poisoned Pt catalysts.[b] All values are reported in ^oC.

Reactant	Pt/γ-Al_2O_3	Pt/TiO_2	Pt/ZrO_2	Pt/SiO_2
CO	+63	+75	+24	+33
CH_4	+78	+15	+45	-7
C_2H_6	-26	-10	-15	-63
C_2H_4	-12	+7	+20	+14
C_2H_2	+11	-1	-18	+19
C_3H_8	-55	-21	-44	-70
C_3H_6	+17			
n-C_4H_{10}	-72	-42	-39	-61

Notes: (a) ΔT_{50} is the difference between 50 % conversion temperatures of H_2S-poisoned and fresh catalysts.
(b) These values are taken from data listed in Tables 4.1, 4.2, 4.3, and 4.4.

Table 5.2: A summary of ΔT_{50}[a] values obtained for oxidation reactions on SO_2-poisoned Pt catalysts.[b] The corresponding values for H_2S-poisoned Pt catalysts are shown in parentheses for comparison. All values are reported in °C.

Reactant	Pt/γ-Al_2O_3	Pt/SiO_2
CO	+61 (+63)	+33 (+33)
CH_4	+74 (+78)	-23 (-7)
n-C_4H_{10}	-39 (-72)	-69 (-61)

Notes: (a) ΔT_{50} is the difference between 50 % conversion temperatures of sulfur-poisoned and fresh catalysts.
(b) These values are taken from data listed in Tables 4.1 and 4.4.

Table 5.3: A summary of catalyst characterization experiments for fresh and H_2S-poisoned Pt catalysts. The values shown in the table represent the differences in values between fresh and H_2S-poisoned Pt catalysts.

	Pt/γ-Al_2O_3	Pt/TiO_2	Pt/ZrO_2	Pt/SiO_2
Pt Dispersion[a]	-34.0 % (-63.4 %)	-36.1 % (-62.2 %)	-9.9 % (-47.6 %)	-5.6 % (-26.9 %)
Surface Area (m^2/g)[b]	-12 (-16 %)	-9 (-22.5 %)	-16 (-25 %)	+2 (+1.5 %)

Notes: a) Pt Dispersion values were determined by H_2 chemisorption (Ch. 4, section 4.2). The first value listed in each column is the absolute change in the Pt dispersion %. The number in parentheses represents the percentage change in Pt dispersion.
b) Surface area was calculated using the BET method (Ch. 4, section 4.3). The first value listed in each column is the absolute change in the surface area. The number in parentheses represents the percentage change in surface area.

5.1 Overview of Sulfur Poisoning

In Chapter 2, several potential mechanisms were presented to account for the effects of sulfur poisoning on the observed activity for various reactions catalyzed by supported Pt catalysts. The mechanisms are a summary of ideas gathered from numerous published research reports. Brief descriptions of the proposed mechanisms are listed below:

(1) The interaction of sulfur compounds (H_2S, SO_2, SO_3, and SO_4^{2-}) with Pt catalysts induces the structural rearrangement of exposed Pt crystal planes from predominantly Pt (111) surfaces to Pt (100) surfaces. Certain reactions are inhibited on the Pt (100)

surface while others are enhanced. Still other reactions are completely unaffected by the surface change. Specifically, this mechanism has been proposed to account for the enhancement of C_3H_8 oxidation on sulfur-poisoned Pt catalysts.

(2) The formation of oxidized sulfur compounds and anions on the Pt surface or at the Pt/support interface induces electronic perturbations on the Pt particles that alter the catalyst activity for various reactions. Electronic effects are expected to inhibit the dissociative chemisorption of CO and O_2 on Pt particles while simultaneously enhancing the alkane activity on Pt particles.

(3) The oxidation of sulfur compounds (H_2S, SO_2, and SO_3) on supported Pt catalysts leads to the formation of sulfate on the catalyst support or at the Pt/support interface. This results in the formation of new active sites, which promote C-H bond activation in hydrocarbon compounds. This mechanism is proposed to account for enhanced alkane oxidation on sulfur-poisoned catalysts. Additionally, an increase in the surface acidity resulting from sulfate formation may enhance alkane oxidation by promoting the formation of stable carbocations on the support surface.

(4) The oxidation of sulfur compounds (H_2S, SO_2, and SO_3) also results in the formation of small amounts of oxidized sulfur compounds and/or anions on Pt particles. The effects of this phenomenon include the blocking of active sites for CO and O_2 chemisorption, but also the creation of new active sites for alkane reactions as described in the previous mechanism.

(5) The reaction of sulfur compounds (H_2S, SO_2, and SO_3) on supported Pt catalysts results in the reduction and crystal growth of Pt particles. Larger Pt crystals may be less active for CO and O_2 reactions, but more active for alkane reactions.

(6) The formation of sulfate on the Pt catalyst support material causes the blockage of pores and, thus, a decrease in the number of active sites available for all reactions. This is expected to occur on γ-Al_2O_3, TiO_2, and ZrO_2, but does not occur on SiO_2.

Some catalysis researchers have considered each of these mechanisms as a singular explanation for observed activity changes on Pt catalysts following sulfur poisoning. However, it is entirely possible and quite likely, considering the results of this study, that many or all of these mechanisms play a role in the sulfur-induced activity changes observed on Pt catalysts.

Some of the proposed mechanisms were not directly investigated in this study. For example, the restructuring of Pt crystal surfaces from (111) to (100) planes was not determined in these experiments, nor were the electronic effects of sulfur deposition determined. It is only possible to conclude that the experimental results are consistent with the proposed effects of both mechanisms. That is, the occurrence of structural recrystallization or electronic effects cannot be ruled out by the experimental results.

In the proceeding sections, a summary of the interactions of sulfur compounds and the associated activity changes is presented for each catalyst.

5.2 Pt/γ-Al_2O_3

Temperature-programmed reduction studies revealed a large amount of sulfate formation on Pt/γ-Al_2O_3 following H_2S poisoning. However, this was not accompanied by a large loss in surface area as determined by the BET method. The small decrease in surface area observed combined with a large decrease in Pt dispersion indicates that a significant amount of Pt crystal growth has occurred. FTIR analysis confirmed the presence of

aluminum sulfate as well as coordinated sulfate ions, and the presence of sulfate on Pt particles cannot be ruled out.

The combination of Pt crystal growth, aluminum sulfate formation, adsorbed sulfate ions on the support, and sulfate formation on Pt, each contribute to the significant decrease in activity observed for CO oxidation and CH_4 oxidation. The enhancement of alkane oxidation reactions on sulfur-poisoned Pt/ γ-Al_2O_3 is due to the combination of Pt crystal growth and formation of new active sites as a result of sulfate formation on Pt, γ-Al_2O_3, and/or the Pt-γ-Al_2O_3 interface. The formation of new active sites was confirmed by TPD studies, which showed a large increase in the amount of C_3H_8 adsorbed on the sulfur-poisoned catalyst. Additionally, it was found that the desorption temperature of C_3H_8 was significantly shifted to a lower temperature following sulfur-poisoning, indicating increased reactivity. The formation of new active sites due to sulfate formation is further confirmed by the results found for the oxidation of C_2H_6. The activity enhancement resulting from the formation of sulfate sites involves an enhancement of C-H bond activation. The fact that C_2H_6 oxidation was enhanced to a lesser extent than C_3H_8 or C_4H_{10} oxidation on the sulfur-poisoned catalysts is evidence that C-H bond activation is involved in the observed activity enhancement.

Relatively minor changes in activity for the oxidation of C_2H_4, C_3H_6, and C_2H_2 were found for H_2S-poisoned Pt/γ-Al_2O_3 catalysts. These reactions are thought to occur by a Langmuir-Rideal mechanism involving the interaction of gas-phase hydrocarbon molecules with dissociatively chemisorbed O_2. It is expected, therefore, that Pt crystal growth and the formation of sulfate on Pt and the support surface would deactivate the catalyst for the oxidation of unsaturated hydrocarbons by inhibition of dissociative

chemisorption of O_2. However, this inhibition effect may not have been observed due to the large excess of O_2 present in the system (~20 % O_2, 1 % hydrocarbon). (Similar results were found on Pt/TiO_2, Pt/ZrO_2, and Pt/SiO_2, and this explanation applies to these catalysts as well.)

5.3 Pt/TiO_2

FTIR spectroscopy and TPR experiments both suggest that H_2S poisoning of Pt/TiO_2 results in the formation of sulfate predominantly in the form of coordinated sulfate anions on the catalyst surface. Although most of the adsorbed sulfate anions probably reside on the TiO_2 surface, the presence of small amounts of sulfate on Pt is possible and cannot be ruled out. Since the formation of $Ti(SO_4)_2$ appears to be minimal, the large loss in Pt dispersion as determined by H_2 chemisorption can be a result of either Pt crystal growth, the adsorption of sulfate on active sites, or a combination of both. However, the BET surface area decreased by 22.5 % on the H_2S-poisoned catalyst and this result is difficult to justify considering other experiments showing little $Ti(SO_4)_2$ formation. A possible conclusion is that sulfur poisoning caused support sintering. Support sintering occurs when reaction conditions cause the pore network of the support to partially collapse resulting in the occlusion of active Pt sites. Although TiO_2 is reported to be stable at temperatures up to 500°C, impurities in the support material itself or exposure to reactive gases such as sulfur compounds can cause support sintering at lower temperatures. If support sintering occurred in this case, it represents an additional cause for the low Pt dispersion values obtained for the H_2S-poisoned Pt/TiO_2 catalyst.

The deactivation of CO and CH_4 oxidation on H_2S-poisoned Pt/TiO_2 is attributed to all of the following: Pt crystal growth, the adsorption of sulfate on active sites, and possibly, the sintering of the TiO_2 support. Enhancement of alkane oxidation on H_2S-poisoned Pt/TiO_2 is the result of Pt crystal growth and the formation of new active sites due the presence of coordinated sulfate ions on both Pt and the TiO_2 surface. As in the case of $Pt/\gamma\text{-}Al_2O_3$, the new active site hypothesis is substantiated by the smaller enhancement seen for C_2H_6 oxidation as opposed to C_3H_8 and C_4H_{10} oxidation. Curiously, however, TPD studies did not show any increase in C_3H_8 adsorption capacity on the H_2S-poisoned Pt/TiO_2 catalyst unlike $Pt/\gamma\text{-}Al_2O_3$ and Pt/ZrO_2, which showed substantial increases in the adsorption capacity for C_3H_8 following H_2S-poisoning. This result may suggest the possibility that electronic effects of sulfate adsorption are influencing catalyst activity. Although the existence of electronic effects due to sulfate adsorption on supported Pt catalysts is considered questionable at best, Pt/TiO_2 would be the most likely catalyst of the group to exhibit this behavior considering the electronic properties of TiO_2. Electronic effects of sulfur deposition have been predicted to inhibit CO oxidation and enhance alkane oxidation on Pt catalysts, which is consistent with the results obtained in these experiments.

5.4 Pt/ZrO_2

Catalyst characterization experiments including H_2 chemisorption, BET surface area, and FTIR spectroscopy indicate that the oxidation of H_2S on Pt/ZrO_2 results in both Pt crystal growth and sulfate formation. Sulfate is deposited in the form of both molecular $Zr(SO_4)_2$ and adsorbed sulfate ions on the ZrO_2 surface. The presence of a small amount

of sulfate on Pt particles is also probable and cannot be ruled out by the experimental results.

Oxidation activity for CO and CH_4 on H_2S-poisoned Pt/ZrO_2 is inhibited due to a combination of Pt crystal growth, pore blockage due to $Zr(SO_4)_2$ formation, and the adsorption of sulfate on active sites. The enhancement for alkane oxidation observed on H_2S-poisoned Pt/ZrO_2 is a result of the combined effects of Pt crystal growth and the formation of new active sites resulting from the formation of sulfate on the catalyst surface. As in the case of Pt/γ-Al_2O_3, the formation of new active sites that are active for C-H bond scission is confirmed by TPD results and C_2H_6 oxidation activity experiments. TPD experiments show an increased adsorption capacity as well as a decreased desorption temperature for C_3H_8 adsorption on H_2S-poisoned Pt/ZrO_2 catalysts, which is consistent with the formation of new active sites. Activity experiments show an enhancement for C_2H_6 oxidation on H_2S-poisoned Pt/ZrO_2 that is much smaller than the enhancement observed for C_3H_8 or C_4H_{10} oxidation. This is evidence that C-H bond activation is important to the enhancement effects observed.

5.5 Pt/SiO_2

The oxidation of H_2S or SO_2 on Pt/SiO_2 results in the crystal growth of Pt particles as well as the formation of a small amount of sulfate on Pt particles. BET surface area was unaffected while Pt dispersion dropped approximately 25 %.

Pt crystal growth and the adsorption of sulfate on active Pt sites account for the deactivation observed on sulfur-poisoned Pt/SiO_2 catalysts for CO oxidation. CH_4 oxidation was largely unaffected by sulfur poisoning, presumably because sulfate did not

form on the SiO_2 surface and, therefore, the diffusion of reactants through the catalysts' pore network was not adversely affected. The enhancement in oxidation activity for alkanes observed on sulfur-poisoned Pt/SiO_2 is mainly due to the creation of more active sites as a result of Pt crystal growth. It is also expected that the formation of sulfate on Pt particles yields active sites for C-H bond activation and this is an additional source for alkane oxidation reaction enhancement. These effects have not previously been observed on Pt/SiO_2 catalysts and, therefore, the results are a major contribution provided by this study to the current body of catalysis research.

5.6 Effects of H_2O on Catalyst Poisoning

It can be concluded, based on preliminary results obtained for SO_2-poisoned Pt/γ-Al_2O_3 and Pt/SiO_2, that H_2O enhances the poisoning effects of sulfur gases on certain catalyst surfaces. Specifically, a comparison of the activity of fresh, H_2S-poisoned, and SO_2-poisoned Pt/γ-Al_2O_3 and Pt/SiO_2 for C_4H_{10} oxidation activity suggests that H_2O enhances the formation of sulfate on γ-Al_2O_3 surfaces. No effect was observed on Pt/SiO_2 since this catalyst does not undergo sulfate formation on the support surface but a similar enhancement of sulfation is expected to occur on TiO_2 and ZrO_2. However, further research is required in this area to clearly establish the observed effect of H_2O.

5.7 General Conclusions

In the previous sections of Ch. 5, a discussion of the interactions of sulfur compounds and associated changes in catalyst activity on each of the four catalyst samples

investigated in this work was presented. A summary of the major conclusions is presented below:

- The poisoning of supported Pt catalysts by H_2S under oxidizing conditions results in the enhancement of activity for the complete oxidation of C_2H_6, C_3H_8, and C_4H_{10}. This enhancement was observed for Pt catalysts supported on γ-Al_2O_3, TiO_2, ZrO_2, and SiO_2.
- The enhancement of alkane oxidation on H_2S-poisoned Pt catalysts supported on γ-Al_2O_3, TiO_2, and ZrO_2 results from a combination of the formation of support sulfate compounds, the adsorption of sulfate anions on the support surface, formation of oxidized sulfur groups on the Pt metal sites, and Pt sintering. Each of these effects appear to result in the formation of new active sites which facilitate the hydrocarbon oxidation reaction.
- The enhancement of alkane oxidation on H_2S-poisoned Pt/SiO_2 has not been observed previously and is primarily associated with Pt crystal growth. An additional enhancement effect is due to the formation of small amounts of sulfate on the Pt metal sites, yielding new sites active for the alkane oxidation reactions.
- The oxidation of CO on each of the supported Pt catalysts was severely deactivated following H_2S-poisoning. The deactivation was a result of the combined effects of pore blockage, Pt crystal growth, and adsorbed sulfate groups on active Pt sites.
- The oxidation of CH_4 on H_2S-poisoned Pt catalysts was slightly deactivated on all of the catalyst samples except Pt/SiO_2 and is primarily a result of pore blockage due to sulfate formation on the support.

- The effects of H_2S-poisoning on alkene and alkyne oxidation reactions on supported Pt catalysts were minimal. These reactions are proposed to occur by a Langmuir-Rideal mechanism in which a gas-phase hydrocarbon molecule reacts with a dissociatively adsorbed O atom. Although the effects of H_2S-poisoning of supported Pt catalysts is expected to inhibit the dissociative chemisorption of O_2, the activity changes observed were minimal since the reactions were carried out in excess O_2 (~20 % O_2, 1 % HC).
- The sulfur-induced restructuring of the Pt crystal surface structure from (111) to (100) planes and the electronic effects of adsorbed sulfur on Pt crystals were not directly determined. However, the occurrence of these effects is consistent with the experimental results and, thus, cannot be ruled out.

CHAPTER 6

RECOMENDATIONS FOR FUTURE WORK

The experimental results and conclusions presented in Ch.'s 4 and 5 reveal the complex nature of processes occurring on the surface of practical supported Pt catalysts. The results present many opportunities for additional research in this subject area. Several recommendations for interesting and valuable research are suggested below.

- Since, neither alkane oxidation enhancement nor sulfur adsorption has previously been observed on Pt/SiO_2 catalysts, a more in-depth study of the interactions of sulfur compounds on this catalyst would be beneficial.
- FTIR spectroscopy and temperature-programmed reduction were utilized in these experiments to identify the presence of sulfur compounds on the catalyst surface and to suggest the form in which sulfur compounds were present. However, more sophisticated surface analytical techniques such as XPS, AES, LEED, or EXAFS could be useful in determining the exact sulfur compounds and anions present.
- Sulfur poisoning of Pt/TiO_2 catalysts has not been studied extensively, unlike $Pt/\gamma\text{-}Al_2O_3$ and Pt/SiO_2. Further studies of this catalyst are recommended since the effects of sulfur poisoning on this catalyst appear to be significantly different from that of $Pt/\gamma\text{-}Al_2O_3$. Additionally, electronic effects of sulfur and other adsorbed compounds on Pt activity may be more likely to occur on Pt/TiO_2 than other similar catalysts, due to the electronic properties of TiO_2. Experiments in this area could potentially reveal fundamental changes in Pt activity due to adsorbed compounds,

which previously have not been unequivocally shown to occur on supported Pt catalysts.

- The role that acidity has in the promotion of alkane oxidation activity on sulfur-poisoned catalysts is not clearly understood. Characterization of the changes in catalyst acidity due to sulfate formation may be correlated to observed changes in catalyst activity.
- The interaction of H_2O with sulfur compounds and the effects on supported Pt catalysts is also an important topic that is not currently understood clearly. Preliminary experiments have shown that H_2O appears to enhance the sulfation of $Pt/\gamma\text{-}Al_2O_3$ catalysts. However, more in-depth catalyst characterization studies are required to accurately determine the effects of H_2O on catalyst poisoning.
- Very small effects of sulfur poisoning were observed for alkene and alkyne oxidation on supported Pt catalysts. It was suggested that the effects were minimal since O_2 was present in excess in the reactant feedstream. Thus, it would be beneficial to perform similar experiments using much lower O_2 concentrations.

APPENDIX A

GAS SPECIFICATIONS

All analytical gases were purchased from Matheson Gas Products. Listed in the tables below are analytical grades, purity, and concentration for all gases used in this study.

Table A.1: Pure gases

Gas	Grade	Purity[a]	Application
Air	Dry	-	FID flame, sulfur mixtures
Helium	High Purity	99.995 %	GC carrier gas
Hydrogen	Prepurified	99.99 %	FID flame, H_2 chemisorption
Nitrogen	Prepurified	99.998 %	H_2 chemisorption, BET surface area, TPR, TPD
Argon	High Purity	99.995 %	H_2 chemisorption, TPD (CO)

Notes: a) Percentages represent minimum values for gas purity

Table A.2: Gas mixtures

Gas	Concentration	Balance gas (grade)[a]	Application
Carbon monoxide	0.931 %	Air (Dry)	Activity experiments
Methane	0.986 %	Air (Dry)	Activity experiments
Ethane	1.1 %	Air (Dry)	Activity experiments
Ethylene	1.0 %	Air (Dry)	Activity experiments
Acetylene	1.07 %	Air (Dry)	Activity experiments
Propane	0.98 %	Air (Dry)	Activity experiments
Propylene	0.993 %	Air (Dry)	Activity experiments
Butane	0.912 %	Air (Dry)	Activity experiments
Hydrogen sulfide	0.61 %	Nitrogen (Prepurified)	Catalyst poisoning
Sulfur dioxide	491 ppm	Nitrogen (Prepurified)	Catalyst poisoning
Carbon monoxide	984 ppm	Helium (High purity)	TP Desorption
Propane	1207 ppm	Helium (High purity)	TP Desorption
Ethylene	920 ppm	Helium (High purity)	TP Desorption
Propylene	1020 ppm	Helium (High purity)	TP Desorption
Hydrogen	5.06 %	Argon	TP Reduction
Ammonia	4.97 %	Helium (High purity)	Ammonia titration
Nitrogen	10.21 %	Helium	BET surface area
Nitrogen	19.78 %	Helium	BET surface area
Nitrogen	29.18 %	Helium	BET surface area
Calibration Std.	1038.7 ppm CO 980.0 ppm CH_4 987.1 ppm CO_2	Nitrogen	GC calibration

Notes: a) For balance gas purity, see data in Table 1

APPENDIX B

H_2 CHEMISORPTION DATA

The figures presented below contain the experimental data used to calculate Pt dispersion values. Each figure contains all 15 H_2 pulses displayed on one plot. Also shown are calculated peak areas for each pulse.

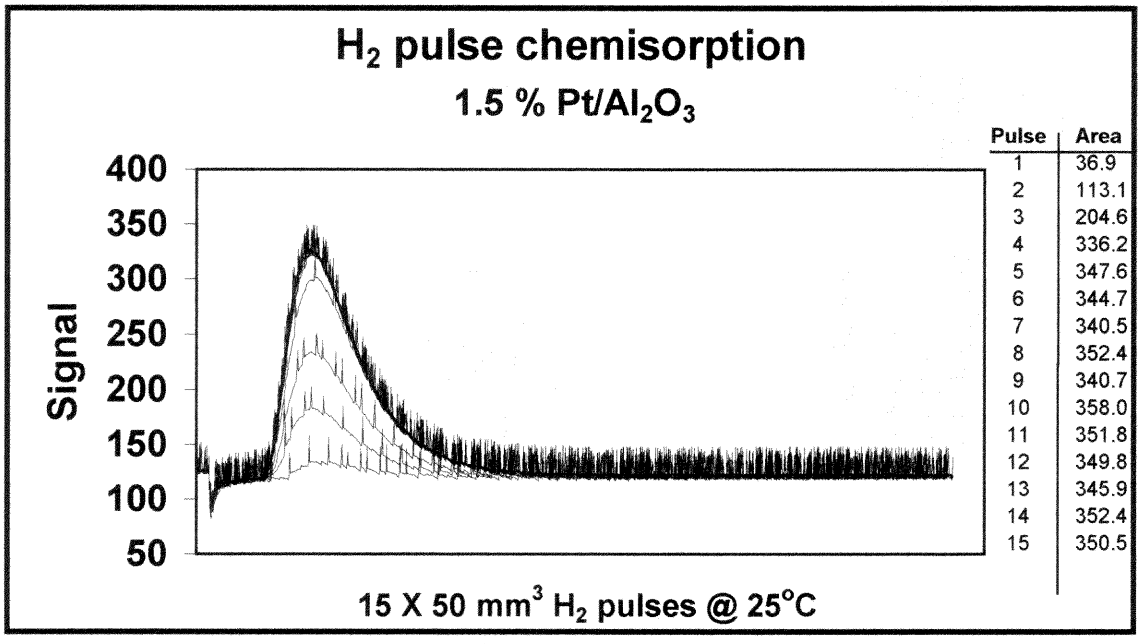

Pulse	Area
1	36.9
2	113.1
3	204.6
4	336.2
5	347.6
6	344.7
7	340.5
8	352.4
9	340.7
10	358.0
11	351.8
12	349.8
13	345.9
14	352.4
15	350.5

Figure B.1: H_2 chemisorption data for 1.5 % Pt/γ-Al_2O_3

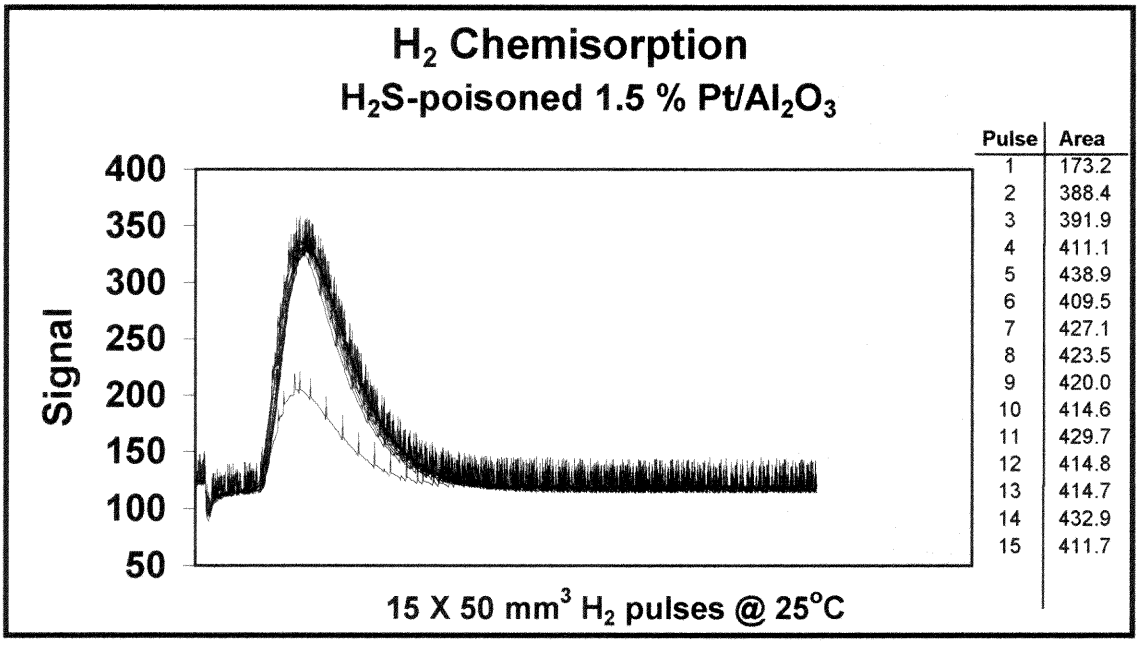

Pulse	Area
1	173.2
2	388.4
3	391.9
4	411.1
5	438.9
6	409.5
7	427.1
8	423.5
9	420.0
10	414.6
11	429.7
12	414.8
13	414.7
14	432.9
15	411.7

Figure B.2: H_2 chemisorption data for H_2S-poisoned 1.5 % Pt/γ-Al_2O_3

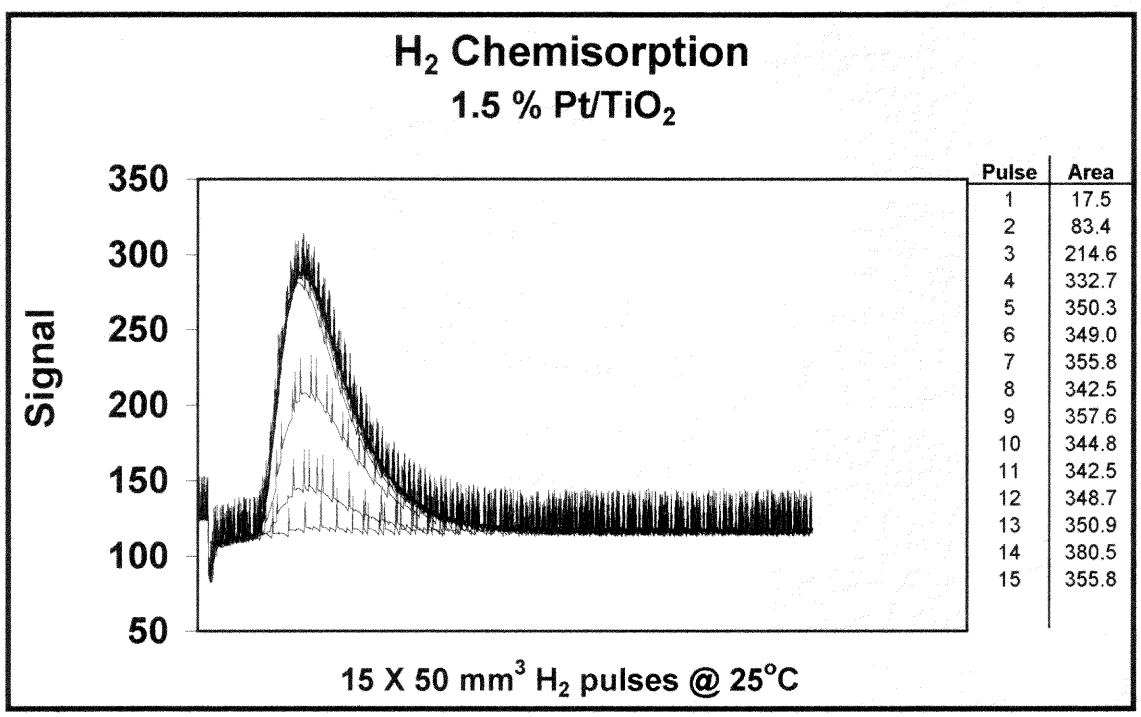

Figure B.3: H_2 chemisorption data for 1.5 % Pt/TiO_2

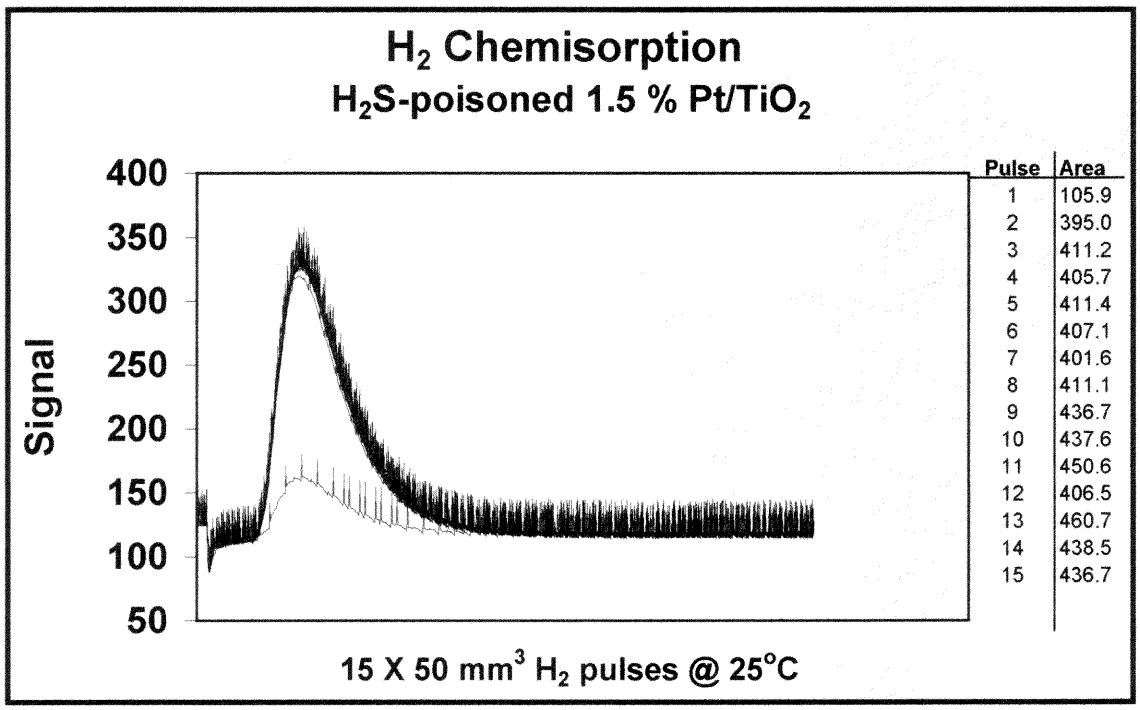

Figure B.4: H_2 chemisorption data for H_2S-poisoned 1.5 % Pt/TiO_2

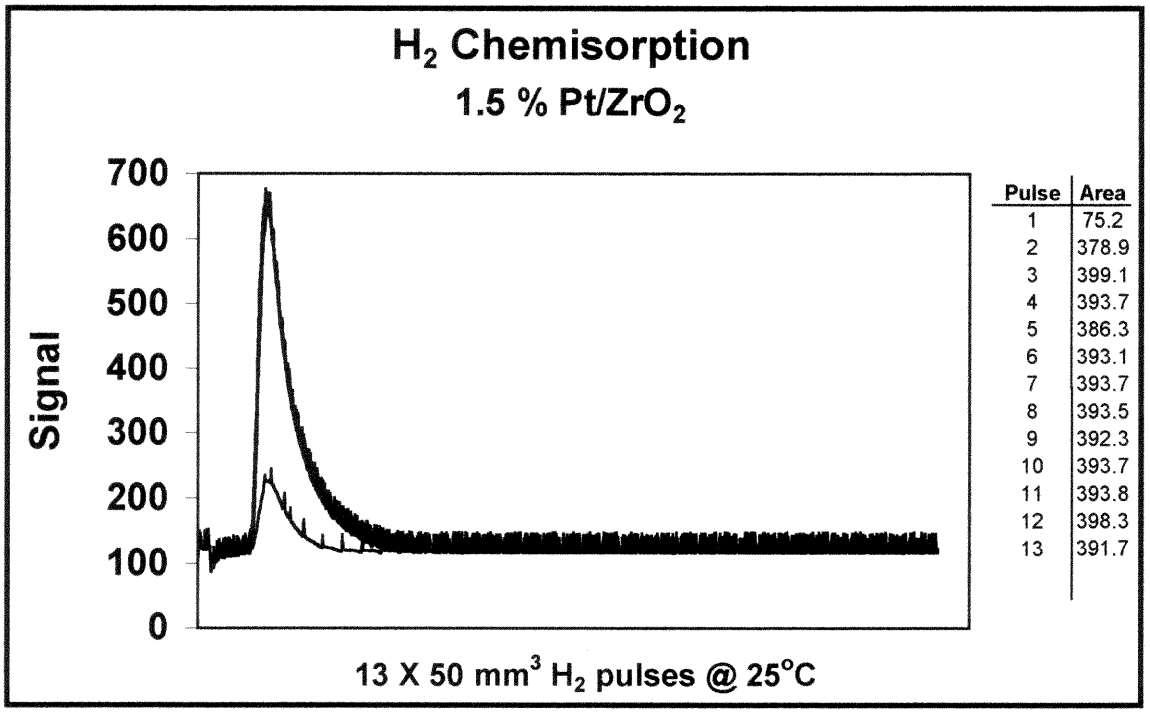

Figure B.5: H_2 chemisorption data for 1.5 % Pt/ZrO_2

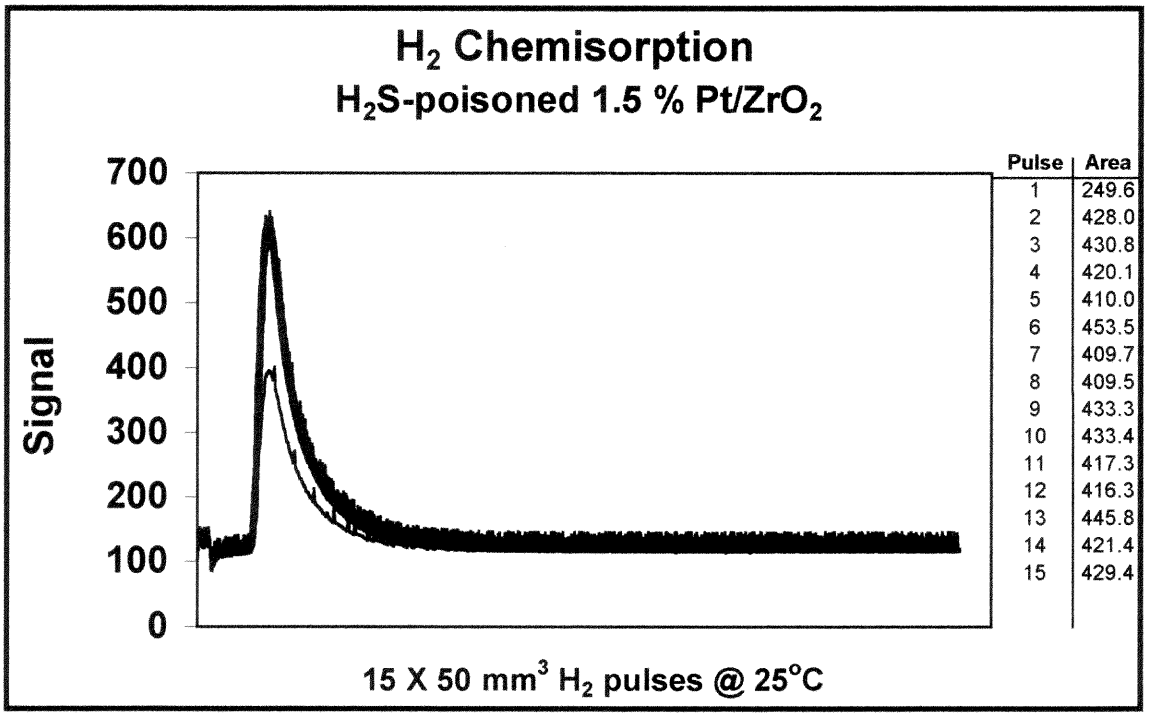

Figure B.6: H_2 chemisorption data for H_2S-poisoned 1.5 % Pt/ZrO_2

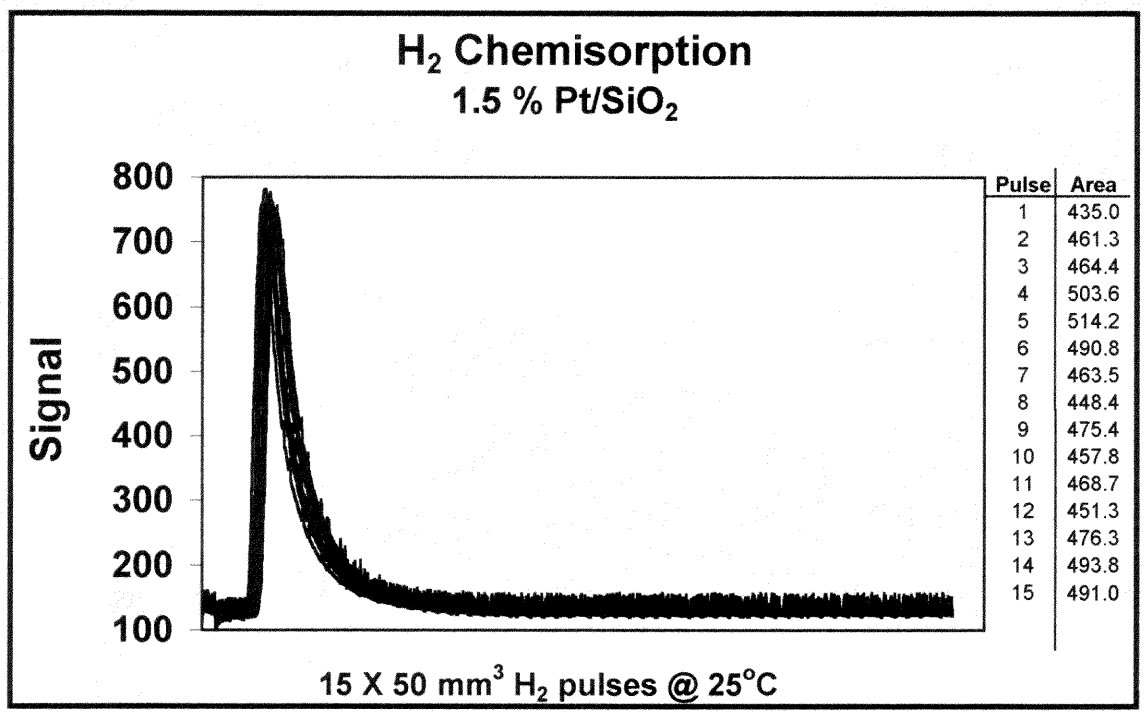

Figure B.7: H_2 chemisorption data for 1.5 % Pt/SiO_2

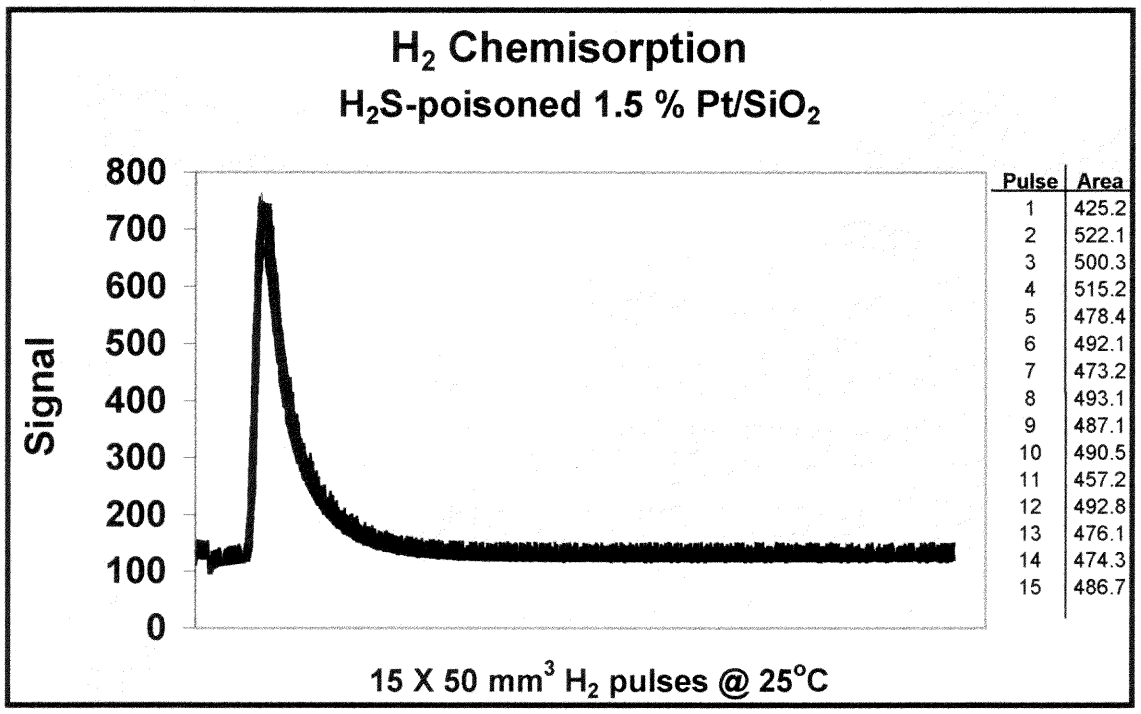

Figure B.8: H_2 chemisorption data for H_2S-poisoned 1.5 % Pt/SiO_2

REFERENCES

1. Farrauto, R.J.; Heck, R.M.; "Catalytic Converters: State of the Art and Perspective" Catal. Today, 51, 351, 1999.

2. Heck, R.M.; Farrauto, R.J.; Catalytic Air Pollution Control; Commercial Technology Van Nostrand Reinhold: New York; 1995.

3. www.epa.gov; May, 2000.

4. Johnson, J.; "Cleaner Vehicles, Gas to be Required by EPA" Chem. & Eng. News, 9, January 3, 2000.

5. Ansell, G.P.; Golunski, S.E.; Hatcher, H.A.; Rajaram, R.R.; "Effects of SO_2 on the Alkane Activity of Three-Way Catalysts" Catal. Lett., 11, 183, 1991.

6. Oudar, J.; "Sulfur Adsorption and Poisoning of Metallic Catalysts" Catal. Rev.-Sci. Eng., 22(2), 171, 1980.

7. Wilson, K.; Hardacre, C.; Lambert, R.M.; "SO_2-Promoted Chemisorption and Oxidation of Propane Over Pt(111)" J. Phys. Chem., 99(38), 13755, 1995.

8. "Fuel Refiners Want Sulfur Rule Withdrawn" Chem. Eng. News; 32, March 20, 2000.

9. Satterfield, C.N.; Heterogeneous Catalysis in Industrial Practice, 2nd ed.; McGraw Hill, Inc.: New York; 1991.

10. Deo, A.V.; Dalla Lana, I.G.; Habgood, H.W.; "Infrared Studies of the Adsorption and Surface Reactions of Hydrogen Sulfide and Sulfur Dioxide on Some Aluminas and Zeolites" J. Catal., 21,270, 1971.

11. Chang, C.C.; "IR Studies of SO_2 on γ-Alumina" J. Catal., 53(3), 374, 1978.

12. Okamoto, Y.; Oh-Hara, M.; Maezawa, A.; Imanaka, T.; Teranishi, S.; "H_2S Adsorption on Al_2O_3, Modified Al_2O_3, and MoO_3/Al_2O_3" J. Phys. Chem., 90, 2396, 1986.

13. Yanxin, C.; Yi, J.; Wenzhao, L.; Rongchao, J.; Shaozhen, T.; Wenbin, H.; "Adsorption and Interaction of H_2S/SO_2 on TiO_2" Catal. Today, 50, 39, 1999.

14. Yamaguchi, T.; Jin, T.; Tanabe, K.; "Structure of Acid Sites on Sulfur-Promoted Iron Oxide" J. Phys. Chem., 90, 3148, 1986.

15. Somorjai, G.A.; "On the Mechanism of Sulfur Poisoning of Platinum Catalysts" J. Catal., 27(3), 453, 1972.

16. Schmidt, L.D.; Luss, D.; "Physical and Chemical Characterization of Platinum-Rhodium Gauze Catalysts" J. Catal., 22, 269, (1971).

17. Harris, P.J.F.; "Sulphur-Induced Faceting of Platinum Catalyst Particles" Nature, 323, 792, 1986.

18. Halachev, T.; Ruckenstein, E.; "Poisoning and Promoting Effects of Additives on the Catalytic Behavior of Metal Clusters" J. Catal., 73, 171, 1982.

19. Kummer, J.T.; "Laboratory Experiments Evaluating the Effects of S and Cu on a Pt-Al_2O_3 Auto Exhaust Oxidation Catalysts" J. Catal., 38, 166, 1975.

20. Kiskinova, M.; Szabo, A.; Yates Jr., J.T.; "CO adsorption on Pt(111) Modified with Sulfur" J. Chem. Phys., 89(12), 7599, 1988.

21. Feibelman, P.J.; Hamann, D.R.; "Electronic Structure of a Poisoned Transition-Metal Surface" Phys. Rev. Lett., 52(1), 61, 1984.

22. Wimmer, E.; Fu, C.L.; Freeman, A.J.; "Catalytic Promotion and Poisoning: All-Electron Local-Density-Functional Theory of CO on Ni(001) Surfaces Coadsorbed with K or S" Phys. Rev. Lett., 55(23), 2618, 1985.

23. Apesteguia, C.R.; Brema, C.E.; Garetto, T.F.; Borgna, A.; Parera, J.M.; "Sulfurization of Pt/Al_2O_3-Cl Catalysts VI. Sulfur-Platinum Interaction Studied by Infrared Spectroscopy" J. Catal., 89, 52, 1984.

24. Wilson, K.; Hardacre, C.; Lambert, R.M.; "SO_2-Promoted and Propane Oxidation Over Pt(111) and $Pt(111)/AlO_x$ Model Systems" Preprint, Symp. Heterogeneous Hydrocarbon Oxidation, Div. Pet. Chem., Am. Chem. Soc., 41(1), 37, 1996.

25. Burch, R.; Halpin, E.; Hayes, M.; Ruth, K.; Sullivan, J.A.; "The Nature of Activity Enhancement for Propane Oxidation Over Supported Pt Catalysts Exposed to Sulphur Dioxide" Appl. Catal. B: Env., 19, 199, 1998.

26. Ruth, K.; Hayes, M.; Burch, R.; Tsubota, S.; Haruta, M.; "The Effects of SO_2 on the Oxidation of CO and Propane on Supported Pt and Au Catalysts" Appl. Catal. B: Env., 24, L133, 2000.

27. Wilson, K.; Lambert, R.M.; Hardacre, C.; "SO_2-Promoted Propane Oxidation Over Pt(111) and $Pt(111)/AlO_x$ Model Systems" Programme - 11th Int. Congr. Catal. - 40th Anniv., June 30-July 5, 1996; Po-278.

28. Wilson, K.; Lee, A.F.; Hardacre, C.; Lambert, R.M.; "Electronic, Structural, and Reactive Properties of Ultrathin Aluminum Oxide Films on Pt(111)" J. Phys. Chem. B, 102, 1736, 1998.

29. Lee, A.F.; Wilson, K.; Lambert, R.M.; Hubbard, C.P.; Hurley, R.G.; McCabe, R.W.; Gandhi, H.S.; "The Origin of SO_2 Promotion of Propane Oxidation Over Pt/Al_2O_3 Catalysts" J. Catal.; 184, 491, 1999.

30. Meeyoo, V.; Trimm, D.L.; Cant, N.W.; "The Effect of Sulphur Containing Pollutants on the Oxidation Activity of Precious Metals Used in Vehicle Exhaust Catalysts" Appl. Catal. B: Env.; 16, L101, 1998.

31. Wang, Yi; "The Effect of Sulfur and Phosphorous Compounds on Supported Platinum Catalyst Activity" Ph.D. Dissertation, New Jersey Institute of Technology, 1995.

32. Burch, R.; Fornaserio, P.; Southward, B.W.L.; "Particle Size and Support Effects on the Activity and Deactivation of Pt-based Catalysts for the Reduction of NO by n-octane Under Lean-Burn Conditions" Chem. Comm., 625, 1998.

33. George, Z.M.; "Poisoning and Regeneration of Claus Alumina Catalysts" Can. J. Chem. Eng., 56, 711, 1978.

34. Spenadel, L.; Boudart, M.; "Dispersion of Platinum on Supported Catalysts" J. Phys. Chem.; 64, 204, 1960.

35. Renouprez, A.; Hoang-Van, C.; Compagnon, P.A.; "Supported Platinum Catalysts-Small Angle X-Ray Scattering and Chemisorption" J. Catal., 34, 411, 1974.

36. Parkash, S.; "Determining Surface Area" Chemtech, 572, Sept. 1980.

37. Brunauer, A.; Emmett, P.H.; Teller, E.; "Adsorption of Gases in Multimolecular Layers" J. Am. Chem. Soc., 60, 309, 1938.

38. Chia, L.; Ricketts, S.; "Basic Techniques and Experiments in Infrared and FTIR Spectroscopy" Perkin Elmer, 1988.

39. Burch, R.; Watling, T.C.; "The Effect of Sulphur on the Reduction of NO by C_3H_6 and C_3H_8 Over Pt/Al_2O_3 Under Lean-burn Conditions" Appl. Catal. B: Env.; 17, 131, 1998.

40. Mowery, D.L.; Graboski, M.S.; Ohno, T.R.; McCormick, R.L.; "Deactivation of $PdO-Al_2O_3$ Oxidation Catalyst in Lean-Burn Natural Gas Engine Exhaust: Aged Catalyst Characterization and Studies of Poisoning by H_2O and SO_2" Appl. Catal. B: Environmental; 21, 157, 1999.